U.S.NRC
United States Nuclear Regulatory Commission
Protecting People and the Environment

Technical Letter Report
TLR-RES/DE/MEB-2026-01
PNNL-38917

Nondestructive Evaluation of Carbon Fiber Reinforced Polymers

April 2026

Prepared by:

Muthu Elen, Nick Conway, Matt Prowant, Richard Jacob

Pacific Northwest National Laboratory
Richland, Washington 99354

NRC Project Manager:

Chinthaka M. Silva
Materials Engineering Branch

Division of Engineering
Office of Nuclear Regulatory Research
U.S. Nuclear Regulatory Commission
Rockville, MD 20852

This report does not contain or imply legally binding requirements. Nor does this report establish or modify any regulatory guidance or positions of the U.S. Nuclear Regulatory Commission and is not binding on the Commission.

Pacific Northwest
NATIONAL LABORATORY

PNNL-38917

Nondestructive Evaluation of Carbon Fiber Reinforced Polymers

April 2026

Muthu Elen
Nick Conway
Matt Prowant
Richard Jacob

Prepared for the U.S. Nuclear Regulatory Commission
Office of Nuclear Regulatory Research
Under Contract DE-AC05-76RL01830
Interagency Agreement: A2307-031-089-048662
Task Order Number: 31310024S0062

DISCLAIMER

PACIFIC NORTHWEST NATIONAL LABORATORY
operated by
BATTELLE
for the
UNITED STATES DEPARTMENT OF ENERGY
under Contract DE-AC05-76RL01830

Printed in the United States of America

Available to DOE and DOE contractors from
the Office of Scientific and Technical Information,
P.O. Box 62, Oak Ridge, TN 37831-0062
www.osti.gov
ph: (865) 576-8401
fox: (865) 576-5728
email: reports@osti.gov

Available to the public from the National Technical Information Service
5301 Shawnee Rd., Alexandria, VA 22312
ph: (800) 553-NTIS (6847)
or (703) 605-6000
email: info@ntis.gov
Online ordering: http://www.ntis.gov

PNNL-38917

Nondestructive Evaluation of Carbon Fiber Reinforced Polymers

April 2026

Muthu Elen
Nick Conway
Matt Prowant
Richard Jacob

Prepared for the U.S. Nuclear Regulatory Commission
Office of Nuclear Regulatory Research
Under Contract DE-AC05-76RL01830
Interagency Agreement: A2307-031-089-048662
Task Order Number: 31310024S0062

Pacific Northwest National Laboratory
Richland, Washington 99354

Abstract

The American Society of Mechanical Engineers Boiler and Pressure Vessel Code requires repair and replacement of safety-related piping materials to meet the original Construction Code; however, no construction criteria currently exist for carbon fiber reinforced polymer (CFRP) materials in the nuclear industry. Although nondestructive examination (NDE) techniques for cast and wrought ferritic and austenitic steels are well established, licensees are increasingly deploying novel materials such as CFRP for which assessment of the use of NDE is required, as the inspectability of such materials and the influence of manufacturing processes on inspectability remain insufficiently understood. To address these gaps, Pacific Northwest National Laboratory (PNNL) evaluated the fabrication of several CFRP repair mockups and the effectiveness of NDE methods to support regulatory review of CFRP repairs in nuclear power plant applications. Representative flat-plate mockups containing realistic fabrication defects were manufactured and inspected using manual and automated tap testing, dynamic response spectroscopy (DRS), and ultrasonic testing (UT). The study identified significant fabrication variability, particularly in controlling defect size and epoxy thickness, which strongly influenced defect detectability by NDE methods. Tap testing was effective for shallow defects in thin epoxy configurations but unreliable for thicker repairs and deeper flaws. DRS demonstrated higher sensitivity to dry spots but produced unconfirmed indications for thicker plates, requiring further validation. Conventional UT, particularly at 1.0 MHz, showed the strongest overall capability for detecting a range of defects, although performance degraded with increasing repair thickness and complexity. The results highlight the need to better define critical defect sizes, develop reliable mockup fabrication methods, and validate NDE methods needed to support CFRP repairs.

Summary

Keeping reactors in operation and maintaining reliable power generation is a current priority for the U.S. Nuclear Regulatory Commission (NRC). Utilities have proposed the use of carbon fiber reinforced polymer (CFRP) systems to repair degraded safety-related piping, particularly where replacement would result in extended outages or significant operational burden. However, the American Society of Mechanical Engineers Boiler and Pressure Vessel Code requires repair and replacement items to meet the original Construction Code, and no construction criteria currently exist for fiber-reinforced polymer materials. As a result, licensees seeking to use CFRP repairs may submit a request for an alternative to codes and standards requirements under 10 Code of Federal Regulations (CFR) 50.55a(z)(1) and demonstrate that the proposed alternative provides an acceptable level of safety. Several such requests have already been submitted, creating the need for a technical basis to support NRC review with respect to nondestructive evaluation (NDE) of CFRP repairs.

This study was undertaken as part of confirmatory research to evaluate the fabrication of representative CFRP repair mockups and to assess the effectiveness and limitations of commercially available NDE methods for detecting fabrication and installation defects. The work focused on fabricating mockups designed to be nominally realistic and representative of field conditions, defect detectability, and the practicality of inspection techniques that could reasonably be deployed in the field.

Key findings on CFRP mockup fabrication include the following:

- CFRP mockup fabrication was highly sensitive to process control, including epoxy and putty mixing, cure timing, and installer skill. Small variations in these parameters resulted in meaningful differences in repair quality and defect formation.
- Defects, including dry spots, gaps in the fabric layer, fabric overlaps, and wrinkles, were intentionally introduced. Controlling final dry spot size and geometry proved difficult because of resin bleed-in during saturation.
- The variability observed during fabrication raises concerns about repeatability and consistency of qualification mockups and highlights the importance of fabrication controls in both mockup development and field repairs.

Key findings on NDE techniques evaluated include the following:

- Thicker putty layers significantly altered defect visibility and detectability, masking deeper defects and reducing inspection effectiveness of all NDE methods.
- Manual tap testing (MTT) and automated tap testing (ATT) were effective at detecting the 3 in^2 dry spots in repairs with thin putty layers but were unreliable for thicker putty repairs and detecting other defects such as gaps, overlaps, and wrinkles.
- MTT generally demonstrated higher sensitivity than ATT but required significant inspector experience and was negatively impacted by industrial noise, potentially reducing its reliability for field deployment.
- Dynamic response spectroscopy (DRS) showed higher sensitivity to dry spots than tap testing; however, it also identified numerous additional indications that could not be confirmed without destructive testing, limiting confidence in result interpretation.

- Conventional ultrasonic testing (UT), particularly at 1.0 MHz, demonstrated the strongest overall performance, detecting dry spots, overlaps, and some wrinkles. UT performance degraded with increasing repair thickness and laminate complexity, and analysis required experienced interpretation.
- None of the methods reliably detected gaps or wrinkles. Gaps were filled in with putty during the fabrication process, which limited detectability.
- Among the evaluated methods, UT appears to offer the greatest potential as a primary technique for inspecting the CFRP layers, while tap testing is best suited as a screening tool. DRS is primarily intended for substrate inspection and warrants further study to address false-call concerns.

Beyond fabrication and inspection performance, the study found that putty thickness and defect depth were the dominant parameters affecting defect detectability, outweighing the influence of individual defect types. The results also indicate that reliance on post-installation inspection alone may be insufficient to ensure repair quality, particularly for thicker CFRP systems. While this study did not explicitly evaluate layer-by-layer inspection, the findings suggest that such inspections conducted during fabrication, in addition to final inspections, would improve confidence in repair integrity.

Finally, there is a lack of technical basis linking specific defect sizes referenced in current guidance or code cases to the structural performance of CFRP repairs. Additional work is needed to identify critical defect sizes, validate that such defects can be detected and characterized, and confirm inspection results through destructive testing. These efforts would strengthen the technical foundation for reviewing CFRP repair applications and support informed regulatory decisions as CFRP technologies continue to be proposed for safety-related service.

Acronyms and Abbreviations

ASME	American Society of Mechanical Engineers
ATT	automated tap testing
CC	code case
CFR	Code of Federal Regulations
CFRP	carbon fiber-reinforced polymer
CoR	Coefficient of Restitution
dB	decibels
DMA	dynamic mechanical analysis
DPO	differing professional opinion
DRS	dynamic response spectroscopy
DSC	differential scanning calorimetry
EMC^2	Engineering Mechanics Corporation of Columbus
EPRI	Electric Power Research Institute
GFRP	glass fiber-reinforced polymer
ISI	In-service inspection
MFC	mel frequency cepstral
MTT	manual tap testing
NDE	nondestructive evaluation
NPP	nuclear power plant
NRC	Nuclear Regulatory Commission
PCC	Post Construction Committee
PE	pulse echo
PEC	pulsed eddy current
PNNL	Pacific Northwest National Laboratory
TIE	technical information exchange
UT	ultrasonic testing

Contents

Figures

Tables

1.0 Introduction

1.1 Background

Pacific Northwest National Laboratory (PNNL) was contracted by the U.S. Nuclear Regulatory Commission (NRC) to perform confirmatory research to evaluate the capabilities and limitations of nondestructive examination (NDE) methods for inspecting carbon fiber reinforced polymer (CFRP) repairs in commercial nuclear power plants (NPPs). NPP piping systems are exposed to various degradation mechanisms, such as corrosion, that may result in wall thinning and compromise their structural integrity and fitness-for-service. When significant degradation occurs, plant operators must decide whether to repair or replace affected piping. For buried piping, these decisions become more complex and costly because of the need for excavation, which increases project time, expense, and operational disruption.

To address these challenges, the nuclear power industry is increasingly adopting CFRP composites as an advanced repair solution (NRC 2023). CFRP systems consist of high-strength carbon fiber fabrics impregnated or saturated with polymer resins and applied in multiple alternating layers to restore or enhance the pipe's mechanical performance. Depending on the application, CFRP repairs can be installed on the external or internal surface of the pipe, provided there is sufficient access. These composite systems can either supplement the remaining strength of a degraded pipe or may serve as a fully structural, stand-alone system capable of carrying all design loads even if the host pipe continues to deteriorate. Importantly, CFRP repairs have the potential to reduce the downtime of operating reactors.

CFRP technology has been used for non-safety-critical applications in the commercial nuclear power industry for many years, primarily on piping systems such as circulating water, service water, and cooling systems (Olshan 2008; Stang 2011). For example, in 2007, QuakeWrap, Inc., repaired and strengthened the interior surface of a 3 m (10 ft.) diameter prestressed concrete cylinder pipe with CFRP at the San Juan Generating Station (Concrete Repair Bulletin 2008; QuakeWrap, Inc. 2009). 256 lineal m (840 lineal ft.) were targeted at the repair, which was completed within three weeks. At the Hope Creek Nuclear Generating Station, 17.4 lineal m (57 lineal ft.) of 366 cm (144 in.) diameter prestressed concrete cylinder pipe were repaired by Structural Technologies (Structural [no date]). Cracking was repaired in the cement mortar liner of a 213 cm (84 in.) diameter steel pipe at the Brunswick Nuclear Power Plant by Fyfe Company and Fibrwrap Construction (Gerard and Jimenez 2015).

The application of CFRP repairs in nuclear-safety-related systems is relatively recent. In 2020, the American Society of Mechanical Engineers (ASME) Boiler and Pressure Vessel Code Committee approved Code Case (CC) N-871-1, "Internal Repair of Class 2 & 3 Buried Piping using Carbon Fiber Composite Materials," which outlines the use of CFRP for internal repairs of Class 2 and Class 3 piping under Service Levels A, B, C, and D, with a qualified service life of 50 years. However, the NRC has not yet approved the Code Case for inclusion in its Regulatory Guides, meaning utilities must submit a request for alternative to codes and standards requirements under 10 Code of Federal Regulations (CFR) 50.55a(z)(1), which must be approved before using the Code Case.

The potential application of CFRP repairs in safety-related piping systems has drawn increasing regulatory attention. In recent years, the NRC has received several requests for alternative from utilities seeking to apply CFRP repairs to safety-class piping components under certain conditions, as the ASME Code does not specifically address using fiber-reinforced polymers in

either Section III or Section XI (Ramirez and Veil 2025). These include the requests from Surry Power Station Units 1 and 2, South Texas Project Units 1 and 2, Arkansas Nuclear One Units 1 and 2, Brunswick Steam Electric Plant Units 1 and 2, and Calvert Cliffs Nuclear Power Plant Units 1 and 2 (Sartain 2016; Dominion 2016; Helker 2022; Gaston 2020; Entergy Operations, Inc. 2020; Dunn 2019; Helker 2024; Gonzalez 2024). These requests involve using a CFRP repair system for internal structural upgrade of selected piping systems. The requests propose to perform visual inspection, surface preparation verification, and ultrasonic testing (UT) readings of the substrate at the terminal ends. The inservice inspection (ISI) requirements mentioned included determination of biological fouling, sediment buildup, and corrosion; assessment of the effectiveness of biofouling control mechanisms; and monitoring the material integrity of the metallic components, CFRP, concrete, and all joints. However, no specific technical details about the NDE methods and acceptance criteria were identified. The requests mentioned the use of a third-party inspection provider and internal quality assurance and control process, which are proprietary to the CFRP designer and installer.

1.2 Project Scope

Given the growing interest in extending CFRP technology to safety-related applications, it is important to evaluate the reliability and effectiveness of NDE methods used to inspect these composite repairs. An understanding of NDE capabilities, such as defect detection sensitivity, depth profiling, and long-term monitoring potential, is critical to ensuring the structural integrity, regulatory compliance, and service performance of CFRP-repaired piping within the safety requirements of the nuclear industry.

With direction and input from NRC, PNNL developed a two-phase plan for mockup fabrication and NDE analysis. For the mockup fabrication phase, PNNL aimed to identify appropriate guidance and best practices for the construction of qualification mockups in accordance with requirements in ASME CC N-871-1 and ASME Post Construction Committee (PCC) standard PCC-2-2022, “Repair of Pressure Equipment and Piping” (see Section 2.1). The fabrication included a set of representative flat-plate mockups that incorporated realistic flaws and variations in substrate and amount of putty. These mockups were intended to imitate field conditions, providing a credible and consistent basis for evaluating NDE performance. In addition to this work, NRC had previously sponsored research at Engineering Mechanics Corporation of Columbus (EMC^2), including CFRP mockup fabrication, testing, and evaluation of CFRP performance (Hioe et al. 2021; Hioe et al. 2022). The manufacturer followed their own proprietary procedure for the fabrication and inspection process, but this research work did not include evaluating the NDE methods.

For the NDE analysis phase, PNNL assessed commercially available and readily deployable methods to determine their effectiveness in detecting and characterizing flaws in the mockups. This study evaluated whether tap testing—a simple and cost-effective screening technique—can serve as a preliminary method to identify potential areas of concern. UT methods were also tested, including conventional UT and dynamic response spectroscopy (DRS), a commercial inspection technology described in Section 1.3.3.3. This study aimed to determine the challenges and best practices for CFRP repair inspections.

1.3 Key Concepts

1.3.1 Carbon Fiber Reinforced Polymer Repairs

"CFRP repair" or "composite repair" refers to the complete composite system, consisting of primers, laminae, epoxy, putty, and top coatings installed onto a metallic substrate in accordance with defined laminate design/architecture. CFRP repairs can be applied to both internal and external areas of the pipe, depending on the application. This work and the ASME Code Case are focused on internal CFRP repairs. A common CFRP repair system design is illustrated in Figure 1. The key elements of the repair process are described in the subsections below.

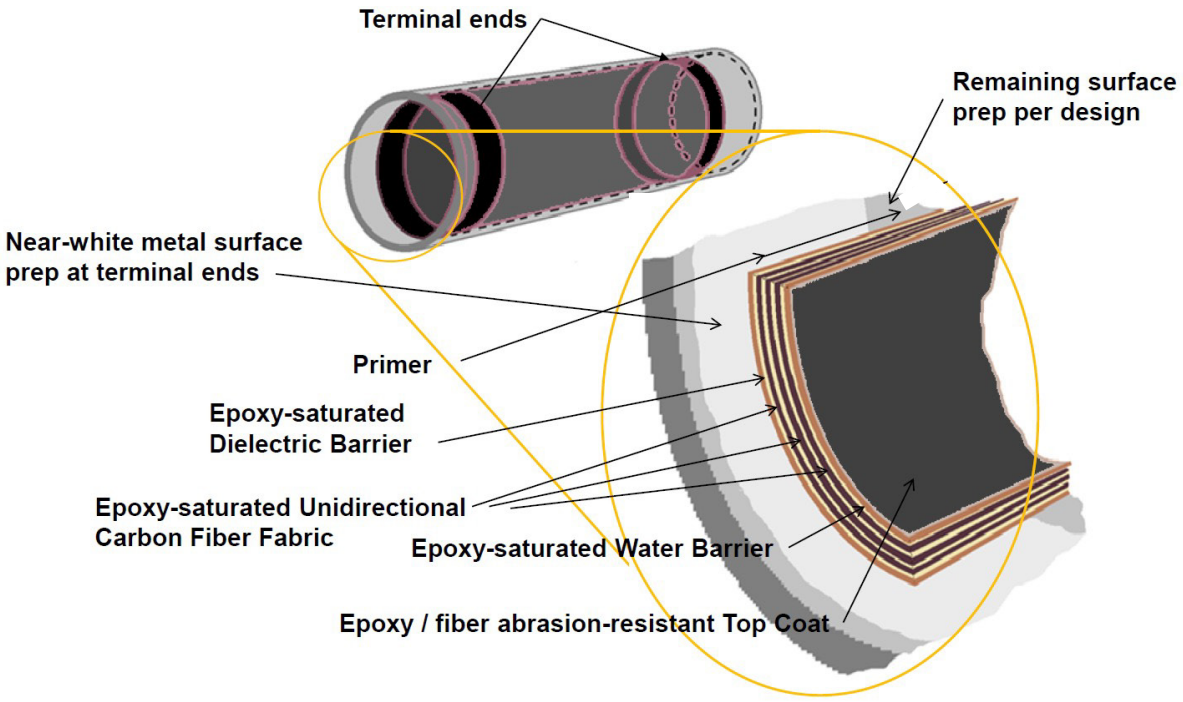

Figure 1. Example of a CFRP repair (Sullivan 2020).

1.3.1.1 Material Systems

A typical CFRP repair consists of a substrate, carbon fiber fabric, a dielectric layer (glass fiber fabric), matrix material, and epoxy or thickened epoxy. The substrate is the original pipe to be repaired/modified. The fabric is a cloth-like material constructed of interlaced carbon fibers, yarns, or filaments. It may be unidirectional or bidirectional, or other forms, depending on the fiber orientation and weave type. Carbon fiber is the principal component of the fabric and acts as the primary load-carrying member. The dielectric layer is a glass fiber fabric barrier intended to prevent galvanic corrosion of the substrate. The fabric is embedded in a matrix (also referred to as the resin or epoxy) to form a ply, or lamina. The epoxy is a two-part thermosetting polymer containing one or more epoxide or oxirane groups, curable by reaction with amines or alcohols. The matrix does not include fillers or thickening agents. The thickened epoxy, referred to as putty, is a mixture of epoxy and a prescribed thickening agent (e.g., fumed silica) in an

appropriate ratio. The putty is applied to the substrate to provide a smooth surface for the application of the dielectric layer. The putty is also applied as a protective topcoat.

1.3.1.2 Design

The design and architecture of the CFRP materials should be carefully tailored by the manufacturer to meet the structural and performance requirements of the specific application and, if applicable, the Code Case. The mechanical properties and long-term behavior of the repair depend not only on the individual materials but also on how they are combined, configured, and applied.

A well-engineered CFRP design must account for several interrelated factors. The orientation and layering of the carbon fibers determine the system's ability to resist different types of stresses, such as axial, hoop (circumferential), or bending loads. The epoxy must be selected for compatibility with both the fibers and the substrate material, while providing effective bonding, load transfer, chemical resistance, and environmental durability. The putty or filler materials used in substrate surface preparation play a key role in achieving proper adhesion and uniform bonding to the host pipe, especially when repairing irregular or corroded surfaces.

In addition, the geometry of the repair—including the shape, taper, and thickness of the CFRP layers—must be designed according to the pipe's dimensions, curvature, and load distribution to ensure that stresses are evenly transferred and localized strain concentrations are minimized. Environmental and operational factors, such as temperature, pressure, fluid type, and radiation exposure, must also be considered to ensure long-term durability and reliability.

1.3.1.3 Fabrication

The fabrication process begins with the preparation of the substrate according to the Code Case or design requirements. Each layer of fabric (also referred to as a lamina or a ply) is thoroughly saturated with epoxy resin to ensure complete impregnation of the fibers. This saturation process is critical, as it enables effective bonding between the fibers and the polymer matrix during the curing process, allowing efficient load transfer and maximizing mechanical performance. Multiple laminae are then successively layered to create a composite laminate, where the orientation, thickness, and number of laminae are tailored to meet specific structural and design requirements. Putty is used between each lamina to strengthen the structure and avoid sagging of the fabrics in the upper half of the pipe during internal repairs. A final top-coat is applied to finish the repair.

1.3.1.4 Terminal Ends

The terminal ends are the regions where the laminae are most securely attached to the substrate. CC N-871-1 primarily focuses on the integrity of the underlying metal substrate at the terminal end and the composite-to-substrate bond. The integrity of the terminal ends is critical to the integrity of the entire repair, because the terminal ends are responsible for the load transfer from the substrate to the repair. If a terminal end or bond to the substrate fails, the entire repair has a high probability of failure. The criteria for design and inspection are categorized into two phases, one for the terminal ends and the other for the rest of the repair. Because the terminal ends are so critical to the repair, those regions have more rigorous inspection requirements.

Expansion rings or compression rings are installed in the region connecting the terminal ends and CFRP repair, as per the manufacturer's design requirements. These stainless-steel rings

include a shim, a rubber strip, and are expanded using a hydraulic expander. Due to the installation of these expansion rings, there is compressive force applied to the repair.

1.3.2 Failure Mechanisms of CFRP Repairs

1.3.2.1 Manufacturing Defects

Defects in CFRP composite repairs can arise during material preparation, resin impregnation, layup, or curing processes. Defects can significantly affect the mechanical performance and durability of the composite. Common defects are listed in Table 1 and illustrated in Figure 2. Preventing, detecting, and mitigating these defects through strict process control, quality assurance, and NDE are essential to ensure the reliability and long-term performance of CFRP repairs.

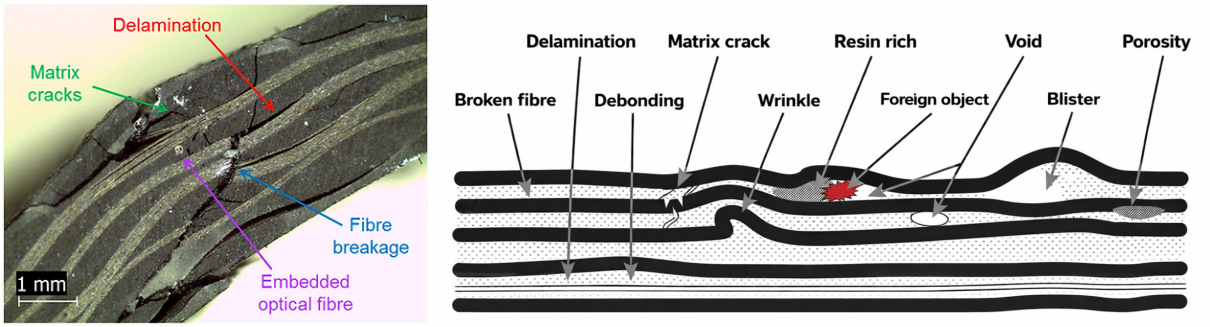

Figure 2. Illustration of defects in CFRP composites (Bowkett and Thanapalan 2017; Chandarana et al. 2017).

Table 1. Common defects in CFRP composites.

Defect	Cause
blisters, voids, or porosities	incomplete resin impregnation or trapped air from improper layup
fiber misalignment or wrinkling	improper layup, improper curing, incorrect resin impregnation
resin-rich or resin-starved areas	uneven resin distribution
delamination	improper compaction or curing between laminae
inclusions or contamination	improper layup, dirty environmental conditions
incomplete polymerization, residual stresses	improper curing cycles
disbond	improper bonding to the substrate, improper substrate preparation

1.3.2.2 Service-Induced Defects

Service-induced defects in CFRP repairs can develop over time due to operational stresses, environmental exposure, or issues introduced during installation and curing. Such defects include cracks or fiber breakage that occur under excessive mechanical or thermal stress that can compromise the load-carrying capacity of the repair; resin degradation from chemical exposure, radiation, or elevated temperatures that can reduce the material's stiffness and long-term durability; and moisture ingress through microcracks or imperfect seals that can further

accelerate damage. Identifying and characterizing service-induced defects through reliable NDE methods is therefore essential to ensure the continued structural integrity, leak-tightness, and performance of CFRP repairs.

1.3.3 Nondestructive Evaluation Methods Overview

There are several NDE methods that can be used for inspecting CFRP repairs, depending on the needs and application (Ramli et al. 2020; Chen et al. 2022; Vaara and Leinonen 2012; Tai et al. 2025). The methods primarily fall into several general categories: ultrasonic, acoustic, radiographic, thermographic, and electromagnetic. Table 2 lists some of the most common methods described in the references.

Table 2. Common NDE methods for composite repair inspections

Category	Methods
ultrasonic	pulse-echo, through-transmission, phased-array, advanced phased-array, laser, DRS
acoustic	manual tap testing, automated tap testing
radiographic	x-ray, digital x-ray, computed tomography, gamma-ray
electromagnetic	eddy current, pulsed eddy current, microwave, terahertz
thermographic	passive, pulsed, lock-in

The scope of this work was to investigate a few methods that are being used or are being considered for use in the nuclear industry, per CC N-871-1. These methods are pulse-echo (PE) UT (conventional), manual and automated tap testing, laser UT,[1] and DRS. The methods are introduced below; details of their implementation are provided in Section 4.0.

1.3.3.1 Tap Testing

Tap testing is a simple, low-cost method that can detect delamination or disbonding in CFRP structures. A trained analyst listens for changes in sound response when different regions of the surface are tapped with a small hammer or impact tool. Well-bonded areas sound solid, while unbonded areas sound hollow or have a different pitch (typically an increased pitch). Automated tap testers are also available. These units have a built-in tapper, and some have a microphone that records the sound response for computational analysis. An additional feature of some automated tap testers is a piezoelectric sensor that can detect changes in stiffness when it strikes the surface, allowing it to identify internal defects. For any tap testing, it is important to calibrate on a region that is known to be well bonded and defect-free. For manual tap testing or tap testers that do not have digital encoding capability, it is also important to work in an environment free of noise that could interfere with the inspector's ability to hear and distinguish the pitches of the tap responses. Tap testing is rapid and readily deployable, but the method can be highly subjective, deep defects may not be detectable, and defect localization and sizing lack precision.

[1] Laser UT was included in the original scope because it was offered by the same vendor that was contracted to perform the DRS tests; however, due to technical issues the vendor was not able to complete the laser UT work in time for this report, so the work was cancelled per NRC's direction.

1.3.3.2 Ultrasonic Testing

Ultrasonic testing is one of the most commonly used NDE methods. It is a volumetric inspection method that uses high-frequency sound waves to detect and characterize internal flaws. PE UT uses a single transducer to emit and detect the sound. PE UT is particularly sensitive to changes in acoustic impedance caused by density variations and discontinuities such as voids, delaminations, and inclusions. The location and timing of the echo responses provide information about the size and depth of defects. Encoded UT records the signals as a function of probe position to create an image for analysis. UT of CFRP repairs can be challenging because variations in acoustic properties between the different layers can attenuate and distort the sound field (Jodhani et al. 2023). UT can be slow for inspecting large areas and is difficult to deploy inside piping. UT also requires direct and continuous contact with the CFRP surface via a couplant (such as water or gel), so the surface needs to be smooth, clean, and free of defects.

1.3.3.3 Dynamic Response Spectroscopy

DRS is an ultrasonic method primarily intended to measure the metal substrate thickness. Figure 3 illustrates the application of DRS. A custom ultrasonic probe on the CFRP side of the pipe is used to interrogate the specimen (panel A). DRS works on the principle of constructive and destructive interference. When the wall thickness is one-half of the wavelength (or an integer multiple thereof), a dip occurs in the detected frequency spectrum from which the substrate thickness can be calculated (Alhamdan et al. 2019; Krautkrämer and Krautkrämer 2013). Defects in the CFRP that block the sound, such as dry spots, bubbles, delaminations, and disbonds, prevent thickness values from being obtained (panel B); however, regions where the sound is blocked appear as a lack of signal and can be used to identify the location and size (but not depth) of the defects. The result is a substrate thickness map with missing pixels indicating defects (panel C). DRS is not well suited for detecting other defects, such as overlaps, wrinkles, and gaps.

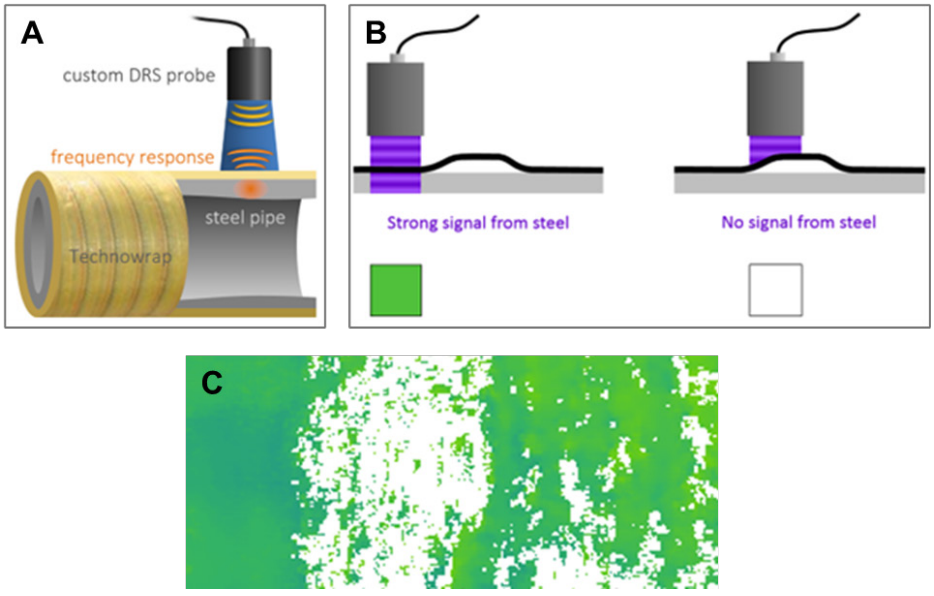

Figure 3. A: DRS is conducted through the CFRP layers. B: DRS signals are blocked by air, so bubbles, delaminations, and disbonds are evident where signals from the substrate are missing. C: Example of a DRS map showing the coating anomalies in white where signals from the substrate are lost. Images courtesy of Sonomatic, Ltd.

1.4 Literature Review

1.4.1 NDE of Composite Repairs

The widespread interest across all industries in using CFRP is evidenced by the steadily increasing number of citations in the open literature focused on NDE of CFRP. Figure 4 shows the results of a Google Scholar search[2] of "CFRP NDT" for each of the past eight years. There was nearly a two-fold increase in the number of citations from 2018 to 2025. A search of "CFRP NDT nuclear" showed that the fraction of citations that included "nuclear" is about 10% each year. This suggests a steadily growing interest in CFRP inspections related to nuclear applications. Note that articles that include "nuclear" at least mention in passing or cite nuclear applications but are not necessarily focused on nuclear.

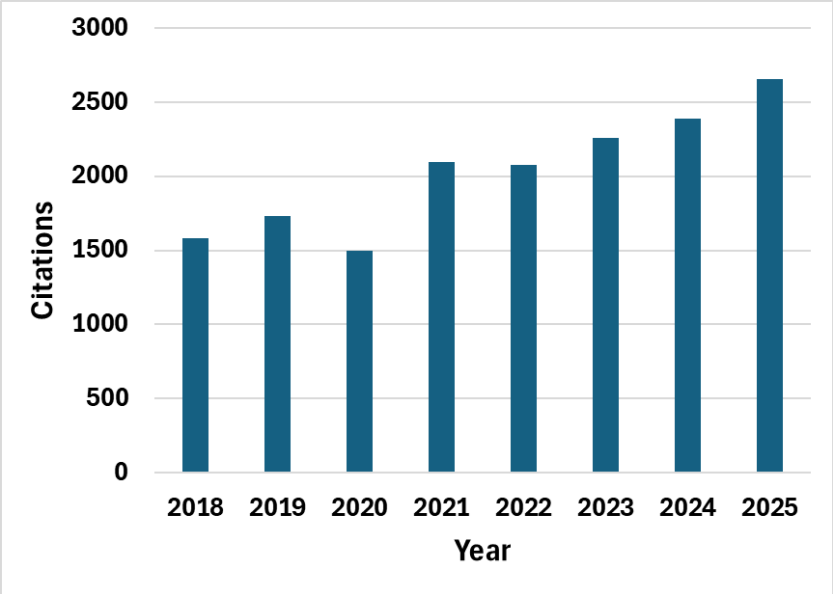

Figure 4. The number of Google Scholar citations found for the search "CFRP NDT".

A search that restricted results to those that had "nuclear" in the title resulted in only 26 citations, none of which were directly applicable to the subject of this report. Search results suggest that little to no research directly relevant to CFRP repair inspections in the nuclear power industry has been done. To understand why, it is important to understand the difference between conventional CFRP used in other industries versus the CFRP repair materials used for nuclear piping applications. Advanced CFRP structures are mostly fabricated in well-controlled environments, such as autoclave equipment and temperature-controlled ovens. The CFRP repairs in piping systems, on the other hand, are done on-site in the NPPs, mostly underground, by a manual layup process, and at room or ambient temperature. Additionally, as per certain design requirements, fabricators may use 40 oz fabrics instead of 20 oz lower weight options. Due to the added weight of the fabrics, putty may be used between the fabric layers to avoid sagging of the CFRP repair pipe, which makes the CFRP repair structure unique compared to other applications. Due to these primary differences, it is critical to evaluate the NDE technologies specific to and suitable for the NPP's inspection and regulatory standards.

[2] Search conducted November 14, 2025.

Even with the lack of nuclear-specific publications, there are many review articles that provide comprehensive overviews of NDE of CFRP and other fiber-reinforced polymers (cf. Sharma and Vijayakumar 2023; Chen et al. 2022; Tai et al. 2025; Panagiotis 2024). Particularly relevant to this report are reviews that cover tap testing (acoustic impact testing) (Vaara and Leinonen 2012) and ultrasonic methods (Jodhani et al. 2023; Wang et al. 2022). Overall, tap testing is well established and, therefore, does not garner much attention in the published literature. The same is true for conventional UT, whereas advanced UT (such as phased-array and full matrix capture), non-contact UT (such as laser UT and air-coupled techniques), and emerging methods tend to get more attention.

Of the research articles, most focus on specific CFRP constructs or substrates; specific NDE techniques, including novel, exploratory, or experimental methods; or specific data analysis methods, including artificial intelligence applications. Pertinent to this report, a search for "'dynamic response spectroscopy' NDT" gave only 11 results, including one in Korean and one in German. Most results were abstracts and not actual articles or reports. Four of the 11 were freely available reports or papers, but all only mentioned DRS and did not describe the method. One paper by Alhamand, et al. (2019) was obtained that had a brief description of DRS. They described DRS as a UT technique that uses a resonance condition that is met when the wavelength matches that of the substrate. They state that "a signal that disappears is an indication of disbonding between the composite repair and the substrate or an internal delamination in the composite repair," such as shown in Figure 3.

Studies on marine composites NDE highlight that no single inspection method can detect all defect types, underscoring the need for multi-technique approaches (Battley et al. 2002; Weitzenböck et al. 1999). The recommended strategy begins with simple, low-cost screening tools, like tap testing, followed by more advanced, high-resolution techniques, such as UT, for detailed flaw characterization. The Pipeline Research Council International also noted that while inspection of the substrate beneath composite repairs is feasible, interfacial delaminations continue to pose significant detection challenges, reinforcing the need for combined NDE methods and optimized mockup designs (Lee and Wall 2012).

The Electric Power Research Institute (EPRI) has published two reports focused on the NDE of CFRP repairs, providing key insights into the performance of emerging and conventional inspection technologies (EPRI 2018; EPRI 2022) (currently only the 2022 report is publicly available). The 2018 report is focused on measuring the properties of the substrate and not defects in the laminae. Key findings from these studies indicate that DRS and pulsed eddy current (PEC) methods were successful in measuring steel substrate thickness through CFRP layers, whereas phased-array UT techniques were ineffective due to high attenuation within the composite. Both DRS and PEC produced corrosion maps of steel substrates that closely matched baseline single-element PE UT results obtained before CFRP installation. PEC demonstrated the highest accuracy when substrate thickness was uniform, though it tended to underestimate localized corrosion smaller than the probe's averaging area. The studies also noted that applying advanced signal-processing algorithms can enhance thickness measurement accuracy by compensating for localized discontinuities within the inspection zone.

1.4.2 CFRP Mockup Design

Mockups are essential for the demonstration and qualification of NDE techniques used in CFRP repair inspections, as they serve as a foundation for identifying and refining best practices in inspection and evaluation. Pridmore et al. (2014) discuss their experience with large-diameter piping repairs using CFRP. They discuss materials selection and requirements, surface

preparation, installation of the CFRP system, terminal end preparation, and testing (per ASTM standards). Relevant mockups can be designed and built following real-world experience and lessons learned from piping installations. However, appropriate flaws and defects need to be included in the mockups.

Lessons from other industries can be used to inform mockup design for the nuclear industry. According to recommendations from Sandia National Laboratories (SNL), based on a Federal Aviation Administration (FAA) study (Roach 2015; Roach and Dorrell 1999; Roach et al. 1998), mockups should

- vary in substrate and laminate thickness
- include disbonds between the substrate and composite layers
- simulate interply delaminations
- be fabricated by multiple suppliers under identical specifications to ensure consistency
- accurately represent real-world repair scenarios encountered in the intended applications.

The FAA test specimen criteria specify maintaining a 5.1 cm (2 in.) flaw separation to avoid signal interference while also introducing closely spaced flaws to assess the ability of NDE methods to resolve boundaries. Flaws should be at least 3.8 cm (1.5 in.) from mockup edges, with minimum flaw sizes at half the target detection threshold and five discrete flaw sizes across specimens, including at least one large flaw for consistent detection across all techniques. These specifications help ensure that mockups challenge the full detection capabilities of each NDE method. The types, sizes, and locations of defects relevant to NPP applications are still open questions.

Realistic flaw fabrication methods identified by SNL include the pillow insert method (Kapton tape wrapped around tissue layers), brass shims coated with silicone release, and Teflon disk inserts of varying or stacked thicknesses (0.08 to 0.20 mm [0.003 to 0.008 in.]). Disbonds can be simulated by machining core sections and inserting pull tabs, and delaminations can be replicated using pillow or stacked Teflon inserts, allowing controlled flaw reproduction.

1.4.3 Literature Summary and NDE Gaps

The most critical areas for examination are

- the substrate at the terminal end under the composite
- the bond between the substrate and composite
- the integrity of the underlying substrate at the terminal end and the composite-to-metal bond, which is critical for load transfer
  - If the terminal end fails to retain structural integrity or the bond fails, it is reasonable to expect that the repair will fail to function as intended.
- laminar flaws (voids or delaminations) within the composite laminate itself.

The following key variables were identified for the fabrication of CFRP repair mockups:

- Substrate and laminate thickness
- Curvature of the piping substrates

- Weight of the fabrics
- Thickened epoxy
  - Whether or not to use it
  - Required quantities
- Potential flaw types and how they affect structural integrity
  - Substrate-to-laminate disbond
  - Interply delaminations
  - Others: Air bubbles, blisters, matrix cracking, moisture ingress, wrinkles, resin-rich and starved (dry) areas, voids, porosity, foreign debris, orientational variations, barely visible impact damage.

The following NDE questions and gaps were identified:

- What critical defects are expected to be observed during inspections? Specifically, are substrate-to-laminate disbond, interply delamination, porosity, and water intrusion among them?
- Among the defects mentioned, which ones are the most challenging to detect using the current inspection methods (i.e., UT and tap testing)? Are there other available and readily deployable methods that could detect these difficult-to-identify defects?
- Are there any defects that are considered undetectable with the currently available NDE methods?
- What are the critical flaw sizes and locations of concern? For example, what would be the impact of finding a 51 mm × 51 mm (2 in. × 2 in.) disbond or delamination along the terminal end versus within the “body” of the repair?
- What is the critical laminar flaw size, and what is the technical basis for this size?
- Have computational models or other technical bases been developed to help establish critical flaw types, sizes, and locations for the CFRP repair process?
- What inspection procedures are in place for the areas immediately upstream and downstream of the compression rings, where non-uniform flow-wear mechanisms may be introduced?
- CC N-871-1 calls only for visual examination of the entire repair but volumetric examination only of the terminal ends. What is the technical basis for not employing volumetric NDE methods of the entire composite repair?

2.0 Industry Activity

2.1 ASME Code

The ASME Boiler and Pressure Vessel Code Section XI, “Rules for Inservice Inspection of Nuclear Power Plant Components,” Paragraph IWA-4221, “Construction Code and Owner’s Requirements,” subparagraph (b), specifies that an item to be used for repair/replacement activities shall meet the requirements of the Construction Code. Subsubparagraph IWA-4221(b)(1) specifies that when replacing an existing item, the new item shall meet the Construction Code to which the original item was constructed. So, in a broad sense, the use of CFRP in repairs is governed by existing Construction Code; however, an assurance that a CFRP repair can meet the Code to which the original item was constructed is difficult to define. More specific documentation, such as code cases, can be used to meet the requirements.

There are two ASME documents related to CFRP repairs and examination. The first is ASME PCC-2-2022, “Repair of Pressure Equipment and Piping.” The section relevant to CFRP is Part 4, “Nonmetallic and Bonded Repairs,” Article 401, “Nonmetallic Composite Repair Systems: High-Risk Applications.” Subarticle 401-5, “Examination,” is specific to inspection of CFRP repairs. Figure 401-5.1-1, “Schematic of a Repair System and Location of Defects,” illustrates the types and locations of potential laminate and substrate defects. Table 401-5.2-1, “Defect Type and Allowable Limits for the Composite Wrap,” lists the defect types and allowable limits, including delamination, foreign matter, blisters, wrinkles, and dry or unimpregnated fiber. Subarticle 401-5 identifies visual inspection, hardness testing, tap testing, and other methods specified by the “repair system supplier” as the inspection methods for the composite repair.

The second document is CC N-871-1 (approved October 9, 2020), “Repair of Buried Class 2 and 3 Piping Using Carbon Fiber-Reinforced Polymer Composite.” The section relevant to CFRP repair inspection is Article 5000, “Examination and Verification Testing.” Table 3 lists the inspection requirements outlined by CC N-871-1 for the terminal ends and for the entire composite repair.

Note that CC N-871-1 is not considered in Revision 21 of NRC’s Regulatory Guide 1.147 and has not been approved for use by the NRC. Special approval to use CC N-871-1 must be obtained from the NRC through a request for alternative to the repair/replacement requirements of Section XI. To address NRC concerns, the ASME Task Group on Repair by Carbon Fiber Composites (under the Working Group on Non-Metallic Repair/Replacement Activities and Subgroup on Repair/Replacement Activities) is currently working on revising CC N-871-1. ASME Codes & Standards record number 24-2395 represents a draft of CC N-871-2, which is modeled after PCC-2 Article 401.

PNNL has participated in the Task Group meetings where CC N-871-2 is being developed and helped review and edit sections involving examination and inspection. PNNL also presented occasional updates on their NDE of CFRP research in order to receive comments and feedback from the Task Group members.

Table 3. Inspection requirements, as per ASME CC N-871-1.

Inspection Requirements	
Terminal End Only	
Prior to Installation of Repair	• Inspect the thickness of metal substrate to ensure structural integrity • Ultrasonic thickness mapping
After Each Layer of Installation	• In-process examination of CFRP layers • Acoustic tap examination
After Installation of the Final Layer	• Volumetric examination of the accessible surface of laminate repair • Metal substrate examination beneath the laminate • Acoustic tap, ultrasonic, or other volumetric examination
Inservice Inspection (ISI)	• Once between 4 to 6 years after repair, and once per 10-year ISI interval • Volumetric methods similar or equivalent to previous step
Entire Composite Repair	
Prior to Installation of Repair	• Visual examination of the prepared pipe surface
During Installation	• Layer-by-layer visual and acoustic tap examination of CFRP
Preservice Exam	• Visual examination after the laminate has achieved tack-free surface
ISI	• Visual examination once between 4 to 6 years after repair, and once per 10-year ISI interval

2.2 2023 Technical Information Exchange

EPRI organized a CFRP Technical Information Exchange (TIE) Workshop in Charlotte, North Carolina, July 25–26, 2023, to bring together key stakeholders from across the nuclear, materials, and NDE communities (Breon and Elen 2024; Elen et al. 2024). Prior to the in-person event, a virtual pre-meeting was held with several CFRP domain experts, during which EPRI and PNNL outlined the workshop's objectives, technical focus, and expected outcomes related to CFRP repair qualification and inspection.

Workshop participants included representatives from EPRI, PNNL, and the NRC, along with major utility organizations such as Framatome, PSEG Nuclear, Ameren, STP Nuclear, and Constellation Energy. CFRP fabricators and material suppliers in attendance included Carbon Fiber Engineered Solutions, Kinectrics, Composite Technology and Infrastructure, Sargent & Lundy, Engineering Mechanics Corp of Columbus, Structural Technologies, A&G Industrial Services, and Thin Film Technology, Inc. Additionally, NDE service providers, such as Sonomatic and academic researchers from Michigan State University and Korea University, contributed to the technical discussions.

Several workshop presentations addressed topics related to CFRP fabrication practices, operator field experience, and ongoing NDE development efforts, emphasizing the need for standardized qualification methods, consistent material performance evaluation, and reliable inspection techniques to support CFRP implementation in both safety- and non-safety-related NPP piping systems.

The following points were the primary topics of discussion at the TIE workshop:

- Key steps in CFRP fabric installation include dewatering of host pipe, thorough surface preparation, adhesion testing, fabric saturation, and weight ratio verification, followed by fabric layup, inspection, installation of expansion rings, and a final quality check.

- Proper surface preparation is critical for achieving strong adhesion between the first fabric layer and the metallic substrate, directly affecting long-term bond performance. The recommended preparation method is to achieve a white-metal blast finish with a 0.076 mm (0.003 in.) surface profile to ensure the resin can flow into the microscopic surface roughness and form a strong mechanical interlock.

- Installation defects typically result from poor workmanship, with most issues occurring at the 12 o'clock position of the pipe—areas that are difficult to access during application or that are prone to sagging. Most defects are relatively minor, with about 90% measuring less than 13 cm^2 (2 $in.^2$).

- Common types of defects include those caused by material quality issues (fabric or epoxy), unfavorable environmental conditions, excessive epoxy thickness, dry spots, wrinkles, air entrapment, fabric bridging[3], and delamination—all of which highlight the need for rigorous quality control during the CFRP installation process. Defect reduction can be achieved through hands-on training, procedure improvements, and refinements to installation systems.

- Computational finite element analysis modeling of defects, combined with NDE analysis, can be used to study the behavior of various composite laminates and assess the impact of potential flaws.

- DRS measurements are highly sensitive to small thickness variations in the substrate, but they have limitations: corrosion pits smaller than 10 mm (0.4 in.) diameter cannot be detected, and DRS cannot evaluate bond quality or directly determine bond strength.

- Beyond CC N-871-1 guidelines, fabricators may follow alternative measures as outlined in "CFRP supplier recommended practices" permitted by the Code Case. It is important to identify uncertainties in the installation process and establish appropriate remedies to ensure consistent quality and performance of the CFRP repair.

- There is no "one-size-fits-all" approach for CFRP repairs, and independent research is necessary to develop best practices and implement consistent policies. Research in aging mechanisms was mentioned in particular. CFRP materials can degrade through mechanisms such as thermo-oxidation, radiation exposure, ultraviolet aging, water ingress, and chemical interactions. Evaluating their long-term performance may require destructive testing of pipe specimens at elevated temperatures to characterize these aging effects..

2.2.1 Workshop Summary

Based on discussions during the TIE workshop, an action plan was developed. Since multiple variables influence the CFRP repair process, it was important to prioritize variables for mockup fabrication. To identify critical variables, it was determined that additional information was required from key stakeholders. Thus, a survey of TIE participants and other stakeholders was recommended (see Section 2.3).

[3] During installation of fabric, fabric bridges over welds, layers, dents, etc. can cause overlaps, wrinkles, and pleats in the installation.

For NDE research, evaluation should focus on methods such as tap testing, UT, DRS, laser UT, microwave, thermography, and shearography. Additional research needs were identified, including bond testing at terminal ends structural testing of CFRP to determine critical flaw sizes for reliable performance assessment.

2.3 Industry Survey on NDE of CFRP

To address key concerns discussed during the workshop, PNNL and EPRI developed a survey to gather insights from the CFRP repair community, including designers, asset owners, fabricators/installers, NDE researchers, and certified technicians (the survey has been reproduced in Appendix C). The survey was designed to collect information on various aspects of internal and external CFRP repairs, such as fabric weight, orientation, number of layers, installation configurations, the use of thickened epoxy (putty), topcoat applications, and repair thickness. It also aimed to identify typical flaw types, including loss of adhesion to the substrate, delamination between layers, air voids/bubbles, epoxy cracking, under-saturation, and foreign material. Respondents were asked to rank the criticality of such flaws, identify additional flaws of concern, list common NDE techniques in use, and describe limitations of current NDE methods. The survey was sent to 40 individuals in October 2023 and yielded eight responses. Some declined to respond citing a lack of expertise, plant-specific requirements, or proprietary restrictions. The results were analyzed and helped inform decisions on mockup fabrication and NDE methods for this project.

The following summarizes the survey responses.

- The weight of fabrics varies between about 0.3 to 1.4 kg/m^2 (10 to 40 oz/yd^2), depending on the fabric type, orientation, and fabricator.
- For both internal and external repairs, three respondents indicated that they use putty between CFRP layers, and five confirmed its use as a topcoat and at the interface between the substrate and CFRP. Additionally, one respondent noted that the thickness of the putty layer tends to vary around the circumference.
- The four flaw types ranked as most critical for CFRP repairs were
  - loss of adhesion to the substrate, especially at terminal ends
  - delamination between layers
  - under-saturation of fabric
  - cracking within the epoxy matrix.
- In addition to the critical flaw types identified, respondents highlighted other potential issues that could occur during fabrication or service. These included
  - high-velocity fluid systems causing the CFRP repair to peel off the substrate, leading to failure
  - the use of excess putty, which may negatively impact the desired performance of the repair
  - fabric misalignment
  - overlapping layers resulting in lifted edges
  - excessive application of topcoat
  - pinholes in the topcoat

  - water ingress significantly affecting the strength of the CFRP system
  - cracks propagating within the repair
  - new bubbles or delamination
  - previously unrepaired flaws that grow over time
  - wear or damage caused by system erosion or debris.
- The NDE techniques that were used or recommended were visual, tap testing, DRS, microwave, thermography, shearography, and laser UT.
- Respondents noted that selecting the correct inspection technique depends strongly on the specific flaws and unique requirements of each inspection scenario. Certain techniques have surface-specific limitations, such as DRS requiring a smooth surface and laser methods needing a dark matte surface for effective results. Concerns regarding CFRP inspection included
  - challenges in effectively measuring degradation
  - the inability to accurately assess bond integrity
  - correctly interpreting results from tap testing.

3.0 Fabrication of CFRP Mockups

A CFRP vendor (Kinectrics, Inc., through a partnership with A&G Industrial Services) was contracted by PNNL to fabricate eight plate mockups. The mockups were fabricated over a period of eight days, during which the PNNL team visited the vendor for two days to observe and understand the fabrication process, address challenges, and gain insights into the placement of defects within the mockups.

The base metallic substrates were 61 cm × 61 cm × 1.3 cm (24 in. × 24 in. × 0.5 in.) carbon steel plates. Each mockup consisted of seven plies: one ply of glass fiber-reinforced polymer (GFRP) as the first layer and six plies of CFRP. The CFRP plies were alternately oriented in a 0°/90° configuration (horizontal/vertical). The materials used for the mockups were Carbon Fiber 2339 (Toray T700S), a unidirectional fabric that is 0.661 kg/m^2 (19.5 oz/yd^2) and has a nominal thickness of 0.97 mm (0.036 in.), and Glass Fiber 1210 (Hybon 2026), a bidirectional fabric that is 0.875 kg/m^2 (25.8 oz/yd^2) and has a nominal thickness of 0.79 mm (0.031 in.). Specific information about the properties of the carbon fiber and glass fiber materials is proprietary. 212N Saturant was used as both a primer and saturant for the fiberglass and carbon fiber, and 130N Tack Coat, thickened with fumed silica, was applied between layers of fabric in layer thicknesses of 0.79 mm or 3.2 mm (0.031 in. or 0.125 in.), as noted in Table 4. 130N putty has 6.3% fumed silica by weight. To achieve different percentages, additional fumed silica was added to the 130N putty and mixed thoroughly.

Intentional defects, or flaws, were included in the mockups. Mockups were divided into four quadrants for flaw placement; flaw types and locations are detailed in Table 4. In the table, “P” indicates the ply and “Q” indicates the quadrant. Note that ply 0 is the glass fiber, ply 1 is the inner-most carbon fiber ply (closest to the substrate), and ply 6 is the outer-most. Mockups 1 through 6 had identical flaws in each quadrant and at each depth, but the locations of the flaws within each quadrant were varied. Note that the 58 cm^2 (9 in.^{2}) dry spots were intended to be 19 cm^2 (3 in.^{2}) dry spots, but through a miscommunication, the vendor interpreted this as 7.6 cm × 7.6 cm (3 in. × 3 in.) square (communications with the vendor used only English units, and “three square inches” was interpreted as “three inches square”). This was noticed during the PNNL visit to the vendor, so additional circular dry spots of 19.4 cm^2 (3 in.^{2}), or 5.0 cm (2.0 in.) diameter, were included on ply 5.

Figure 5 shows a schematic (not to scale) top view of the approximate flaw placements in Mockup 1. Quadrants are labeled 1 through 4, clockwise, starting from the top right. Appendix B shows sketches of all eight mockup designs. Figure 6 shows an example cross-section view, illustrating the placement of the different flaws in the laminae strata. Note that flaws were placed such that they did not overlap to avoid confounding signals during the inspections.

Table 4. Test matrix of CFRP mockup fabrication.

Mockup	1	2	3	4	5	6	7	8
% of Fumed Silica	6.3	8.3	10.3	6.3	8.3	10.3	8.3	8.3
Thickness of Putty Between Each Layer (in.)	0.031	0.031	0.031	0.125	0.125	0.125	0.031	0.125
Dry Spot (58 cm^2 [9 $in.^2$] square)	P2-Q1 P4-Q3	P2-Q1 P4-Q3	P2-Q1 P4-Q3	P2-Q1 P4-Q3	P2-Q1 P4-Q3	P2-Q1 P4-Q3	P0-Q1	P0-Q1
Dry Spot (19 cm^2 [3 $in.^2$] circle)	P5-Q4	P5-Q4	P5-Q4	P5-Q4	P5-Q4	P5-Q4	P0-Q1	P0-Q1
Wrinkles (5–7.6 cm [2–3 in.])	P1-Q1 P3-Q3	P1-Q1 P3-Q3	P1-Q1 P3-Q3	P1-Q1 P3-Q3	P1-Q1 P3-Q3	P1-Q1 P3-Q3		
Gap (7.6 cm [3 in.] long × 2.5 cm [1 in.] wide)	P3-Q4	P3-Q4	P3-Q4	P3-Q4	P3-Q4	P3-Q4		
Overlap (7.6 cm [3 in.] long × 2.5 cm [1 in.] wide)	P3-Q2	P3-Q2	P3-Q2	P3-Q2	P3-Q2	P3-Q2		
Primer Partial Cure Before Ply							P0-Q2	P0-Q2
Lack of Adhesion (Improper Surface Prep)							P0-Q3	P0-Q3

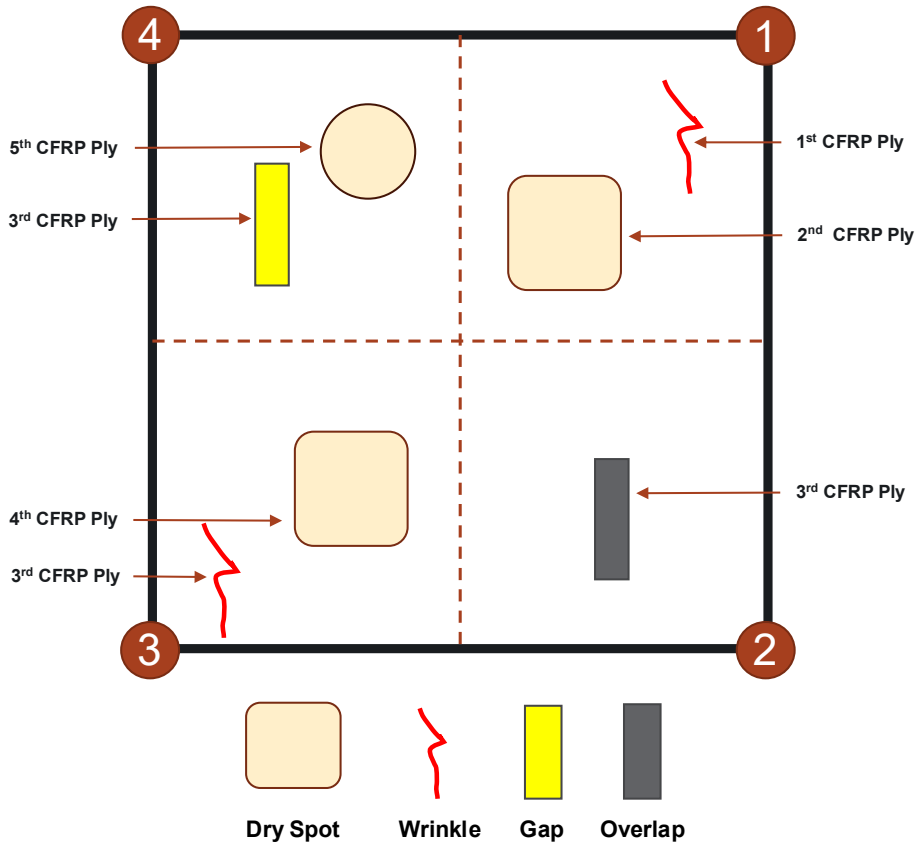

Figure 5. Top view schematic of the CFRP repair Mockup 1 with planned defects.

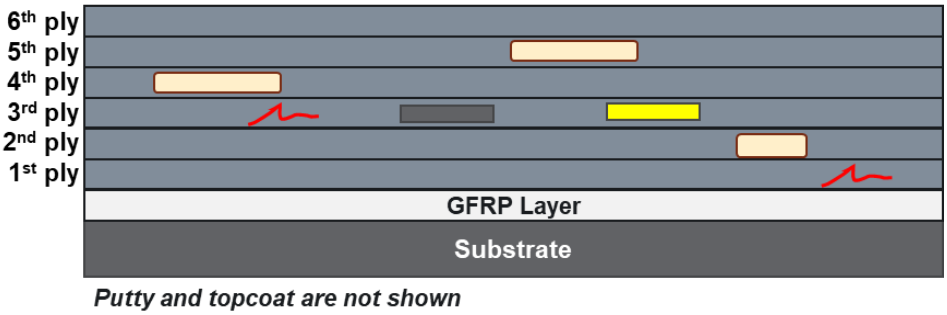

Figure 6. Cross-section schematic of a mockup. Flaw placement is illustrative only.

3.1 The Fabrication Process

The CFRP repair mockup fabrication process involved the following steps, described below and shown in photographs in Figure 7. Additional information and photographs are provided in Appendix A.

1. Surface preparation – Visual inspection was performed on the steel substrate, and the surface was prepared by sandblasting per the design requirements. For Mockups 7 and 8, one quadrant (Q3) was not sandblasted (as shown in Figure 7), so that effects of improper surface finish could be examined with NDE.
2. Application of primer – A thin layer of the primer was applied with a roller on the top surface of the substrate.
3. Preparation of putty – The putty had 6.3% fumed silica content per the manufacture's technical datasheet. Additional fumed silica was added to achieve different fumed silica contents (8.3% and 10.3%).
4. Application of putty – The putty was applied on the top of the primer layer.
5. Fabric saturation – The two-part epoxy was mixed, per the manufacturer's specifications, then manually applied to the fabric. Figure 8 illustrates the difference between the 6.35 mm (0.25 in.) trowel and the 1.59 mm (0.0625 in.) trowel. The saturated fabric was then weighed to ensure that the fiber-matrix ratio met the installation requirements.
6. Fabric installation – The saturated fabric was installed on top of the putty layer. Defects were added according to the test matrix (Table 4). Steps 2 through 6 were repeated for each layer of fabric. The directionality of the fabric layers was alternated.
7. Application of topcoat and paint layer – A final layer of putty was applied as a topcoat, followed by paint for the final finish layer.

The CFRP mockups were fabricated one layer per day, allowing each lamina to cure completely at room temperature. During the mockup fabrication process, an infrared thermometer was used to measure the temperature distribution after each layer and after applying the putty. Since the epoxy and putty were room temperature cure systems and were spread uniformly in a thin layer, the information obtained from the thermography did not reveal any interesting results. However, it was able to identify the dry spots.

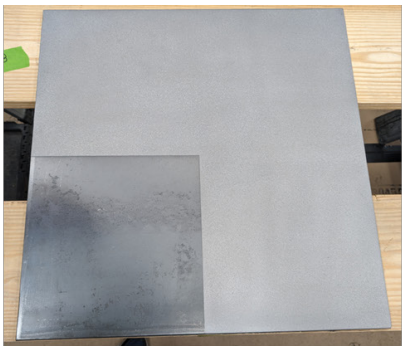

Step 1: Surface Preparation

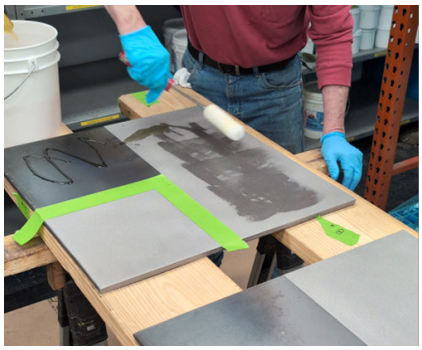

Step 2: Primer Application

Step 3: Preparation of Putty

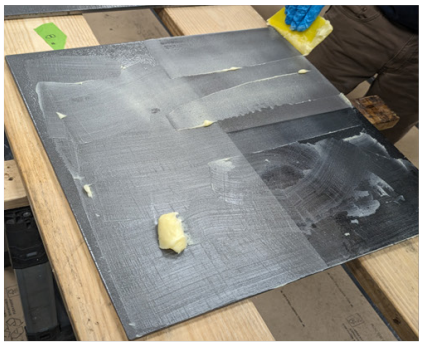

Step 4: Putty Application

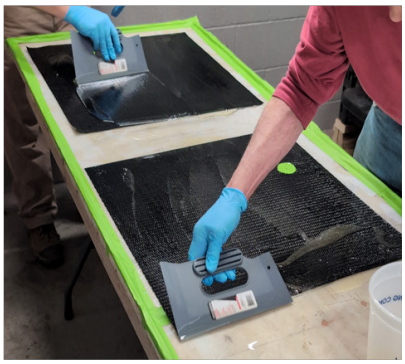

Step 5: Fabric Saturation

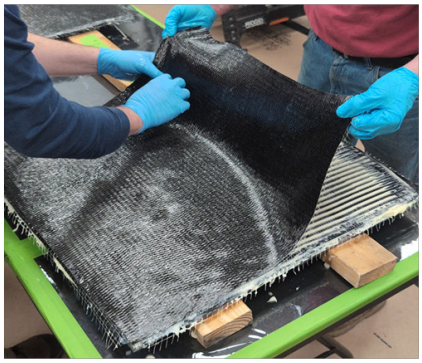

Step 6: Fabric Installation

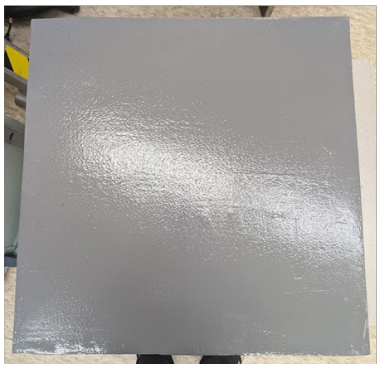

Step 7: Application of Top Coat and Finish

Figure 7. Mockup preparation steps.

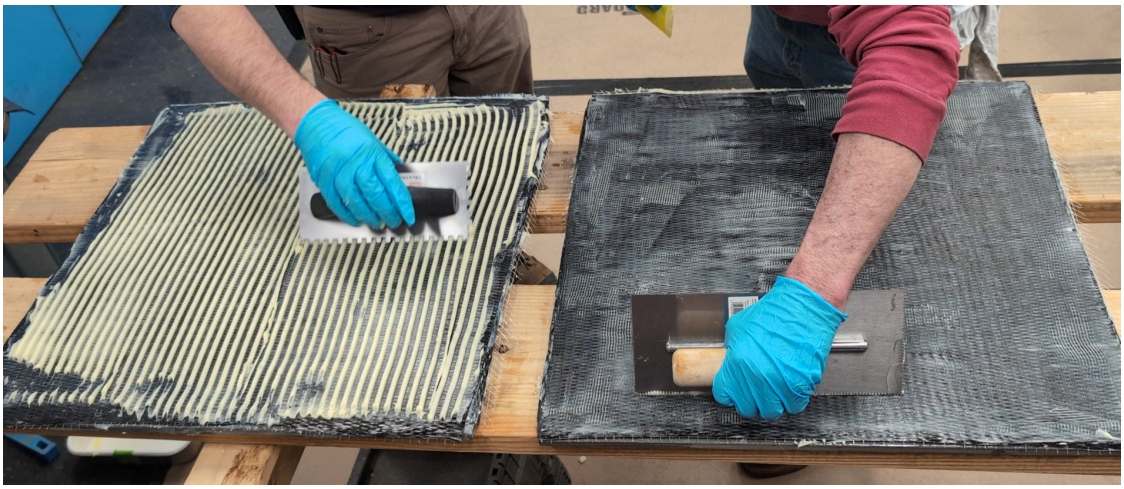

Figure 8. Photograph of putty being applied with the 6.35 mm (1/4 in.) trowel (left) and the 1.59 mm (1/16 in.) trowel (right).

3.2 Description of Added Defects

Dry Spots

Dry spots or undersaturated spots were created by covering the desired region with a Teflon cutout of the appropriate size and shape, as shown in Figure 9, then applying the epoxy. After the epoxy was applied, the cutout was removed, revealing the dry spot underneath.

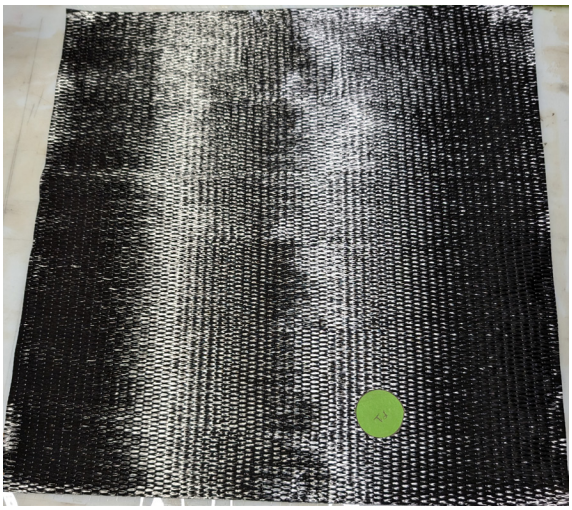

Figure 9. Fabrication of a dry spot.

Figure 10 shows two dry spots, one in the carbon fiber and one in the glass fiber. Both spots were intended to be 7.6 cm × 7.6 cm (3 in. × 3 in.), with an area of 58 cm^2 (9 $in.^2$). However, due to the wicking of the epoxy, the actual sizes of the spots were reduced somewhat. For example, the glass fiber shows a region that is totally dry within an approximately 5 cm × 6.4 cm (2 in. × 2.5 in.) undersaturated region. Unfortunately, the final true-state dimensions of the dry spots are unknown and would require destructive testing. It was also visually observed during fabrication that the 7.6 cm × 7.6 cm (3 in. × 3 in.) square dry spot in Mockup 8 was fully saturated, while only the circle dry spot was fabricated as intended. Hence, overall, the planned

dry spots may be a combination of undersaturated and dry spots. Note that CC N-871-1 requires defects in terminal ends larger than 12.9 cm^2 (2 $in.^2$) to be repaired; essentially all the dry spots in the mockups exceed this and must therefore be detectable with NDE.

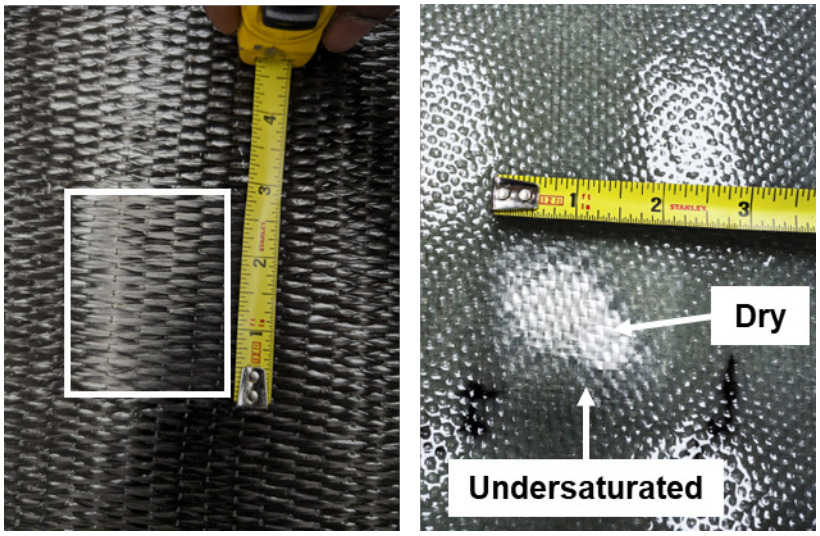

Figure 10. Dry spots after resin saturation. Left: in a carbon fiber ply. Right: in a glass fiber ply. Note that glare from the overhead lights makes the dry spots difficult to discern in photographs.

Wrinkles, Gaps, and Overlaps

Wrinkles were made by pinching the fabric layer after laying it up on the putty layer. Gaps in the fabric were made by cutting out the desired size from the fabric (Figure 11). Overlaps were made by placing the cut piece on a fabric layer. Figure 12 shows an example of all three on one ply. Note that gaps were ultimately filled with epoxy or putty when the next lamina was applied.

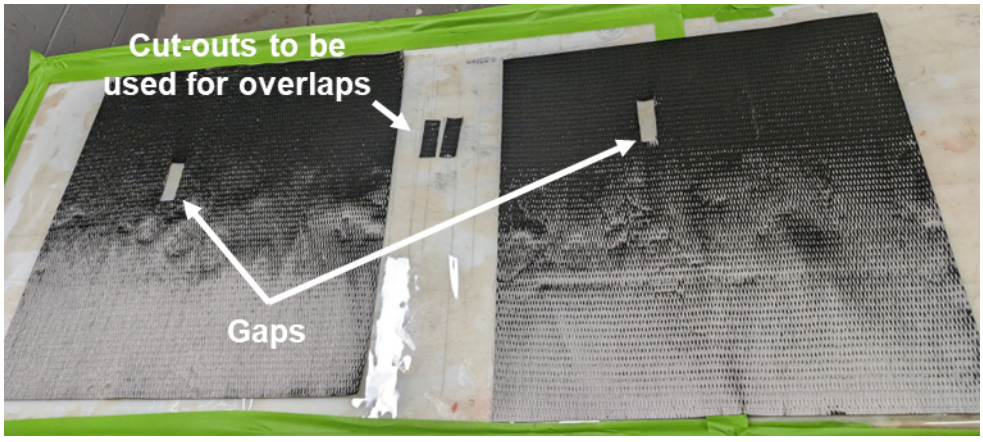

Figure 11. Fabrication of gaps and overlaps.

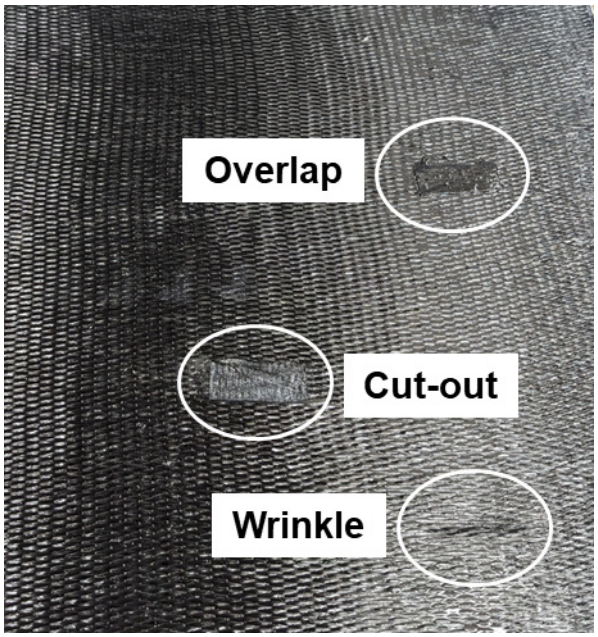

Figure 12. Example of an overlap, cut-out, and wrinkle.

Surface Preparation

Mockups 7 and 8 each had one quadrant of their substrates that was fabricated without sandblasting, as shown in Figure 13. All other mockups had the surface grit blasted to an SSPC-SP 10 Near White Metal standard with a 3+ mil profile.

Figure 13. Surface preparation of the substrate of Mockup 8.

3.3 CFRP Panels

Two composite panels measuring 30.5 cm × 30.5 cm (12 in. × 12 in.) were fabricated without a substrate using putty with 6.3% and 8.3% fumed silica. These panels were fabricated by the vendor for demonstration purposes and potential tensile testing of mechanical performance with and without defects. The panels followed the same layup sequence as the plate mockups, consisting of one layer of glass fiber followed by six layers of carbon fiber with alternating orientations. A dry spot defect was deliberately introduced on one-half of the panel in the third CFRP ply. The putty thickness was 0.79 mm (0.031 in.). The panels were cut and examined through a Keyence microscope to illustrate the thickness of the putty layers and the dry spots, as shown in Figure 14. Note that no NDE data were acquired on these panels, and mechanical testing was ultimately not included in the work scope, so no further testing was performed.

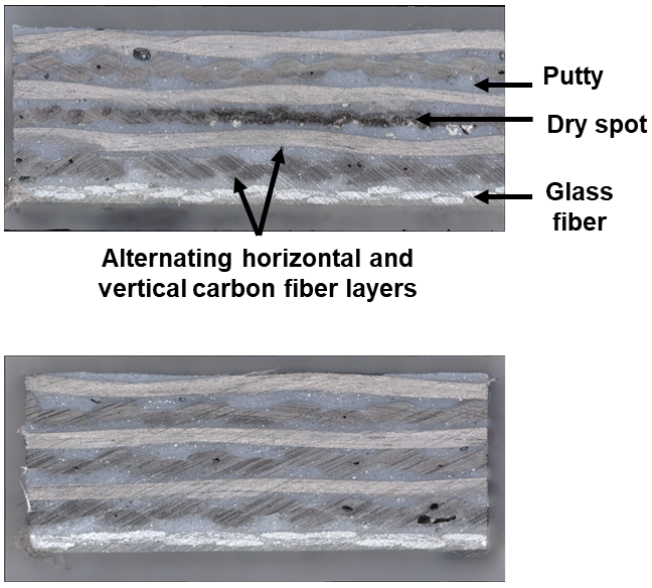

Figure 14. Cross-sectional views of two CFRP panels with 6.3% (top) and 8.3% (bottom) fumed silica.

3.4 Lessons Learned During CFRP Mockup Fabrication

PNNL learned the following while observing the mockup fabrication.

- The size of the dry spots was difficult to control. For example, the final size of the 58 cm^2 (9 $in.^2$) dry spots appeared to be reduced to approximately 5 cm × 5 cm (2 in. × 2 in.), because of resin saturation bleeding in from the edges of the intended defect locations. Similarly, the 19.4 cm^2 (3 $in.^2$) circular dry spots were often reduced to about 13 cm^2 (2 $in.^2$) or less. Thus, the actual dimensions and shapes of the dry spots were not well controlled and may vary from mockup to mockup. This raises concerns about being able to reliably and reproducibly fabricate mockups that meet design specifications. Techniques in the literature suggest using Teflon or similar materials, using wax or a mold release agent, or placing an additional layer of dry fabric over the cured region as means to control the defect dimensions.
- The epoxy and putty preparation process requires careful attention to cure time. The epoxy or putty needs to be properly mixed, but timing is important, so that it is not allowed to cure before it is applied. If the epoxy or putty begins to harden, it is difficult to spread and smooth.

- The laminae layup process requires significant skill and attention to detail. Gaps between layers can form if the putty is not adequately smoothed to achieve uniform thickness or if it is allowed to cure before the next lamina is applied. Also, foreign matter or debris can easily become embedded in the laminae.
- Errors during the layup process need to be recognized and mitigated in a timely manner. If the epoxy or putty begins to cure, then removing a lamina is a significant effort and may damage the repair.

3.5 EPRI Mockups

EPRI fabricated two sets of CFRP mockups using the same vendor and the same (or similar) materials as PNNL, but with different defects. The major difference between PNNL and EPRI mockups is that EPRI did not use putty (thickened epoxy) between each layer. Putty was only applied as a topcoat layer. An EPRI report has been published in which they describe the details of the mockup design and fabrication (this report is currently not publicly available) (EPRI 2025). Below is a summary of the mockups.

Set 1 of EPRI mockups consisted of eight plates with varying numbers of laminae. Like the PNNL mockups, EPRI's mockups were divided into quadrants, and defects placed within various layers of each quadrant (some quadrants were left unflawed); multiple defects within the same quadrant were always in the same layer. The defects were specified as circular interstitial delamination flaws of sizes 1 $in.^2$ (small), 2 $in.^2$ (medium), and 16 $in.^2$ (large). For reference, Table 5 shows the equivalent diameters of the flaws in English and metric units.

The second set of EPRI mockups consisted of 16 plates; eight were made with 0.661 kg/m^2 (19.5 oz/yd^2) fabric and are referred to as Set 2A, and eight were made with 1.42 kg/m^2 (42 oz/yd^2) fabric and comprise Set 2B. The purpose of these mockups was to study the effect of the fabric weight on inspectability and defect detection. Set 2A was made with six layers (1 GFRP + 5 CFRP), and 2B was made with five layers (1 GFRP + 2 CFRP + 1 GFRP + 1 CFRP). The following defects were added to different layers: circular undersaturated dry spots of area 1 $in.^2$, 2 $in.^2$, 4 $in.^2$, 6 $in.^2$, and 10 $in.^2$, filled[4] and unfilled air bubbles (1.6 mm [0.063 in.] thick) of area 4 $in.^2$ and 10 $in.^2$, and a 30.5 cm × 30.5 cm (12 in. x 12 in.) overlap of CFRP fabric. Additionally, one mockup of set 2B (mockup #16) also had a filled air bubbles of 3.2 mm (0.125 in.) and 4.8 mm (0.188 in.) thick.

Table 5. Equivalent diameters of specified flaw areas.

Area ($in.^2$)	Diameter (in.)	Area (cm^2)	Diameter (cm)
1.0	1.1	6.5	2.9
2.0	1.6	12.9	4.1
4.0	2.3	25.8	5.7
6.0	2.8	38.7	7.0
10.0	3.6	64.5	9.1
16.0	4.5	103.2	11.5

PNNL borrowed 22 of the 24 EPRI mockups for NDE. Two mockups from Set 1 were excluded because they did not have GFRP layers as the base layer. Of the 22 mockups, 5 were selected

[4] A filled air bubble is an air bubble that has been repaired by filling with epoxy.

(Mockup 6 of Set 1, 2 of Set 2A, and 9, 10, and 14 of Set 2B) for testing at PNNL using automatic tap testing (ATT), manual tap testing (MTT) in ambient and simulated industrial noise conditions, and UT. These five mockups were chosen because it was believed that they represented the most difficult to detect defects of the available mockups and therefore could be used to test the limitations of the NDE approaches. The remaining 17 mockups were only manually tap tested under ambient laboratory noise conditions and industrial noise conditions. EPRI also performed NDE on their mockups; however, only the results of testing performed at PNNL are presented in this report. EPRI's results are presented separately in their own report (EPRI 2025).

3.6 Pipe Mockup

A CFRP pipe repair mockup was fabricated by Structural Technologies, Inc., and SGH, who were contracted by EMC^2 on a previous project funded by the NRC. The materials used and layup of the CFRP pipe repair were different from the plate mockups. The layup configuration for CFRP repair system was (1D+1H+1L+1W+1H), where dielectric (D) and watertightness (W) layers were bidirectional GFRP, and hoop (H) and longitudinal (L) layers were unidirectional CFRP. Putty was applied between each layer. The pipe had an outer diameter of 102 cm (40 in.), a wall thickness of 0.95 cm (0.375 in.), and was 122 cm (48 in.) long. The nominal CFRP repair thickness was 7.8 mm (0.308 in.), with a total length of 61 cm (24 in.). The pipe also had an internal composite repair where a 61 cm × 102 cm (12 in. × 24 in.) section of steel had been removed. This mockup was fabricated in 2021 and was subjected to hydrostatic pressure testing (Hioe et al. 2022, Hioe et al. 2021). The EMC^2 report states, "The failure mode for the full-scale hydrostatic test with CFRP repair was designated as a "leak" preceded by a significant matrix cracking noise." The mockup was later stored in an outdoor yard at EMC^2 and exposed to environmental conditions. The true state of damage/defects of this pipe is unknown.

PNNL contracted with Sonomatic to inspect the pipe with DRS. Figure 15 shows photographs of the mockup taken by Sonomatic, showing the inspection data on the long seam, the area of the missing steel with CFRP applied internally, and the internal view showing the expansion rings and rough epoxy. Figure 16 shows a CFRP debond from the steel pipe on the outer edge of the CFRP repair pipe mockup. Figure 17 shows the river-like matrix cracking on the CFRP repair pipe mockup after the hydrostatic pressure testing.

Figure 15. Photographs of the pipe mockup.

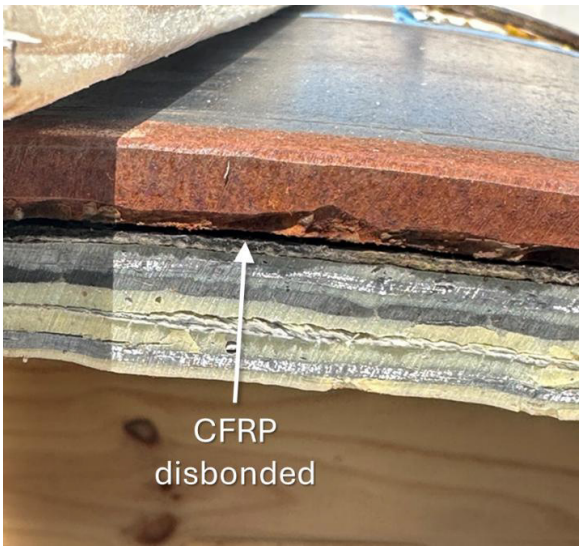

Figure 16. Disbonded CFRP region in the pipe mockup.

Figure 17. River-like matrix cracking on the CFRP pipe after hydrostatic testing. Images from Hioe et al. (2021).

4.0 Description of NDE Methods

4.1 Tap Testing

4.1.1 Manual

An aerospace tap hammer was used for MTT, as shown in Figure 18. It is a low-cost and easily deployable tool commonly used in the field. The inspector gently taps the test material repeatedly while moving the hammer across the test region in an approved inspection pattern. The inspector listens carefully to any changes in the acoustic response. If an anomalous response is heard, the inspector taps with finer spatial increments to better locate and size the indication. While the method is straightforward, it requires a trained inspector to interpret the audible responses to identify flaws accurately. MTT was performed in laboratory conditions at PNNL by a technician who is a formerly certified NDE inspector with qualification in manual tap testing. To better simulate field conditions, additional tests were performed with the ambient noise levels in the lab increased from 40 dB to 80 dB using pre-recorded industrial noise.[5]

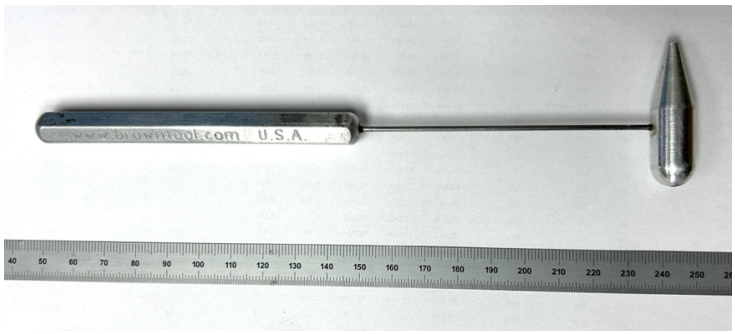

Figure 18. Manual tap hammer.

MTT was performed on the eight PNNL plate mockups and all of the EPRI plate mockups that were shipped to PNNL for analysis.

4.1.2 Woodpecker Automated Tap Tester

A Woodpecker WP-632AM-R (Figure 19) was loaned to PNNL from EPRI for ATT. The Woodpecker measures a ratio of the response in a test location to that of a reference location. Hence, results are objective and not dependent on the inspector's hearing abilities or ambient noise, although they do depend on an appropriately selected reference location. The Woodpecker records the measurement values but not the position. Software called XYplotter was provided by the vendor for position mapping; however, PNNL found the software was not helpful during their analysis, so position information was recorded manually.

The accuracy of the Woodpecker measurements depended on the angle at which it was held, so a fixture was 3-D printed to ensure it was consistently held at the correct angle. To obtain spatially consistent data that could be used to compare methods, a grid with 12.7 mm (0.5 in.) spacing was drawn on a transparent sheet and used as a guide, resulting in a spatial resolution of 12.7 mm × 12.7 mm (0.5 in. × 0.5 in.). A fence was clamped to the mockup to align the grid and help the inspector move the tap tester smoothly and precisely along a single grid row.

[5] 80 dB is roughly comparable to a kitchen garbage disposal, a vacuum cleaner, or heavy street noise.

The Woodpecker alerts the inspector to an indication visually (with two red lights and a yellow light) and audibly. Data were binned into one of four categories based on the Coefficient of Restitution (CoR) ratio (as shown in Table 6), which is the ratio of a measured CoR value to a reference value taken from a well-bonded and defect-free region. Unbonded or flawed regions should have a CoR less than that of the defect-free region, making the CoR ratio always ≤ 1. Results from Mockup 1 are shown in Figure 20. The true-state map was overlaid on the Woodpecker results. It appears that the circular dry spot in Q4 may have been detected, but indications of all other defects were either absent or ambiguous. Overall, there were many false calls and missed detections, and signal responses appeared to be essentially random. Note that the Woodpecker was designed primarily for inspection of thin composite laminates; results confirm that it was not appropriate for use on the thicker composites tested herein. Based on the initial results, use of the Woodpecker was discontinued in this study.

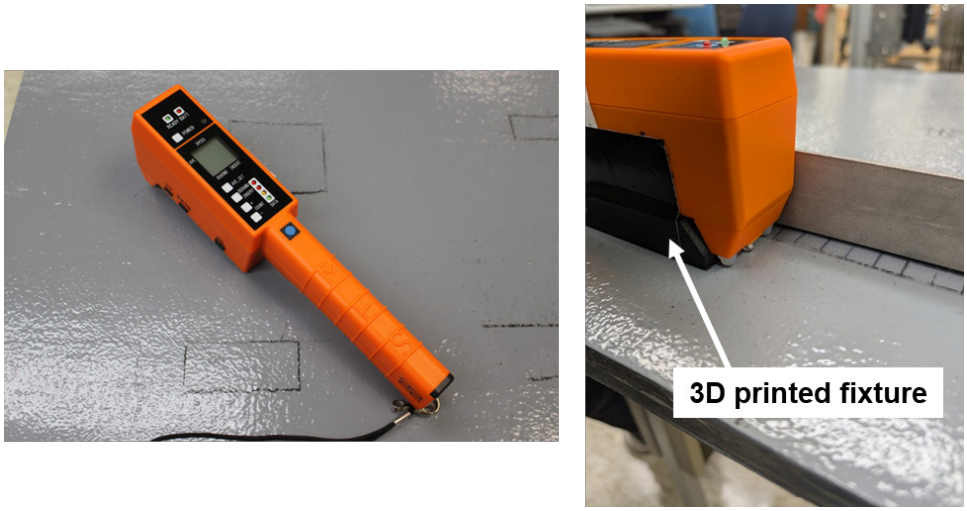

Figure 19. Woodpecker ATT.

Table 6. Color code for the different debond detections bins of the Woodpecker tap tester.

Color Code	Alerts	CoR ratio
A	Red1+Red2+Buzzer	0.3
B	Red2+Buzzer	0.5
C	Red1+Buzzer	0.75
D	Yellow	0.85

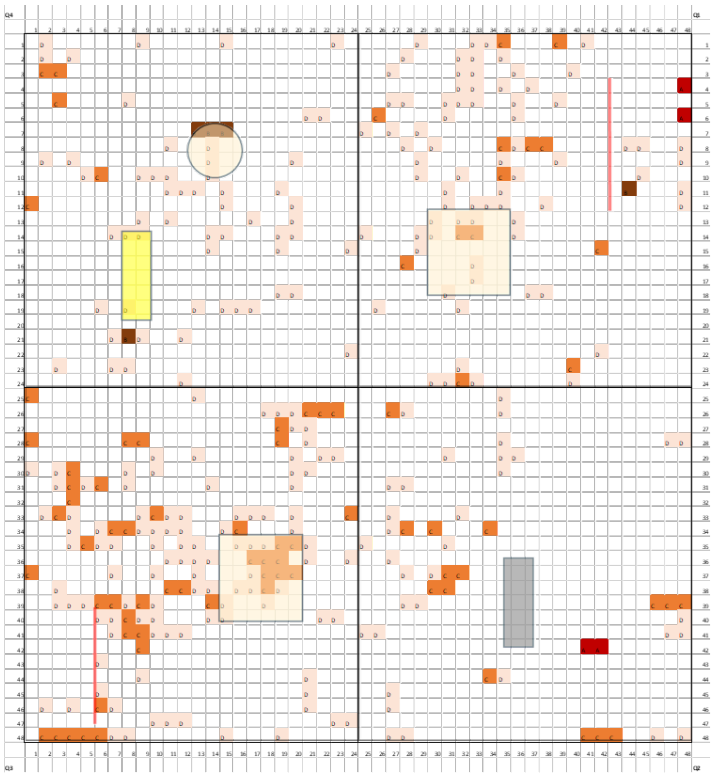

Figure 20. Woodpecker results on Mockup 1 based on the color code shown in Table 6. The intended true state (see Figure 5) is overlayed on the Woodpecker results.

4.1.3 EVOTIS Automated Tap Tester

A second ATT device was borrowed by PNNL from EPRI, an EVOTIS tap tester (see Figure 21). The EVOTIS is intended for use on thick composites. It measures both a piezoelectric and acoustic response and records the data digitally to a computer via a USB connection for real-time visualization. Figure 22 shows an example of recorded waveforms from one row of the grid; location information was recorded manually. These raw data required additional analysis in order to determine whether a defect was present.

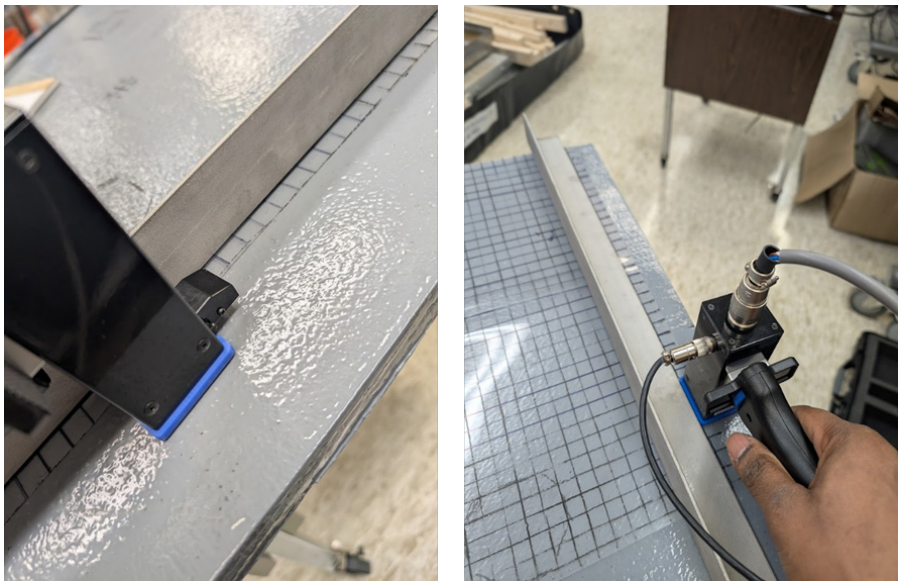

Figure 21. Tap testing a plate with the EVOTIS tap tester.

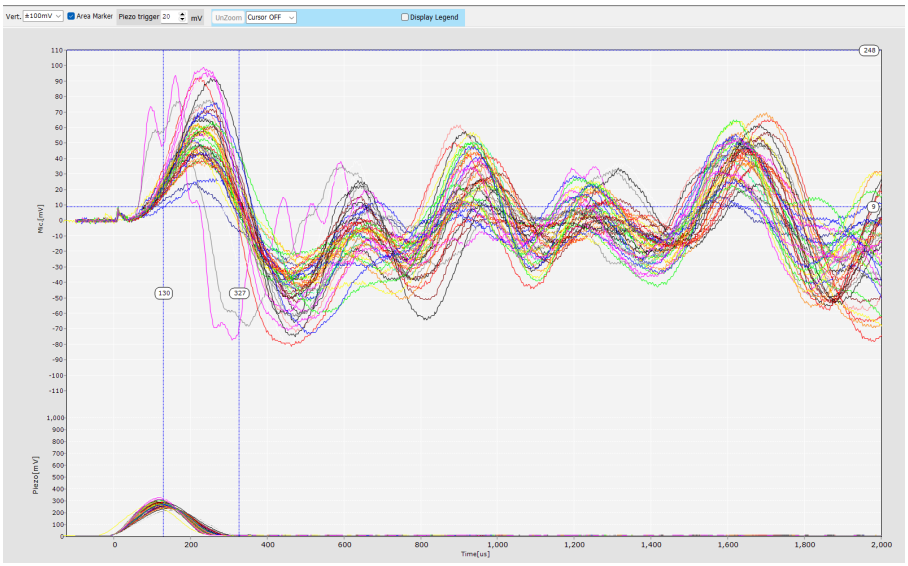

Figure 22. Example EVOTIS signal responses from one grid row.

PNNL analyzed the EVOTIS data using several methods that were then evaluated to decide which method provided the most sensitivity and most accurate results. These methods included basic frequency analysis, signal quality assessment, multi-scale decomposition (wavelet), audio-inspired features, and correlation analysis. A brief summary of these methods is given below. The value of some analysis methods was readily apparent, whereas others may contain information that is less obvious. To avoid spending too much time digging into analytical minutiae, a high-level analysis determined that the wavelet ratio spatial gradient (Figure 25) had the best performance in identifying the flaws. These data will be shown in this report.

1. Basic frequency analysis (Figure 23)
   - What it does: Converts time-based signal into frequencies (like a musical note analyzer)
   - Key outputs:
     - Peak frequency: The strongest frequency in the signal (like the main musical note)
     - Center frequency: The middle point of the active frequency range
     - Bandwidth: The range of frequencies in the signal (how “broad” the sound is)
   - Value: Identifies the main ultrasonic frequencies that interact with the material
   - Conclusion: Appears to be as sensitive or more sensitive to the natural resonances of the plate than to the defects

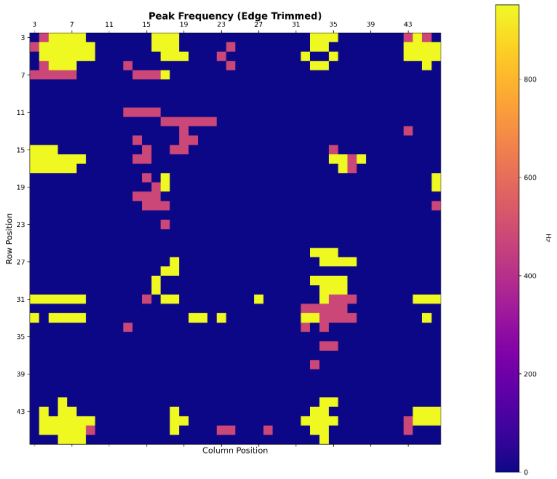

Figure 23. Peak frequency plot of Mockup 1.

2. Signal quality assessment (Figure 24)
   - What it does: Measures how clean and reliable the signal is
   - Key outputs:
     - Signal-to-noise ratio (SNR): Signal strength compared to background noise
     - Confidence score: Overall reliability of the frequency measurement (0 to -100%)
     - Parameters valid: Simple yes/no if measurements are within expected ranges
   - Value: Helps distinguish between reliable and unreliable measurements
   - Conclusion: Insensitive to defects and noisy

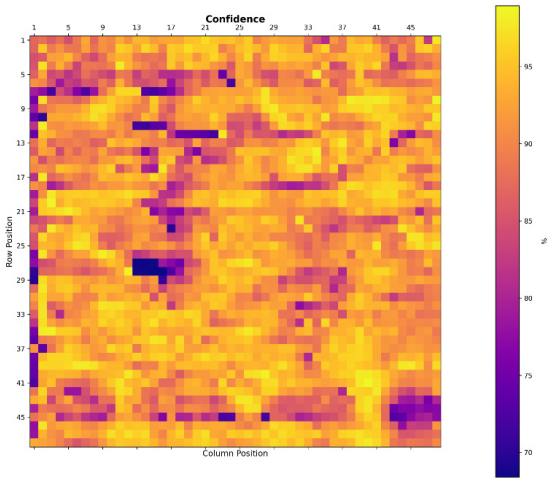

Figure 24. Confidence score plot of Mockup 1.

3. Multi-scale decomposition (wavelet) (Figure 25)
   - What it does: Breaks signal into different components (like separating bass, midrange, and treble in music) and compares the ratio of different components or the spatial gradient of the ratio
   - Key outputs:
     - Approximation energy: energy in the lowest frequencies
     - Detail 1 energy: energy in the highest frequencies
     - Detail 2 energy: energy in the medium-high frequencies
   - Value: Shows which frequency ranges contain most information about the material
   - Conclusion: Appears to be sensitive to defects, has a high contrast-to-noise ratio

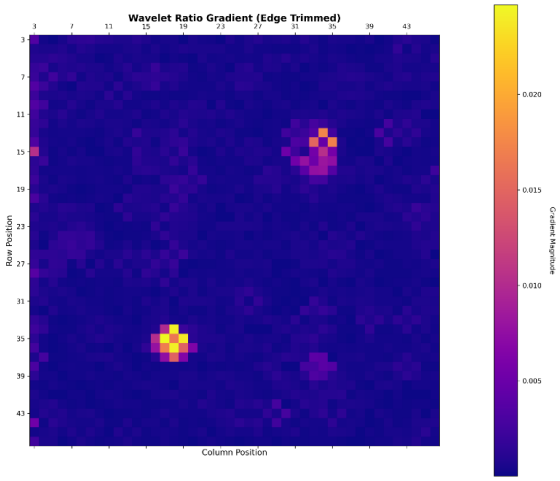

Figure 25. Wavelet ratio gradient plot of Mockup 1.

4. Mel frequency cepstral (MFC) coefficients (Figure 26)
   - What it does: Analyzes signal features and audio descriptors, such as “timbre,” using frequency analysis techniques (Abdul and Al-Talabani 2022)

- Key outputs:
  - MFC coefficients: Numerical values representing spectral patterns
- Value: Captures complex audio patterns that may indicate material properties
- Conclusion: Appears somewhat sensitive to defects but is noisy

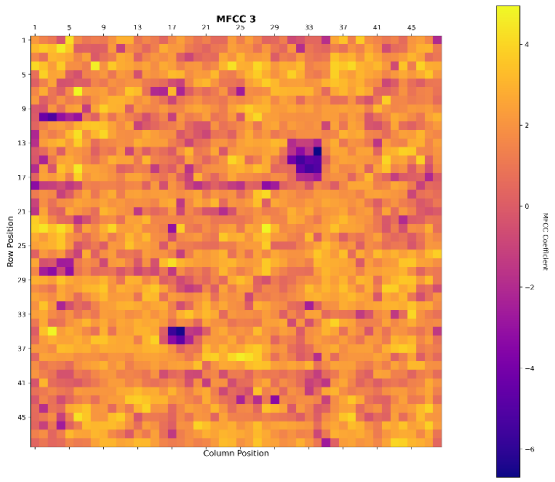

Figure 26. MFC coefficient plot of Mockup 1.

5. Correlation analysis (Figure 27)
   - What it does: Compares the microphone and piezo sensor readings
   - Key outputs:
     - Pearson correlation coefficient: How closely the two sensors' readings correlate (-1 to 1, with -1 being perfect negative correlation and +1 being perfect positive correlation)
   - Value: Shows how consistently material responds to acoustic testing using two different measurements
   - Conclusion: Less sensitive than other methods, some false signals

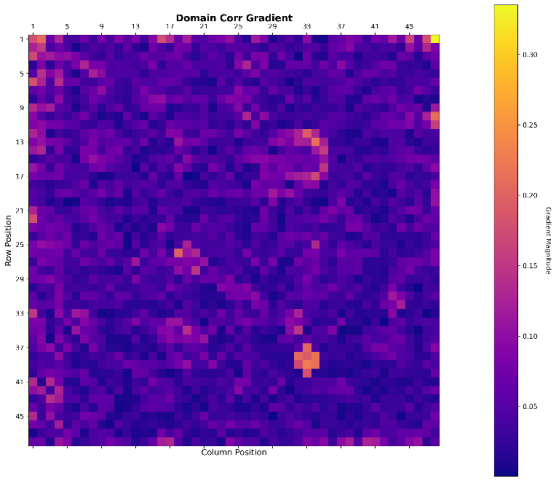

Figure 27. Pearson correlation analysis of Mockup 1.

Automated tap testing was done on the eight PNNL mockups and the five selected EPRI mockups.

4.2 Ultrasonic Testing

PNNL acquired spatially encoded data PE UT using a Zetec DYNARAY with a ZMC2 scanner and UltraVision3 software. The resolution in both the scan and index directions was 2.5 mm (0.1 in.). Probes were single element at frequencies of 0.5 MHz (Olympus V101, 25.4 mm [1.0 in.] diameter aperture) and 1 MHz (Krautkramer 389-057-070 BMC 12.7 mm [0.5 in.] diameter aperture with a 24.5 mm [1 in.] Rexolite delay line) using longitudinal waves and a 0° angle of incidence. Inspection frequencies were selected to optimize penetration and resolution. As shown in Figure 28, mockups were scanned in a basin with water used as the couplant to ensure effective ultrasonic wave transmission between the probe and mockups. Due to the size of the mockups, data were acquired by quadrant in four separate scans.

PE UT was performed on the eight PNNL mockups and the same five EPRI plates that were selected for ATT.

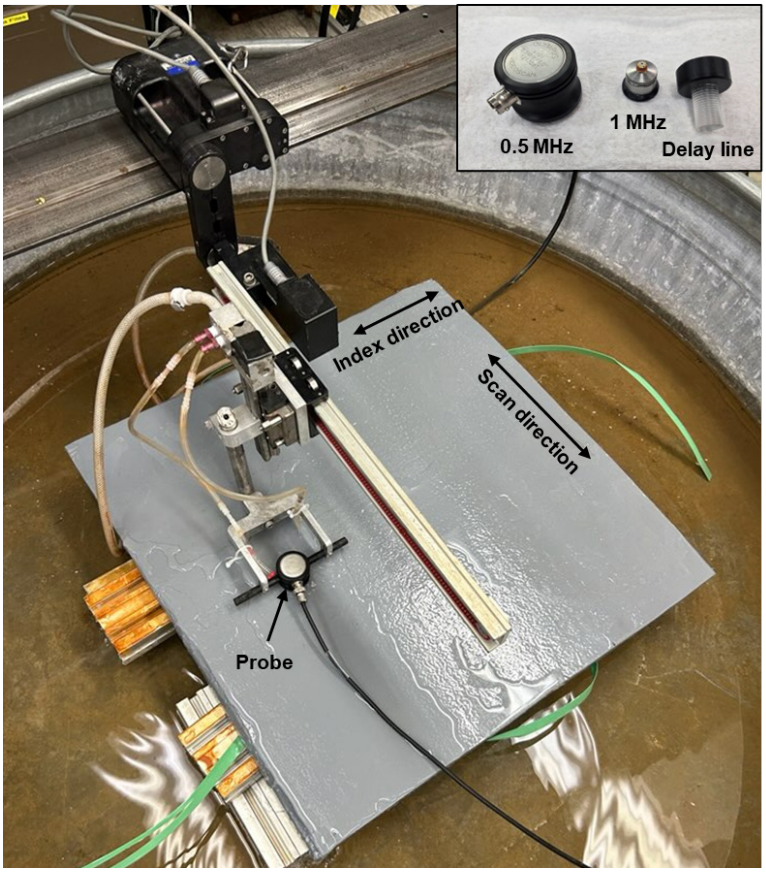

Figure 28. Photograph of a mockup during UT scanning. The inset shows the probes and delay line used.

4.3 DRS

DRS was performed on the eight PNNL mockups and the EPRI pipe mockup by Sonomatic, Ltd., at their facility in Mooresville, North Carolina. The methods used were largely proprietary, but some details were shared in a report provided to PNNL. They used “a range of low ultrasonic frequencies” from a probe “positioned several millimeters above the inspection surface.” The inspection resolution was 1 mm (0.04 in.) in the scan direction and 4 mm (0.16 in.) in the index direction, which “is suitable for detecting CFRP flaws with a diameter of 1/2” [12.7 mm] or larger.” “Advanced signal processing algorithms” were used to extract the results and construct a corrosion map of the steel substrate. Scans of the pipe mockup were completed on regions of the repairs; scans were not performed on the other regions or the expansion rings.

5.0 Results

5.1 PNNL Mockups

The subsections below show example NDE results from the PNNL mockups. These results were selected as representative and illustrative of detections, missed detections, and false calls. Results are summarized in Section 5.1.5, and full results are shown in Appendices D and E. Recall from Figure 5 that Q1 is the upper right quadrant, and numbering proceeds clockwise.

The intended true-states of the mockups' design were assumed as the actual true-states; however, unintended defects may be present and detected by the different NDE methods. Also, as discussed in Section 3.2, the resultant defects based on the intended characteristics may not meet the design criteria because of effects such as epoxy wicking, even though defect detection using some tested techniques was successful as will be discussed later in the document. Because the actual true-states were assumed, probability of detection was not calculated.

5.1.1 Manual Tap Testing

MTT succeeded at finding the dry spots in Mockups 1 through 3, but it struggled in Mockups 4 through 6, which used the thicker putty, and in Mockups 7 and 8, where the flaws were in the glass fiber layer. All the gaps, overlaps, and wrinkles were missed by MTT. As an example, Figure 29 shows the true-state map overlaid on the MTT results of Mockup 2. To show when an indication was detected by MTT, the grid square was filled black. All three dry spots were detected, and the indication sizes agreed well with the intended true-states. One indication in Q1 did not correspond to an intended defect.

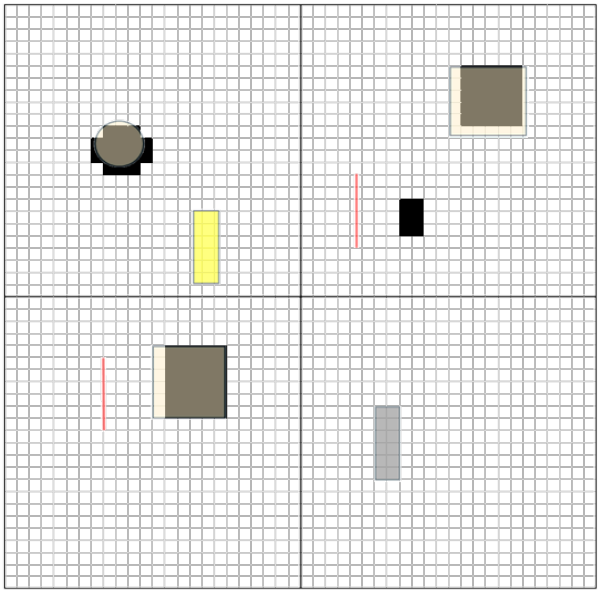

Figure 29. MTT results of Mockup 2 overlaid with true-state map. Filled grid squares show where indications were found.

Figure 30 shows results from Mockups 4 and 6, fabricated with the thick putty layers. Both show several false indications, and the sizes of the dry spots that were detected (in Q1 of Mockup 4 and Q3 of Mockup 6) did not agree well with the true-states.

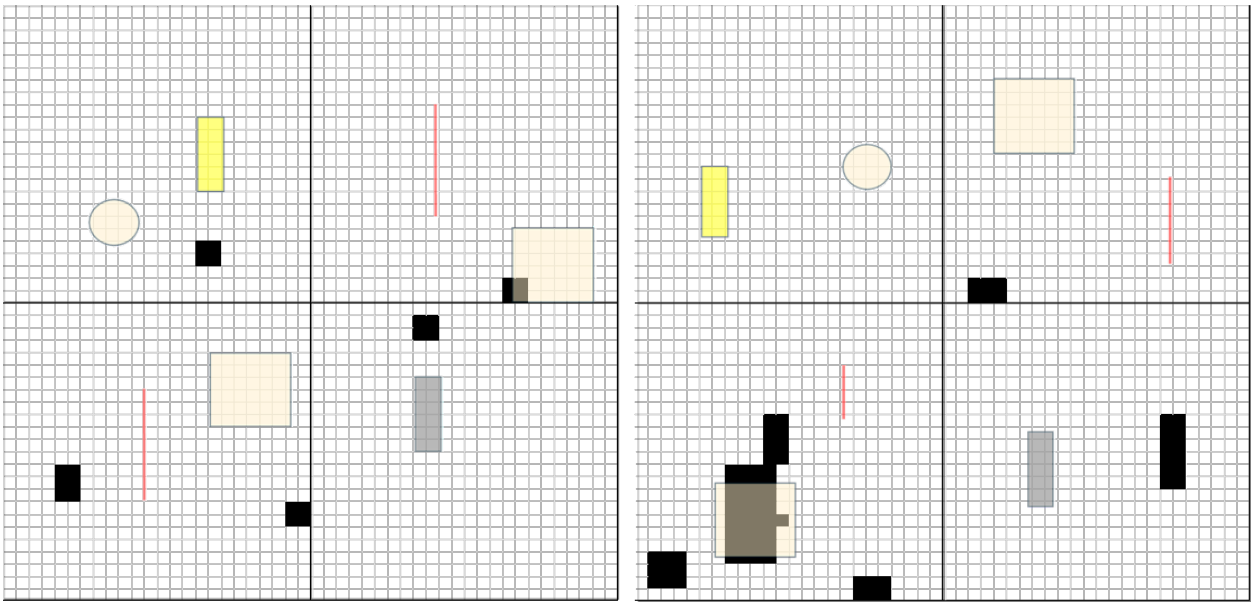

Figure 30. MTT results of Mockup 4 (left) and Mockup 6 (right).

5.1.2 Automated Tap Testing

ATT performed nearly identically to MTT; the only exceptions were two dry spots detected with MTT that were not detected with ATT. Figure 31 shows results from Mockup 3. The color scale in the figure indicates the strength of the measured wavelet ratio gradient; stronger indications appear orange and yellow against the purple background. The dry spot in Q4 was missed, and this mockup had a higher than usual amount of background noise.

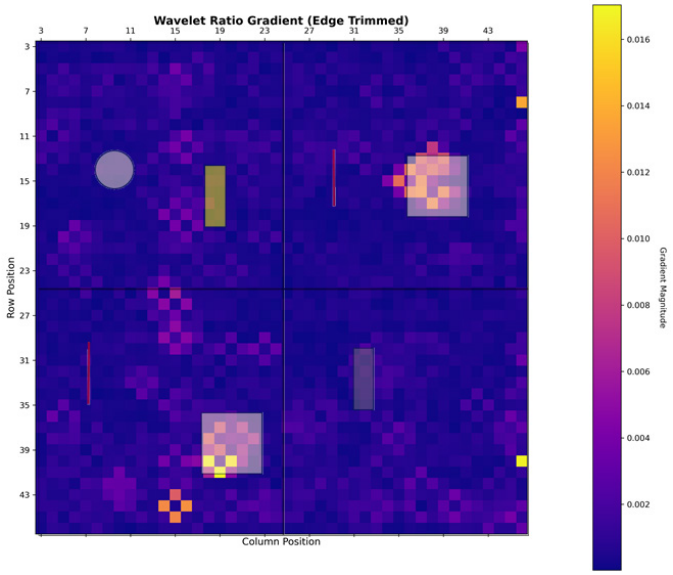

Figure 31. ATT results of Mockup 3.

Figure 32 shows examples from Mockups 4 and 6. There were essentially no indications in Mockup 4 except one near the edge in Q1. This indication was in the approximate vicinity of a dry spot and was credited as a detection, but the indication could have originated from an edge

effect (cf., Figure 31, which has a couple of small indications along the right edge). The ATT results of Mockup 6 were similar to those of the MTT, with one dry spot detected.

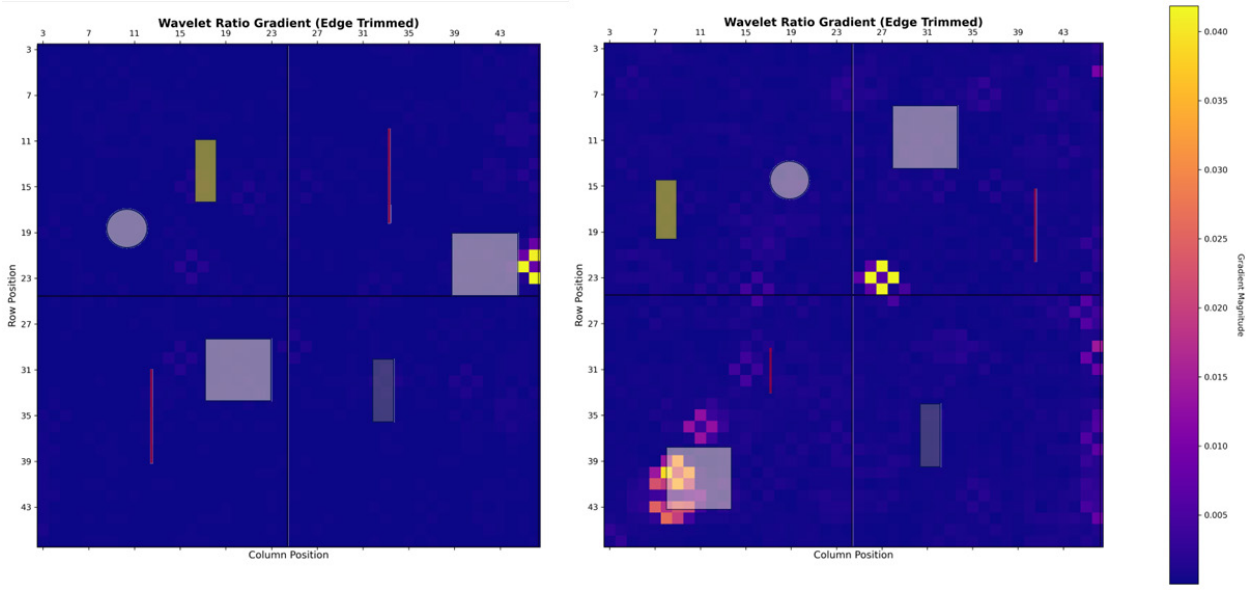

Figure 32. ATT results of Mockup 4 (left) and Mockup 6 (right).

Overall, MTT outperformed ATT for detection of dry spots, although ATT tended to have fewer false indications. MTT did not require a computer for data collection and analysis, so it is more readily deployable, but it does require significant inspector training and experience to distinguish the tap sound.

5.1.3 DRS

Overall, DRS significantly outperformed both ATT and MTT at dry spot detection, only missing three dry spots in the entire mockup set. However, DRS tended to have many additional indications, especially for Mockups 4 though 6 that used the thick putty. At this stage, without destructive testing, it is unclear if these additional indications are false calls or detections of unintended defects.

The DRS results were labeled with numbered indications; however, not every indication was numbered. It is unclear what criteria the vendor used to determine whether an indication was significant enough to warrant as a detection with a number. Figure 33 shows DRS results of Mockups 3 and 6 as examples; DRS was credited for detecting the three dry spots in Mocukup 3 (labeled 1, 2, and 3 in the DRS map) and the three dry spots in Mockup 6 (labeled 2, 3, and 12 in the DRS map). The average thickness of CFRP reported by Sonomatic for Mockups 1, 2, 3, and 7 (mockups with 0.79 mm [0.031 in.] thick putty) are 10.2 mm (0.40 in.), and for Mockups 4, 5, 6, and 8 (mockups with 3.18 mm [0.125 in.] thick putty) are 19.2 mm (0.76 in.). The intended sizes as per fabric dimensions and design for 0.0031 in. thick putty mockups are 0.464 in., and for 0.125 in. thick putty mockups are 1.1 in. The thicker CFRP repairs have more indications of defects.

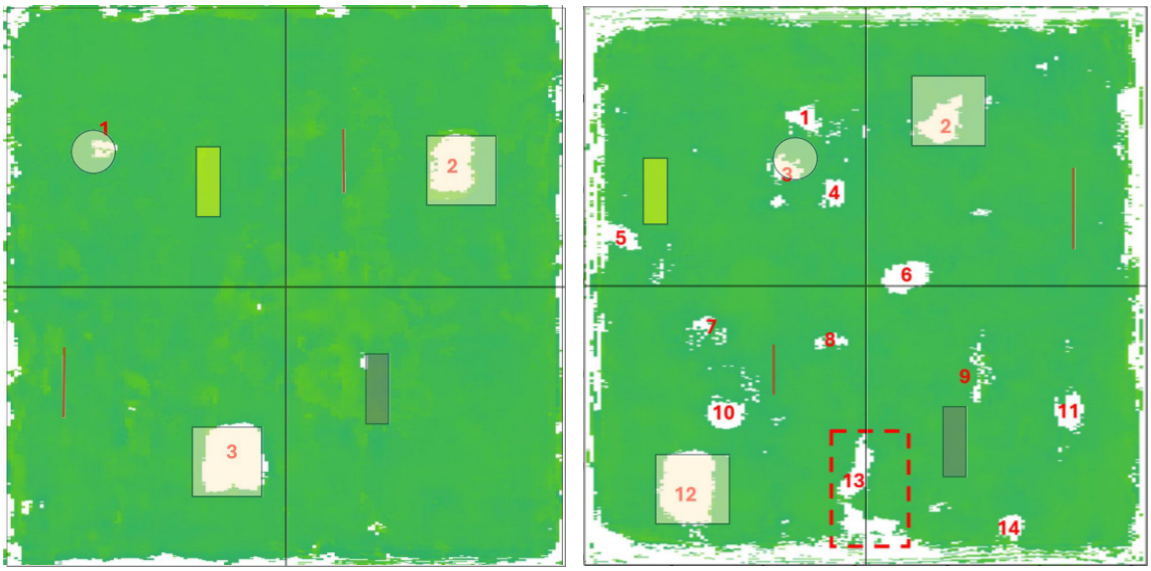

Figure 33. DRS results of Mockup 3 (left) and Mockup 6 (right). Indications numbered from left-to-right and top-to-bottom.

Note that indications in the same location as the indication labeled “6” in Figure 33 were also observed in the ATT and MTT data (see Figure 30 and Figure 32). It is likely an unintended disbond defect.

In Mockup 4 (Figure 34), DRS was credited with detecting two dry spots and a wrinkle in Q3. With all the additional indications in the DRS results, it is unclear if the wrinkle detection was accidental. The wrinkle in Q1 was not credited for detection because none of the white regions in labeled indication 2 overlapped with the actual wrinkle, and the major axis of the indication was not aligned to the orientation of the wrinkle.

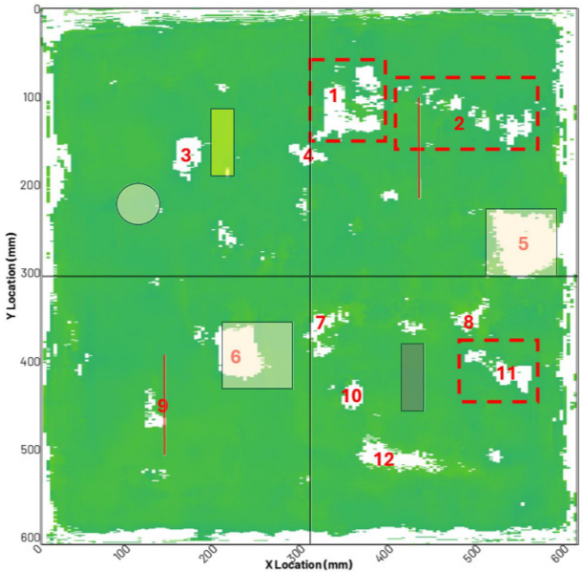

Figure 34. DRS results of Mockup 4.

5.1.4 Ultrasonic Testing

The UT at 1 MHz performed the best of all the methods tested. However, it should be noted that the UT data analysis was not performed blind; analysts knew the locations, types, and sizes of the defects. This project was to assess the ability of UT for finding defects, not to assess the analysts' abilities. UT images were strongly affected by the different laminae and putty. Dry spots were often characterized by strong echo signals in the layer and as a shadow (or lack of signal) in layers below the spot. Sometimes only one or the other was readily detectable. To further complicate analysis, the large aperture of the 0.5 MHz probe resulted in relatively poor spatial resolution and a "splotchy" image appearance. In some cases, when a detection was questionable, a "?" was used in the summary tables in Section 5.1.5.

Figure 35 shows a comparison of the 0.5 MHz (left) and 1.0 MHz data (right) from Q1 of Mockup 1. The light blue region (circled in black) is the shadow of the dry spot. Note the reduced resolution and splotchy appearance of the 0.5 MHz data are due to the large probe aperture. It is likely that some indication signals were lost in the background of the 0.5 MHz data, and, overall, it did not perform as well as the 1.0 MHz UT. Thus, additional 0.5 MHz UT results will not be shown. It is possible that using a delay line with the 0.5 MHz probe or using a focused 0.5 MHz probe may improve results; these approaches were not tested. The 1.0 MHz scan appears to also have echo signals from the wrinkle (circled in white), but the 0.5 MHz scan does not.

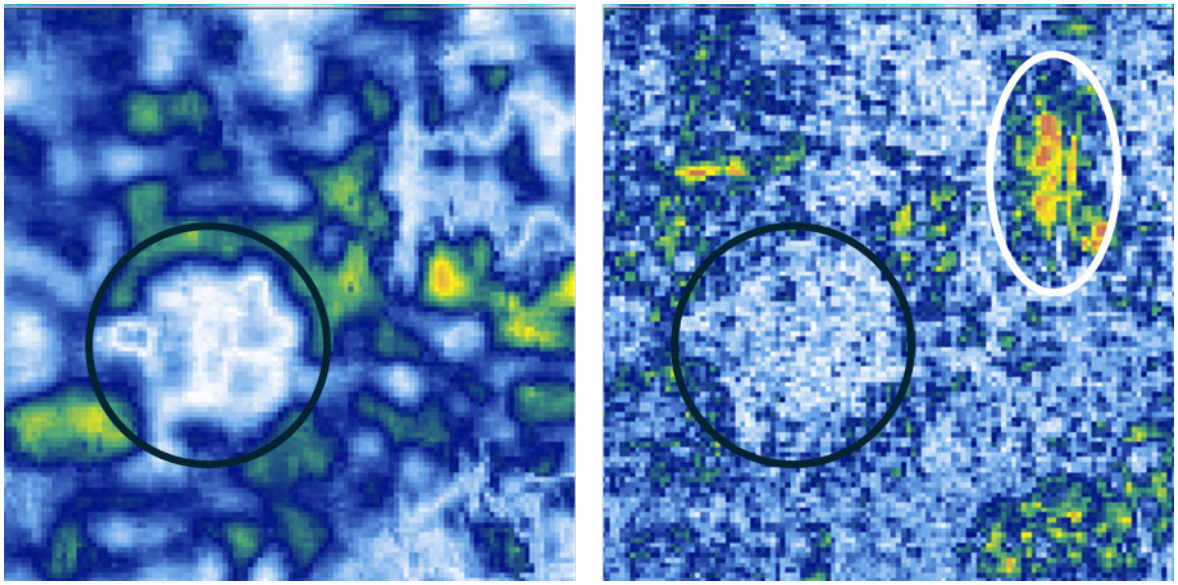

Figure 35. UT data at 0.5 MHz (left) and 1.0 MHz (right). The dry spot in Q1 of Mockup 1 is visible just below and to the left of center as a light blue circular region.

Figure 36 shows 1.0 MHz UT results of Mockup 2. There are several points to note about the figure. First, recall that the mockups were scanned by quadrant. Thus, they were analyzed by quadrant, resulting in the gating and software gains varying from quadrant to quadrant (e.g., Q3 appears light blue with low signal intensities while Q2 and Q4 are largely red with strong signals). Second, the scan region was slightly oversized for each quadrant to assure that there were no gaps between the scans. Thus, the sizing and placement of the true-state overlay is less precise than for the methods shown above. Finally, in quadrants with multiple defects, the defects were often detected with different gate (depth) settings, so they were not necessarily

captured in the same screenshot. In Figure 36, the three dry spots are visible (as shadows in Q1 and Q4), as are signal from the wrinkle in Q1 and the shadow of the overlap in Q2. The wrinkle in Q3 and the gap in Q4 were not detected.

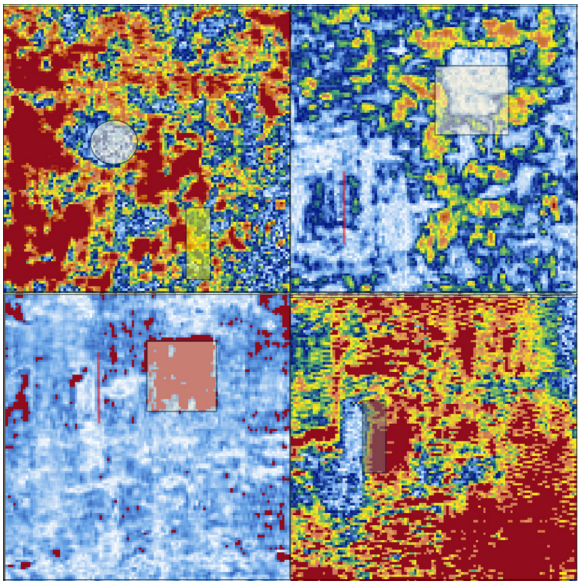

Figure 36. 1.0 MHz UT results of Mockup 2 overlaid with the true-state map.

As with the other methods, detection was more challenging in Mockups 4 through 6, with the thicker putty. There were several questionable indications and missed defects. Figure 37 shows the results from Mockup 6. The dry spot on Q1 was marked as questionable because, although enhanced signal was detected in the region, neither the signal intensity nor the shape of the indication was remarkable or convincing.

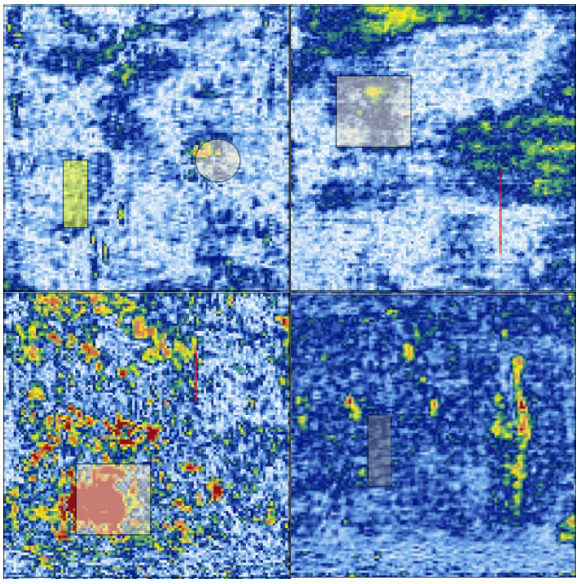

Figure 37. 1.0 MHz UT results of Mockup 6.

The UT and DRS testing on Mockups 7 and 8 did not reveal any remarkable results for the different surface preparation methods between Q3 and other quadrants, indicating that there

was no detectable disbond resulting from the different surface preparation in these mockups. This does not suggest that proper surface preparation is not important.

5.1.5 Results Summary

The tables below summarize the flaw detection results. Overall, the dry spots (Table 7) were readily detected by all methods in Mockups 1 through 3, with the exception of the spot in Q4 of Mockup 1, which was missed by ATT and MTT. In Mockups 4 through 6, with the thick putty, both tap methods struggled, and detection with UT was more challenging. As noted in Section 3.2, the square dry spot in Mockup 8 was saturated, so data were not recorded for it (marked with a "-" in the table).

Table 7. Summary of dry spot detection. "x" and "-" denote flaw detection and unrecorded data, respectively, while "space" denotes failure to detect flaws. Questionable detections are indicated using a question mark.

Mockup	Location (Ply-Quadrant-Size)	0.5 MHz UT	1.0 MHz UT	DRS	MTT	ATT
1	P2-Q1-9 $in.^2$	x	x	x	x	x
1	P4-Q3-9 $in.^2$	x	x	x	x	x
1	P5-Q4-3 $in.^2$	?	x	x		
2	P2-Q1-9 $in.^2$	x	x	x	x	x
2	P4-Q3-9 $in.^2$	x	x	x	x	x
2	P5-Q4-3 $in.^2$	x	x	x	x	x
3	P2-Q1-9 $in.^2$	x	x	x	x	x
3	P4-Q3-9 $in.^2$	x	x	x	x	x
3	P5-Q4-3 $in.^2$	x	x	x	x	
4	P2-Q1-9 $in.^2$		x	x	x	x
4	P4-Q3-9 $in.^2$	x	x	x		
4	P5-Q4-3 $in.^2$	x	x			
5	P2-Q1-9 $in.^2$	x	x	x		
5	P4-Q3-9 $in.^2$		x	x	x	
5	P5-Q4-3 $in.^2$	x	x	x		
6	P2-Q1-9 $in.^2$	x	?	x		
6	P4-Q3-9 $in.^2$	x	x	x	x	x
6	P5-Q4-3 $in.^2$	x	x	x		
7	P0-Q1-9 $in.^2$			x		
7	P0-Q1-3 $in.^2$					
8	P0-Q1-9 $in.^2$	-	-	-	-	-
8	P0-Q1-3 $in.^2$					

Detection of the gaps was very difficult with any method, but overlaps were detected with 1.0 MHz UT (Table 8). Several wrinkles were detected or possibly detected with 1.0 MHz UT, but all other methods struggled or missed the wrinkles entirely (Table 9).

Table 8. Summary of overlap and gap detection. Questionable detections are indicated using a question mark.

Plate	Location (Ply-Quadrant-type)	0.5 MHz UT	1.0 MHz UT	DRS	MTT	ATT
1	P3-Q2-Overlap	?	x			
1	P3-Q4-Gap	?				
2	P3-Q2-Overlap	?	x			
2	P3-Q4-Gap					
3	P3-Q2-Overlap		x			
3	P3-Q4-Gap					
4	P3-Q2-Overlap		x			
4	P3-Q4-Gap		?			
5	P3-Q2-Overlap	?	x			
5	P3-Q4-Gap		x	x		
6	P3-Q2-Overlap					
6	P3-Q4-Gap	?				

Table 9. Summary of wrinkle detection.

Plate	Location (Ply-Quadrant)	0.5 MHz UT	1.0 MHz UT	DRS	MTT	ATT
1	P1-Q1	x	x			
1	P3-Q3	x	x			
2	P1-Q1	?	x			
2	P3-Q3		x			
3	P1-Q1					
3	P3-Q3					
4	P1-Q1		x			
4	P3-Q3		x	x		
5	P1-Q1		x			
5	P3-Q3					
6	P1-Q1					
6	P3-Q3					

5.2 EPRI Mockups

The tables below summarize the NDE test results conducted on the five EPRI plates (refer to Table 5 for equivalent diameters and metric conversions). Overall, UT performed poorly on these mockups, with most of the delaminations detected at 500 kHz, only one air bubble detected, and none of the dry spots detected. The overlap was readily detected by UT. ATT and MTT performed well on the delaminations and air bubbles but poorly on the dry spots. Tap testing did not detect the overlap. When 80 dB of industrial noise was played in the lab space, the MTT missed two defects that were detected under ambient noise conditions. The defect layer "Base" refers to the base metal substrate (i.e., the defects are placed directly on top of the base layer). Layer 1 is the first GFRP layer for Set 1 and the first CFRP layer is numbered as 2. Other details about EPRI mockup fabrication are in Section 3.6.

Table 10. Summary of delamination detection.

Mockup Set	Mockup #	Defect Layer#	Size	1 MHz UT	500 kHz UT	ATT	MTT	MTT with Noise
1	6	Base	Small		x		x	
1	6	Base	Medium		x	x	x	x
1	6	1	Small			x	x	x
1	6	1	Medium			x	x	x
1	6	1	Small		x	x		
1	6	1	Medium		x	x	x	x
1	6	2	Small	?	x	x	x	x
1	6	2	Medium		x	x	x	x

Table 11. Summary of air bubble detection.

Mockup Set	Mockup #	Defect Layer#	Type and Size	1 MHz UT	500 kHz UT	ATT	MTT	MTT with Noise
2A	2	1	Unfilled 4 $in.^2$		?	x	x	x
2A	2	1	Filled 10 $in.^2$	?	?	x	x	x
2B	9	Base substrate	Unfilled 4 $in.^2$			x	x	x
2B	9	Base substrate	Filled 10 $in.^2$			x	x	x
2B	10	1	Unfilled 4 $in.^2$			x	x	x
2B	10	1	Filled 10 $in.^2$					
2B	14	1	Unfilled 10 $in.^2$	x		x	x	x
2B	14	1	Filled 10 $in.^2$					

Table 12. Summary of dry spot detection.

Mockup Set	Mockup #	Defect Layer#	Size	1 MHz UT	500 kHz UT	ATT	MTT	MTT with Noise
2A	2	2	1 in.^{2}					
2A	2	2	2 in.^{2}					
2A	2	2	4 in.^{2}					
2A	2	2	6 in.^{2}			x	x	x
2B	9	1	1 in.^{2}					
2B	9	1	2 in.^{2}					
2B	9	1	4 in.^{2}					
2B	9	1	6 in.^{2}					
2B	10	2	1 in.^{2}					
2B	10	2	2 in.^{2}			x	x	x
2B	10	2	4 in.^{2}				x	
2B	10	2	6 in.^{2}					
2B	14	2	10 in.^{2}			x	x	x

Table 13. Overlap detection.

Mockup Set	Mockup Plate #	Defect Layer#	Size	1 MHz UT	500 kHz UT	ATT	MTT	MTT with Noise
2B	14	4	12 in. × 12 in.	x	x			

For the remaining 17 plates examined only by MTT, one small and one medium delamination spot placed on the base layer were not detected in ambient conditions, while a total of six delamination spots were detected while testing under the industrial noise conditions. All air bubbles (unfilled) were detected by MTT in both conditions, but MTT detected only one filled air bubble 0.188 in. thick. Note that the air bubbles are filled with epoxy and therefore do not have a remarkable tap signature. Among the 35 dry spots in these 17 plates, 12 were not detected under ambient conditions, and 16 were not detected under the industrial noise conditions. The dry spots that were not detected were primarily 1 in.^{2} and 2 in.^{2}. Overlaps were not detected by the MTT testing. More details are provided in Appendix D, Table D.1 through Table D.4.

Table 14 summarizes the MTT results of all the EPRI plates tested at PNNL. Overall, playing industrial noise in the laboratory during MTT caused the inspector to miss 12% of the defects and 33% of the indications (which have potential to be unintended defects in mockups) that were detected under ambient noise conditions.

Table 14. Summary of MTT on EPRI mockups.

	Planned Defects	Total Indications Observed by MTT in Ambient Conditions	Total Indications Observed by MTT in Noise Conditions	Total Flaws Detected by MTT in Ambient Conditions	Total Flaws Detected by MTT in Noise Conditions
Set 1	32	40	27	29	24
Set 2A	42	55	38	28	25
Set 2B	42	37	23	17	14
Total	116	132	88	74	63

5.3 CFRP Pipe Mockup

The pipe mockup, described in Section 3.6, was inspected by Sonomatic from the inner surface using DRS. Figure 38 shows the DRS map. Two circumferential regions were not inspected because of the expansion rings, shown in Figure 15. Overall, the DRS results show that the CFRP was well bonded to the steel pipe. Sonomatic expressed that some areas of the epoxy surface were rough enough to prevent good contact with the scanning head, which resulted in some white pixels in the map that were not flagged as indications. Two large indications, labeled 1 and 2 in Figure 38, were identified.

Indication 1 is the missing steel area, but it also extends further in the circumferential direction than the actual defect. This suggests that delamination occurred during the hydrostatic pressure testing, as evidenced by the water leaking during the pressure tests. Indication 2 correlates to the CFRP disbond flaw identified by visual inspection, as shown in Figure 16, extending from 85 mm (3.35 in.) axially, touching the edge of pipe to 410 mm (16.1 in.) circumferentially. Note that the only other confirmed flaw identified in the EMC^2 report was river-like matrix cracking, as shown in Figure 17. This flaw lies within the area designated as Indication 1, where the metal substrate is absent. Consequently, a limitation of the DRS technique is evident: while it identifies debonding regions, it cannot detect flaws within the CFRP repair itself. This is because the methodology for DRS excites the steel substrate with a range of low ultrasonic frequencies and uses the response to determine thickness and thickness variations, further correlating it to a debond or defect. Hence, without a steel substrate as base, this DRS technology is not valid on the CFRP material alone. It only identifies a region as a flaw if the thickness of the metal substrate is not detected. Furthermore, CC N-871-1 focuses primarily on the terminal end region and requires only visual inspection of the remaining CFRP-repaired area. As a result, inservice defects, such as matrix cracking presented on the CFRP-repaired area (which are not terminal ends), will not be detected under current procedures and standards unless additional NDE techniques are employed.

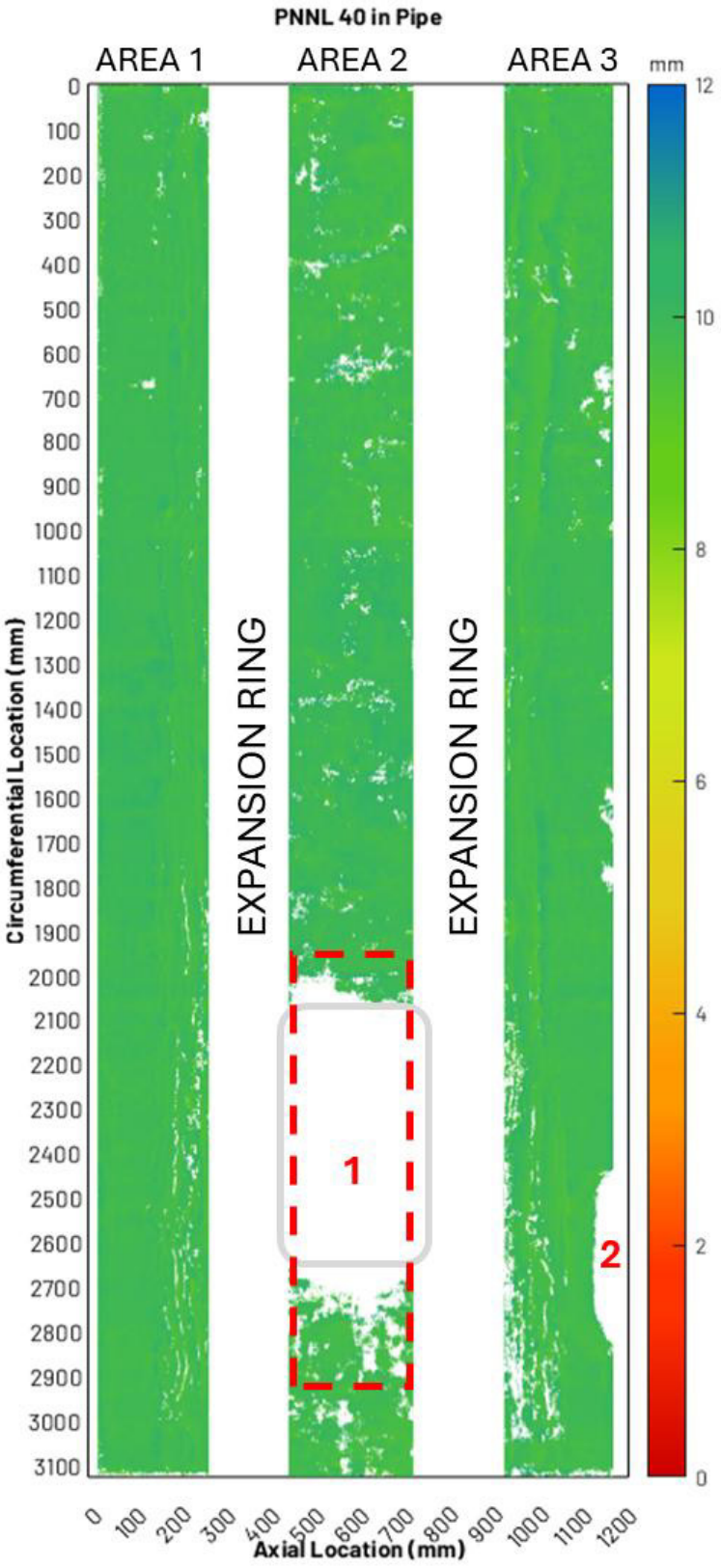

Figure 38. DRS map of the CFRP pipe mockup inspected internally.

6.0 Summary

This study evaluated the fabrication of CFRP repair mockups and the performance of several NDE methods to provide a technical basis for NRC review of requests for alternative using CFRP repairs, including those proposed under CC N-871-1. The work focused on fabrication variability, defect realism and control, and the capabilities and limitations of inspection techniques applied to representative repair configurations.

Mockup Fabrication

- Mockup fabrication was highly sensitive to material handling, cure timing, and installer skill, with small process variations producing meaningful differences in repair quality (Section 3.5).
- Variability in defect geometry and size in fabricated mockups raised concerns regarding the repeatability and consistency of qualification mockups. Control of fabrication of defects—particularly dry spots—was difficult, as resin bleed-in during saturation reduced intended defect size and altered the intended geometry (Sections 3.2 and 3.5).
- The layup process required careful control of epoxy and putty cure times; otherwise, gaps, uneven thickness, and embedded debris could result, and late corrective actions risked damaging the repair. Overall, CFRP repair quality was shown to be strongly process-dependent, consistent with issues identified during industry discussions (Section 2.2).
- Limited confidence in defect size control highlights the need for destructive validation to confirm true-state conditions in future studies.

NDE

- As per code case and EPRI TIE workshop, it was the consensus that defects of size greater than 2 in^2 should be detected and repaired. MTT and ATT were effective for detecting 3 in^2 dry spots in repairs with thin putty layers but performed poorly for thicker repairs and deeper defects. However, neither MTT nor ATT reliably detected gaps, overlaps, or wrinkles. Better MTT results suggest it has generally higher sensitivity than ATT but the whole process required significant inspector experience and was adversely affected by industrial noise, which reduced detection reliability (Section 5.0).
- DRS demonstrated higher sensitivity to dry spots than tap testing on PNNL mockups but produced numerous additional indications that could not be confirmed without destructive testing (Section 5.1.3).
- DRS inspection of the CFRP pipe mockup successfully identified disbond regions where the steel substrate was absent but did not detect internal CFRP damage, such as matrix cracking, highlighting a fundamental limitation of the technique (Section 5.3).
- Conventional UT, particularly at 1.0 MHz, demonstrated the strongest overall performance on PNNL mockups, detecting dry spots, overlaps, some wrinkles, and changes in surface preparation (Section 5.1.4).
- Results from EPRI flat-plate mockups inspected at PNNL demonstrated additional limitations (Section 5.2):
  - UT detected most delaminations only at 0.5 MHz, detected a single air bubble, and failed to detect dry spots, though overlaps were readily detected.

  - MTT and ATT performed well for delaminations and unfilled air bubbles but poorly for dry spots and did not detect overlaps or wrinkles.
  - In an environment with 80 dB industrial noise, MTT missed several defects detected under ambient conditions. Small dry spots (1 to 2 in.^{2}) and epoxy-filled air bubbles were frequently missed, regardless of noise conditions.
  - These results show that defect type, size, repair configuration, and inspection environment strongly influence inspection reliability.
- UT performance degraded with increasing putty thickness, defect depth, and laminate complexity, and data interpretation required significant expertise. UT and DRS were the only methods sensitive to deep defects.
- Putty thickness was the dominant parameter affecting defect detectability across all NDE methods; thicker epoxy layers significantly reduced inspection sensitivity.
- Although layer-by-layer inspections were not performed, the observed limitations of post-installation NDE suggest that inspection only after the repair is fully complete may be insufficient. Combining in-process and post-installation inspections may improve confidence in repair quality.

Remaining Gaps

The current work did not evaluate

- if nominally identical mockups could be fabricated to specification repeatedly and reliably,
- the fabrication of equivalent mockups by different vendors to assess consistency, or
- destructive testing to confirm defect size and NDE indications.

Additional studies focused on identifying critical defect sizes that affect structural performance, as well as on verifying whether available NDE methods can reliably detect those defects under worst-case repair configurations, may provide a stronger technical basis for NRC to review requests for alternatives and for industry to implement CFRP repair code cases.

Early findings already indicate that putty thickness plays a dominant role in defect detectability across all NDE methods, with thicker epoxy layers significantly diminishing inspection sensitivity.

Moreover, although layer-by-layer inspections were not conducted here, the limitations observed in post-installation NDE suggest that relying solely on inspections after the repair is fully complete may be insufficient; combining in-process and post-installation evaluations may improve confidence in repair quality.

Finally, while DRS exhibited greater sensitivity to dry spots than tap testing on the PNNL mockups, it also generated numerous additional indications that could not be verified without destructive examination, underscoring the need for further work to establish reliable confirmation pathways.

7.0 References

Abdul, Z. K., and A. K. Al-Talabani. 2022. Mel Frequency Cepstral Coefficient and Its Applications: A Review. *IEEE Access*, 10: 122136–122158. https://doi.org/10.1109/ACCESS.2022.3223444.

Alhamdan, H., F. A. Asfoor, A. Rehman, and R. Alhajri. 2019. "Techniques for Inspecting Wall Thickness Metal Loss of Pipelines Under Nonmetallic Sleeves." In *Proceedings of CORROSION 2019*, March 24–28, 2019, Nashville, Tennessee. https://doi.org/10.5006/MPWT19-14377.

Battley, M., A. Skeates, R. Simpkin, and A. Holmqvist. 2002. "Non-destructive Inspection of Marine Composite Structures." In High Performance Yacht Design Conference, Auckland, New Zealand, December 4–6, 2002. https://doi.org/10.3940/rina.ya.2002.26.

Bowkett, M., and K. Thanapalan. 2017. "Comparative Analysis of Failure Detection Methods of Composites Materials' Systems." *Systems Science & Control Engineering* 5 (1): 168–177. https://doi.org/10.1080/21642583.2017.1311240.

Breon, L., and M. Elen. 2024. "NDE Considerations for Carbon Fiber Reinforced Polymer (CFRP)." NRC Technical Information Exchange Meetings, January 23–25, 2024. NRC Accession # ML24026A103. https://www.nrc.gov/docs/ML2402/ML24026A103.pdf.

Chandarana, N., D. Martinez Sanchez, C. Soutis, and M. Gresil. 2017. "Early Damage Detection in Composites during Fabrication and Mechanical Testing." *Materials* 10 (7): 685. https://doi.org/10.3390/ma10070685.

Chen, J., Z. Yu, and H. Jin. 2022. "Nondestructive Testing and Evaluation Techniques of Defects in Fiber-reinforced Polymer Composites: A Review." *Frontiers in Materials* 9: 986645. https://doi.org/10.3389/fmats.2022.986645.

Concrete Repair Bulletin. 2008. "Restoration of Large Diameter Prestressed Concrete Cylinder Pipelines." November/December 2008: 45–47. https://www.icri.org/wp-content/uploads/2024/04/CRBNovDec08_ConcretePipeline.pdf.

Dominion. 2016. 09/07/2016 Pre-Submittal Meeting with Surry Power Station Regarding Carbon Fiber Reinforced Polymer Alternative Request. NRC Accession # ML16320A523. https://www.nrc.gov/docs/ML1632/ML16320A523.pdf.

Dunn, R. F. 2019. South Texas Project Unit 1 and 2, Proposed Alternative to ASME Boiler & Pressure Vessel Code Section XI Requirements for Repair/Replacement of Essential Cooling Water (ECW) System Class 3 Buried Piping in Accordance with 10 CFR 50.55a(z)(1). South Texas Project Nuclear Operating Co. NRC Accession # ML19274C393. https://www.nrc.gov/docs/ML1927/ML19274C393.pdf.

Elen, M., N. Conway, and A. Diaz. 2024. "Fabrication and NDE Analysis of CFRP Repair Mockups." NRC/Industry NDE Technical Information Exchange Public Meeting, January 23–25, 2024. PNNL-SA-194066. https://www.nrc.gov/docs/ML2402/ML24026A104.pdf.

Entergy Operations, Inc. 2020. Arkansas Nuclear One (ANO) Carbon Fiber Reinforced Polymer (CFRP) Relief Request Pre-Submittal Meeting with NRC – April 29, 2020. NRC Accession # ML20114E275. https://www.nrc.gov/docs/ML2011/ML20114E275.pdf.

EPRI. 2018. *Non-contact Nondestructive Evaluation Technology: Dynamic Response Spectroscopy and Pulsed Eddy Current.* EPRI Report 3002013174. Electric Power Research Institute. https://www.epri.com/research/products/000000003002013174.

EPRI. 2022. *Nondestructive Evaluation of Metallic Substrates through Carbon Fiber Reinforced Polymer (CFRP) Composite Repair Systems*. EPRI Report 3002020823. Electric Power Research Institute. https://www.epri.com/research/products/000000003002020823.

EPRI. 2025. *Nondestructive Evaluation Performance Characteristics for Carbon Fiber Reinforced Polymer Repair Structures*. EPRI Report 3002032154. Electric Power Research Institute. https://www.epri.com/research/programs/061154/results/3002032154.

Gaston, R. 2020. Arkansas Nuclear One, Unit 1 and Unit 2 – Proposed Alternative to ASME Boiler & Pressure Vessel Code Section XI Requirements for Repair/Replacement of Emergency Cooling Pond (ECP) Supply Piping in accordance with 10 CFR 50.55a(z)(1). Entergy Operations, Inc. NRC Accession # ML20218A672. https://www.nrc.gov/docs/ML2021/ML20218A672.pdf.

Gonzalez H J. 2024. Calvert Cliffs Nuclear Power Plant, Units 1 and 2 - Authorization and Safety Evaluation for Alternative Request ISI-05-021 (EPID L-2023-LLR-0006) - Non-Proprietary. NRC Accession # ML24059A063. https://www.nrc.gov/docs/ML2405/ML24059A063.pdf

Gerard, T. J., and T. T. Jimenez. 2015. “Brunswick Nuclear Plan Circulating Water Piping Discharge Headers Pressure Barrier Replacement Using Advanced Fiber Reinforced Polymer (FRP) Systems.” In SMiRT 2023 Conference Proceedings, Manchester, United Kingdom, August 10–14, 2015.

Helker, D. P. 2022. Calvert Cliffs Nuclear Power Plant, Units 1 and 2, Presentation Information for Pre-Submittal Meeting Regarding Relief Request To Use the Carbon Fiber Reinforced Polymer (CFRP) Composite System. Exelon Generation Co, LLC. NRC Accession # ML22013A394. https://www.nrc.gov/docs/ML2201/ML22013A394.pdf.

Helker, D.P. 2024. Calvert Cliffs Nuclear Power Plant, Units 1 and 2, Proposed Alternative to the Requirements for Repair/Replacement of Saltwater (SW) System Buried Piping. NRC Accession # ML24011A073. https://www.nrc.gov/docs/ML2401/ML24011A073.pdf

Hioe, Y., P. Krishnaswamy, F. Orth, S. Pothana, L. Smith, and M. Uddin. 2021. *Task-3: Mockup Testing and Physical Evaluation of Proposed Carbon Fiber Reinforced Polymer Repair*. Engineering Mechanics Corp of Columbus and the Nuclear Regulatory Commission. NRC Accession # ML21126A334. https://www.nrc.gov/docs/ML2112/ML21126A334.pdf.

Hioe, Y. P. Krishnaswamy, B. Lin, F. Orth, S. Pothana, L. Smith, and M. Uddin. 2022. *EMC2-NRC-CFRP Durability Testing TLR Final, Evaluation Of Factors Affecting Durability Of Carbon Fiber Reinforced Polymer Composite Repairs - Single-Ply Laminate Study*. Engineering Mechanics Corp of Columbus and the Nuclear Regulatory Commission. NRC Accession # ML22118A351. https://www.nrc.gov/docs/ML2211/ML22118A351.pdf.

Jodhani, J., A. Handa, A. Gautam, Ashwni, and R. Rana. 2023. “Ultrasonic Non-destructive Evaluation of Composites: A Review.” *Materials Today: Proceedings* 78 (Part 3): 627–632. https://doi.org/10.1016/j.matpr.2022.12.055.

Krautkrämer, J., H. Krautkrämer. 2013. *Ultrasonic Testing of Materials*. Springer Science & Business Media, pp. 18-23.

Lee, R., S. Burch, and M. Wall. 2012. "PRCI Project NDE 2-3 NDE & Inspection Techniques Applied to Composite Wrap Repairs (PRCI Project No. PR-398-113705)." 2nd Annual Composite Repair Users Group. Houston, Texas.

NRC. 2023. Advisory Committee on Reactor Safeguards – Fuels, Materials, and Structures Subcommittee. Official Transcript of Proceedings, October 18, 2023. Nuclear Regulatory Commission. NRC Accession # ML23325A021. https://www.nrc.gov/docs/ML2332/ML23325A021.pdf.

O'Sullivan, J. 2020. "Code Case N-871-1: Status Update." Electric Power Research Institute, NRC Technical Exchange Meeting in Rockville, Maryland on January 16, 2020. NRC Accession # ML20014E606. https://www.nrc.gov/docs/ML2001/ML20014E606.pdf.

Olshan, L. N. 2008. Oconee, Units 1, 2, and 3, Issuance of Amendments Regarding Use of Fiber-Reinforced Polymer (FRP) (TAC NOS. MD2129, MD2130, MD2131). Letter and amendments from L. N. Olshan, NRC/NRR/ADRO/DORL/LPLII-1, to B. H. Hamilton, Duke Power Co. NRC Accession # ML080320065. https://www.nrc.gov/docs/ML0803/ML080320065.pdf.

Panagiotis, C. J. 2024. "Theoretical Review for Non-Destructive Techniques of Composite Materials." *International Research Journal of Advanced Engineering and Science* 9 (2): 127–136.

Pridmore, A. B., R. Ojdrovic, and M. Geraghty. 2014. "Fifteen Years of Lessons Learned: Design and Construction of CFRP Liners for Large-Diameter Pipelines." *Pipelines 2014: From Underground to the Forefront of Innovation and Sustainability*, 1578-1591. https://doi.org/10.1061/9780784413692.143.

QuakeWrap, Inc. 2009. Project Overview: Repair & Strengthening of PCCP Concrete Pipe with Carbon FRP. https://quakewrap.com/project_sheets/Repair%20and%20Strengthening%20of%20PCCP%20Concrete%20Pipe%20with%20Carbon%20FRP.pdf.

Ramirez, A., and A. D. Veil. 2025. DPO Case File: DPO-2022-002 – Redacted-Public. Nuclear Regulatory Commission/Nuclear Reactor Regulation. NRC Accession # ML25002A153. https://www.nrc.gov/docs/ML2500/ML25002A153.pdf.

Ramli, S. H. M., R. Arifin, and H. Chik. 2020. "Composite Repairs Integrity Assessment: An Overview of Inspection Techniques." *Pertanika Journal of Science and Technology* 28 (S1): 151–158.

Roach, D. 2015. *A Quantitative Assessment of Conventional and Advanced Nondestructive Inspection Techniques for Detecting Flaws in Composite Honeycomb Aircraft Structures*. DOT/FAA/TC-15/63. Albuqurque: Sandia National Laboratories for Federal Aviation Administration. https://rosap.ntl.bts.gov/view/dot/57662.

Roach, D., and L. Dorrell. 1999. *Development of Composite Honeycomb and Solid Laminate Reference Standards to Aid Aircraft Inspections*. SAND99-0540J. Albuquerque: Sandia National Laboratories. https://www.osti.gov/servlets/purl/4187.

Roach, D., L. Dorrell, L., J. Kollgaard, and T. Dreher. 1998. *Improving Aircraft Composite Inspections Using Optimized Reference Standards*. SAND-98-2022C. https://www.osti.gov/biblio/674592.

Sartain, M. 2016. Surry Power Station Units 1 and 2, Proposed Alternative to ASME Section XI Requirements for Repair/Replacement of Circulating and Service Water Class 3 Buried Piping In Accordance with 10 CFR 50.55a(Z)(1). Nuclear Regulatory Commission. NRC Accession # ML16355A346. https://www.nrc.gov/docs/ML1635/ML16355A346.pdf.

Sharma, R. S., and M. N. Vijayakumar. 2023. "Recent Developments in Damage Detection of CFRP Composites Using Non-destructive Techniques – A Review." *Journal of Engineering Research and Reports* 25 (4): 51–65. https://doi.org/10.9734/jerr/2023/v25i4902.

Stang, J. F. 2011. Oconee Nuclear Station, Units 1, 2, and 3, License Amendments, Authorizing Change to the UFSAR Allowing Use of Fiber Reinforced Polymer on Masonry Brick Walls for the Mitigation of Differential Pressure Created by High Winds-TAC ME1710-ME171. Letter and license amendments from J. F. Stang, NRC/NRR/DORL/LPLII-1, to P. T. Gillespie, Duke Energy Carolinas, LLC. NRC Accession # ML11164A257. https://www.nrc.gov/docs/ML1116/ML11164A257.pdf.

Structural. n.d. Pipeline Repairs at Hope Creek Nuclear Generating Station. Accessed Nov. 20, 2025, at https://www.structural.net/case-studies/pipeline-repairs-at-hope-creek-nuclear-generating-station/.

Tai, J. L., M. T. H. Sultan, A. Łukaszewicz, J. Józwik, Z. Oksiuta, and F. S. Shahar. 2025. "Recent Trends in Non-Destructive Testing Approaches for Composite Materials: A Review of Successful Implementations." *Materials* 18 (13): 3146. https://doi.org/10.3390/ma18133146.

Vaara, P., and J. Leinonen. 2012. "Technology Survey on NDT of Carbon-fiber Composites." Kemi-Tornio University of Applied Sciences, ISSN 1799-2834. https://www.theseus.fi/bitstream/handle/10024/54515/vaara%20leinonen%20B%208%202012.pdf.

Wang, B., P. He, Y. Kang, J. Jia, X. Liu, and N. Li. 2022. "Ultrasonic Testing of Carbon Fiber-reinforced Polymer Composites." *Journal of Sensors* 2022 (1): 5462237. https://doi.org/10.1155/2022/5462237.

Weitzenböck, J., A. Echtermeyer, P. Grønlund, F. Artiga-Dubois, and M. Parmar. 1999. "Nondestructive Inspection and Evaluation Methods for Composites Used in the Marine Industry." In 12th International Conference on Composite Materials (ICCM-12). Paris, France.

Appendix A – Fabrication of CFRP Mockups

A.1 Preparation of Thickened Epoxy

The putty used in the CFRP mockup fabrication process (130N Tack) has 6.3% of fumed silica with other proprietary components. However, the percentage of fumed silica varies between different CFRP manufacturers, and it is also varied depending on the weight of the fabric. In order to have this percentage of fumed silica as a variable, an additional 2% or 4% (by weight) was added to the 130N to achieve 8.3% and 10.3%. The fumed silica was mixed well with the 130N tack coat and stirred thoroughly, as shown in Figure A.1.

Figure A.1. Preparation of thickened epoxy.

A.2 Saturation of Fabric

The fabric saturation was achieved by mixing the two-part epoxy and hardener in the appropriate ratio, as specified by the manufacturer and shown in Figure A.2. It was thoroughly mixed and manually applied to the fabric. The fabric was weighed to ensure the fiber-matrix ratio met design criteria and any additional epoxy was removed.

Figure A.2. Manual saturation of fabric.

A.3 Dry Spots in Mockup 7 and 8

As mentioned in Section 3.2, the 9 in.^{2} dry spot in Mockup 8 was completely saturated, as shown in Figure A.3. Hence, this defect was not considered in the analysis, as per Table 7.

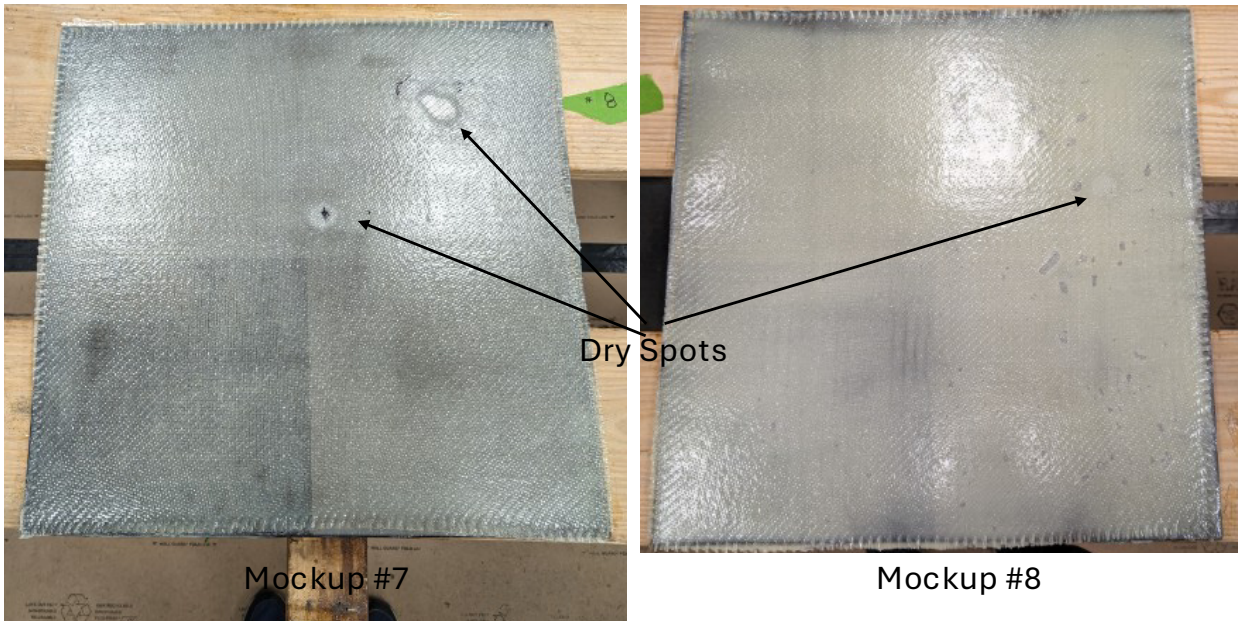

Figure A.3. Comparison of Mockup 7 and Mockup 8 dry spots.

Appendix B – Mockup Design

The tables and figures in this appendix show the planned placement of flaws in the CFRP repair mockups. The color scheme in the figures follows that of Figure 5. Flaw sizes and locations in the figures are approximate.

Table B.1. Plate 1

130N 6.3% (no additional fumed silica) tack coat on primer and between each layer		
1/16" notched trowel for the 130N		
FG Layer	No Defects	
CF1	Q1 – 2 in. to 3 in. wrinkle	21 in. right, 1.5 in. to 6 in. down
CF2	Q1 – Dry spot (3 in. x 3 in. square)	14.5 in. to 17.5 in. right and 6 in. to 9 in. down
CF3	Q2 – 3 in. x 1 in. overlap	17.25 in. to 18.25 in. right and 17.75 in. to 20.75 in. down
	Q3 – 2 in. to 3 in. wrinkle	2.5 in. right and 19.5 in. to 23.5 in. down
	Q4 – 3 in. x 1 in. gap	3.5 in. to 4.5 in. right and 6.75 in. to 9.75 in. down
CF4	Q3 – Dry spot (3 in. x 3 in. square)	7 in. to 10 in. right and 17 in. to 20 in. down
CF5	Q4 – Dry spot (3 $in.^2$ circle)	7.375 in. right and 4 in. down to center
CF6	No Defects	

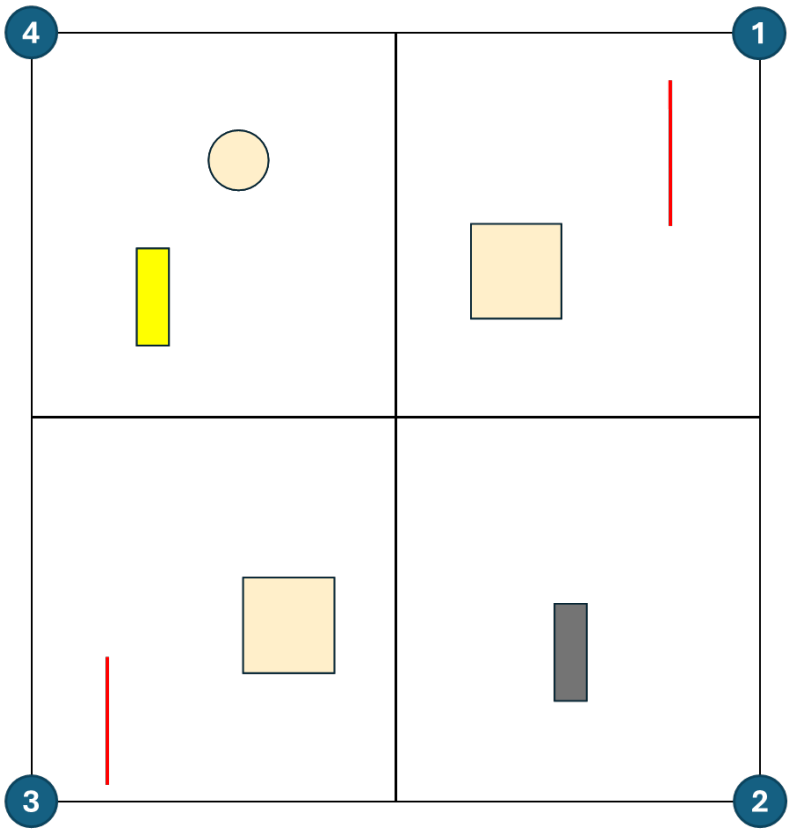

Figure B.1. Plate 1.

Table B.2. Plate 2.

130N 8.3% (additional 2% fumed silica) tack coat on primer and between each layer		
1/16" notched trowel for the 130N		
FG Layer	No Defects	
CF1	Q1 – 2 in. to 3 in. wrinkle	14.25 in. right and 7 in. to 9.5 in. down
CF2	Q1 - Dry spot (3 in. x 3 in. square)	18 in. to 21 in. right and 2.5 in. to 5.5 in. down
CF3	Q2 – 3 in. x 1 in. overlap	15 in. to 16 in. right and 16.5 in. to 19.5 in. down
	Q3 – 2 in. to 3 in. wrinkle	4 in. right and 14.5 in. to 17 in. down
	Q4 – 3 in. x 1 in. gap	7.625 in. to 8.75 in. right and 8.5 in. to 11.5 in. down
CF4	Q3 – Dry spot (3 in. x 3 in. square)	6 in. to 9 in. right and 14 in. to 17 in. down
CF5	Q4 – Dry spot (3 $in.^2$ circle)	5 in. right and 5.75 in. down to center
CF6	No Defects	

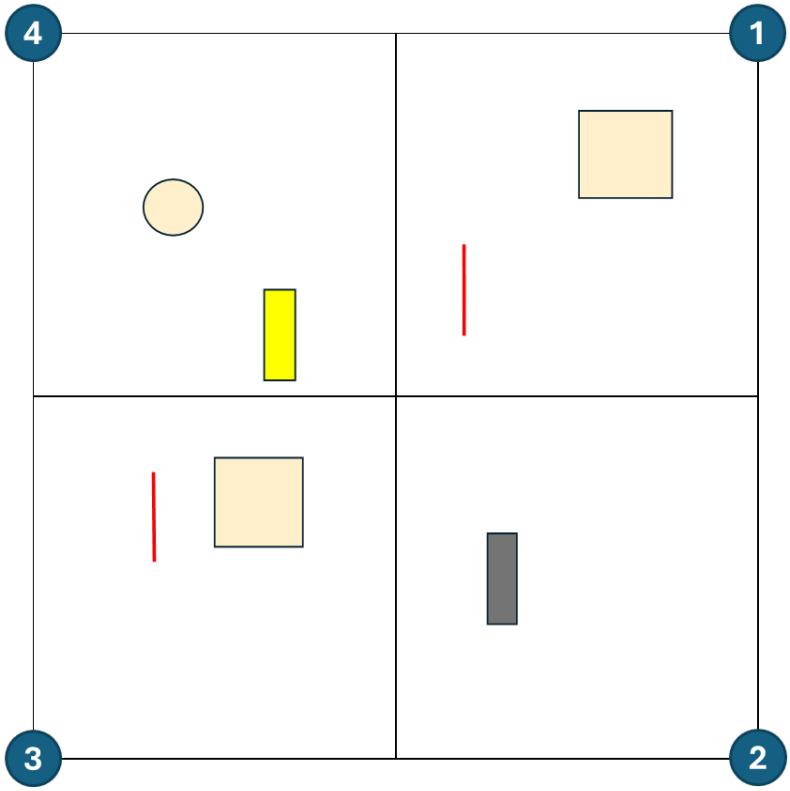

Figure B.2. Plate 2.

Table B.3. Plate 3.

130N 10.3% (additional 4% fumed silica) tack coat on primer and between each layer		
1/16" notched trowel for the 130N		
FG Layer	No Defects	
CF1	Q1 – 2 in. to 3 in. wrinkle	14.5 in. right and 5 in. to 7.5 in. down
CF2	Q1 – Dry spot (3 in. x 3 in. square)	18 in. to 21 in. right and 5.5 in. to 8.5 in. down
CF3	Q2 – 3 in. x 1 in. overlap	15.75 in. to 16.75 in. right and 14.75 in. to 17.625 in. down
	Q3 – 2 in. to 3 in. wrinkle	2.5 in. right and 14.5 in. to 17.5 in. down
	Q4 – 3 in. x 1 in. gap	8.375 in. to 9.375 in. right and 6 in. to 9 in. down
CF4	Q3 – Dry spot (3 in. x 3 in. square)	8 in. to 11 in. right and 18 in. to 21 in. down
CF5	Q4 – Dry spot (3 $in.^2$ circle)	4 in. right and 6.25 in. down to center
CF6	No Defects	

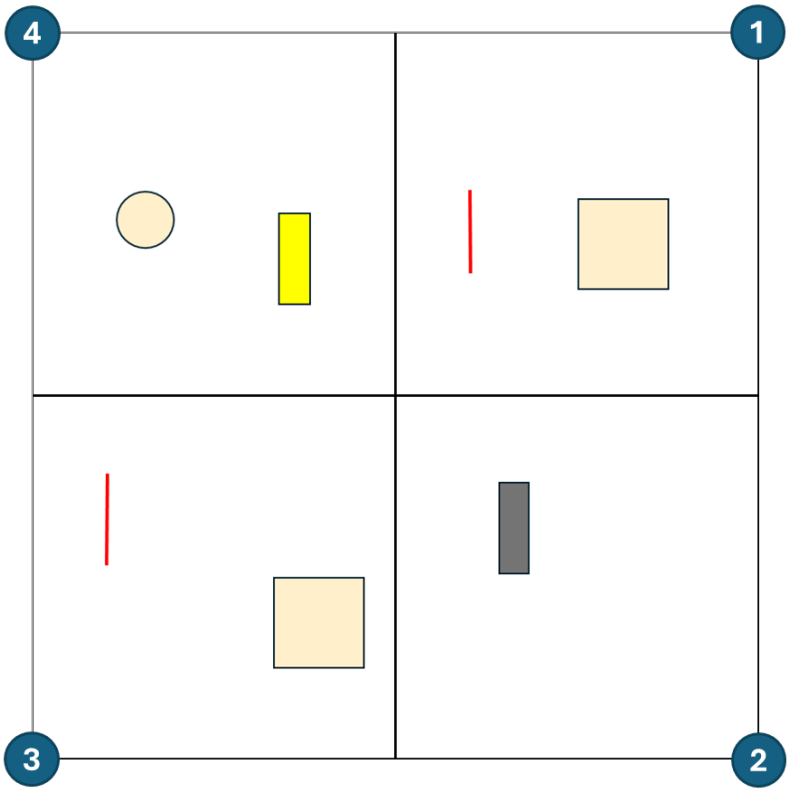

Figure B.3. Plate 3.

Table B.4. Plate 4.

130N 6.3% (no additional fumed silica) tack coat on primer and between each layer		
1/4" notched trowel for the 130N		
FG Layer	No Defects	
CF1	Q1 – 2 in. to 3 in. wrinkle	16.75 in. right, 4 in. to 8.5 in. down
CF2	Q1 – Dry spot (3 in. x 3 in. square)	19.75 in. to 22.75 in. right and 9 in. to 12 in. down
CF3	Q2 – 3 in. x 1 in. overlap	16 in. to 17.375 in. right and 15 in. to 18 in. down
	Q3 – 2 in. to 3 in. wrinkle	5.5 in. right and 15.5 in. to 19.75 in. down
	Q4 – 3 in. x 1 in. gap	7.5 in. to 8.5 in. right and 4.5 in. to 7.5 in. down
CF4	Q3 – Dry spot (3 in. x 3 in. square)	8 in. to 11 in. right and 14 in. to 17 in. down
CF5	Q4 – Dry spot (3 $in.^2$ circle)	4 in. right and 8.75 in. down to center
CF6	No Defects	

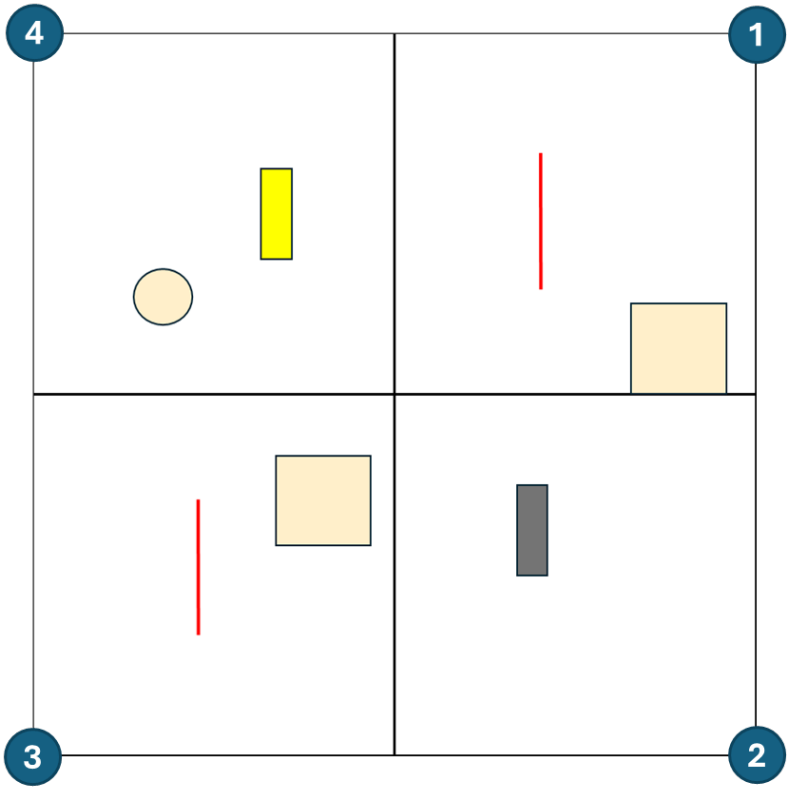

Figure B.4. Plate 4.

Table B.5. Plate 5.

130N 8.3% (additional 2% fumed silica) tack coat on primer and between each layer		
1/4" notched trowel for the 130N		
FG Layer	No Defects	
CF1	Q1 – 2 in. to 3 in. wrinkle	20.5 in. right and 2 in. to 5 in. down
CF2	Q1 – Dry spot (3 in. x 3 in. square)	13 in. to 16 in. right and 3 in. to 6 in. down
CF3	Q2 – 3 in. x 1 in. overlap	17 in. to 18.25 in. right and 14.5 in. to 17.5 in. down
	Q3 – 2 in. to 3 in. wrinkle	4.75 in. right and 15.5 in. to 19 in. down
	Q4 – 3 in. x 1 in. gap	9 in. to 10 in. right and 5 in. to 8 in. down
CF4	Q3 – Dry spot (3 in. x 3 in. square)	7.5 in. to 10.5 in. right and 16 in. to 19 in. down
CF5	Q4 – Dry spot (3 $in.^2$ circle)	4.5 in. right 8.5 in. down to center
CF6	No Defects	

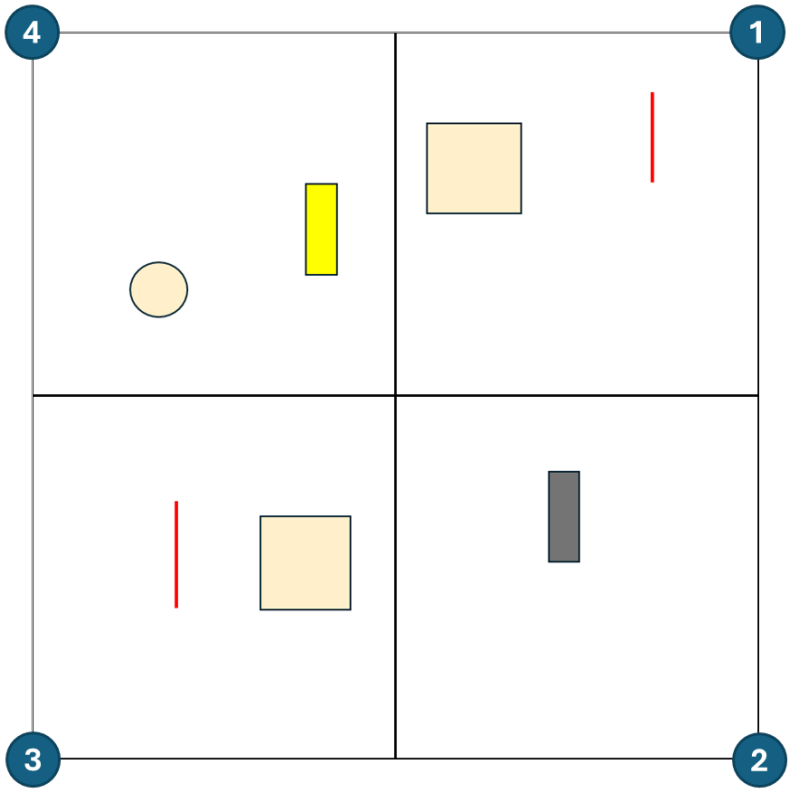

Figure B.5. Plate 5.

Table B.6. Plate 6.

130N 10.3% (additional 4% fumed silica) tack coat on primer and between each layer		
1/4" notched trowel for the 130N		
FG Layer	No Defects	
CF1	Q1 – 2 in. to 3 in. wrinkle	20.75 in. right and 7.5 in. to 10.5 in. down
CF2	Q1 – Dry spot (3 in. x 3 in. square)	14 in. to 17 in. right and 3 in. to 6 in. down
CF3	Q2 – 3 in. x 1 in. overlap	15.375 in. to 16.375 in. right and 17.125 in. to 20.125 in. down
	Q3 – 2 in. to 3 in. wrinkle	8 in. right and 14.5 in. to 16.5 in. down
	Q4 – 3 in. x 1 in. gap	2.5 in. to 3.5 in. right and 6.5 in. to 9.125 in. down
CF4	Q3 – Dry spot (3 in. x 3 in. square)	3 in. to 6 in. right and 19.25 in. to 22.25 in. down
CF5	Q4 – Dry spot (3 in.^{2} circle)	9 in. right and 6.5 in. down to center
CF6	No Defects	

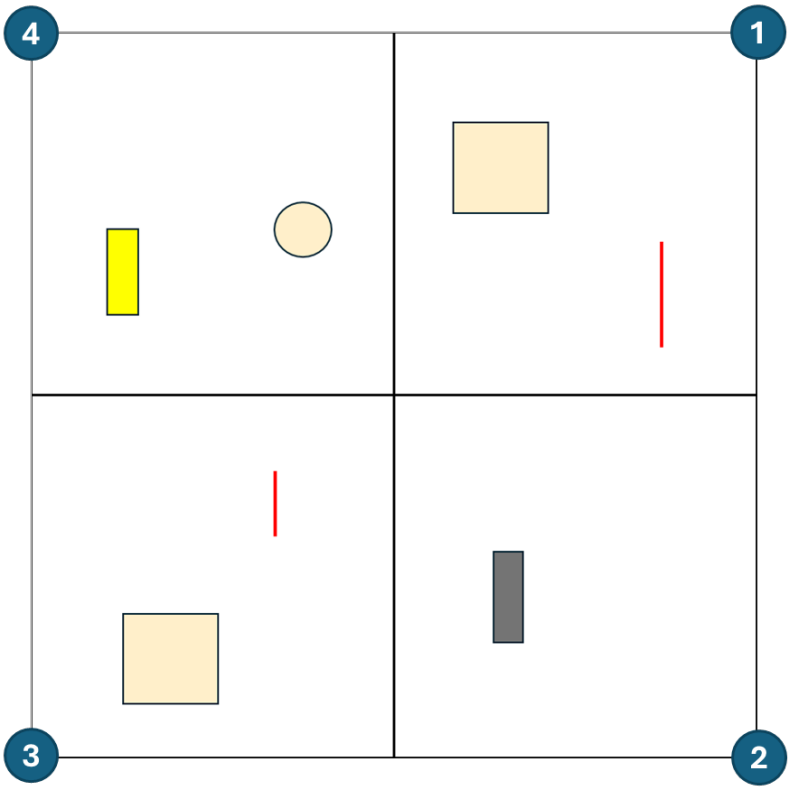

Figure B.6. Plate 6.

Table B.7. Plate 7.

Blast 3 quadrants – Leave Q3 unblasted		
130N 8.3% (additional 2% fumed silica) tack coat on primer and between each layer		
1/16” notched trowel for the 130N		
FG Layer	Q1 – Dry spot (3 $in.^2$ circle)	12.75 in. right and 10 in. down to center
	Q1 – Dry spot (3 in. x 3 in. square)	16.5 in. to 19.5 in. right and 3.25 in. to 6.25 in. down
	Q2 – Primer partial cure before ply	
	Q3 – Improper surface prep – no blast	
CF1	No Defects	
CF2	No Defects	
CF3	No Defects	
CF4	No Defects	
CF5	No Defects	
CF6	No Defects	

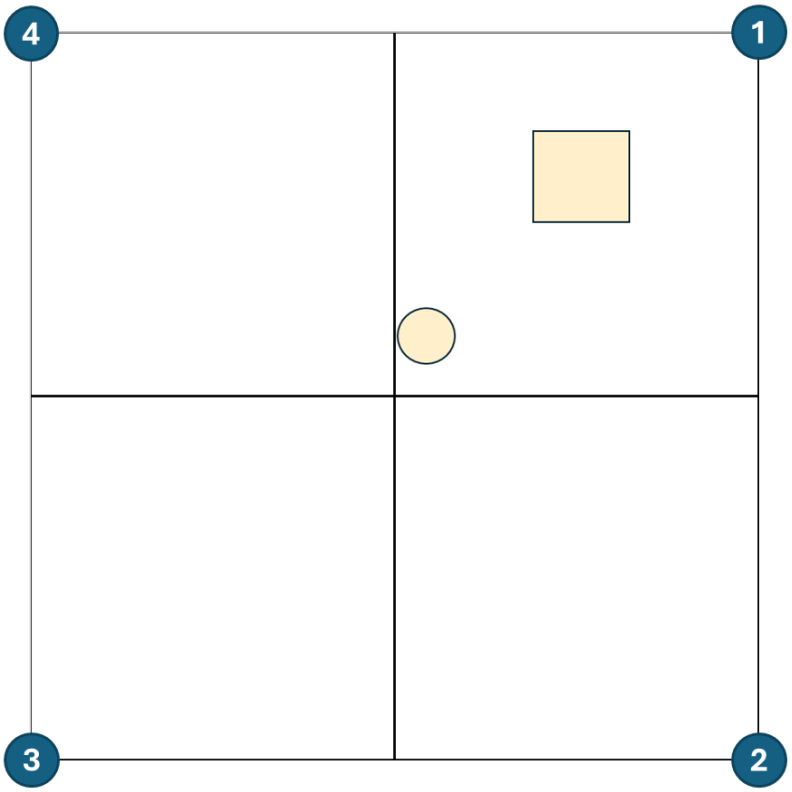

Figure B.7. Plate 7.

Table B.8. Plate 8.

Blast 3 quadrants – Leave Q3 unblasted		
130N 8.3% (additional 2% fumed silica) tack coat on primer and between each layer		
1/4" notched trowel for the 130N		
FG Layer	Q1 – Dry spot (3 $in.^2$ circle)	19.5 in. right and 9.25 in. down
	Q1 – Dry spot (3 in. x 3 in. square)	13 in. to 16 in. right and 3.5 in. to 6.5 in. down
	Q2 – Primer partial cure before ply	
	Q3 – Improper surface prep – no blast	
CF1	No Defects	
CF2	No Defects	
CF3	No Defects	
CF4	No Defects	
CF5	No Defects	
CF6	No Defects	

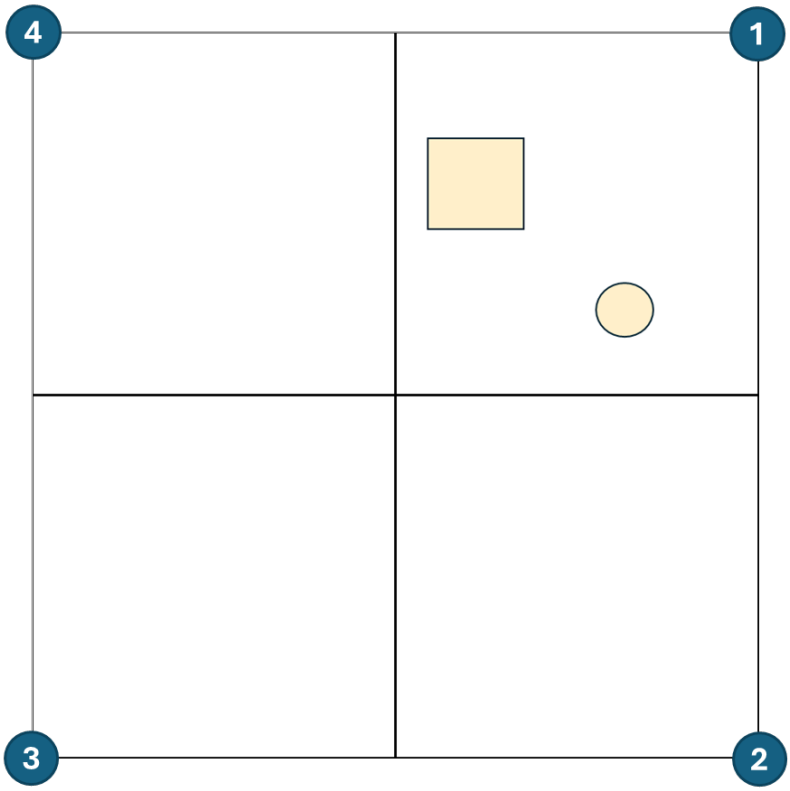

Figure B.8. Plate 8.

Appendix C – NDE Survey

This appendix is a reproduction of the NDE survey, including the included introductory material and questions.

The U.S. Nuclear Regulatory Commission (NRC) Office of Research has sponsored the Pacific Northwest National Laboratory (PNNL) to evaluate nondestructive examination (NDE) for assessing carbon-fiber-reinforced polymer (CFRP) in-ground piping repairs. As part of a memorandum of understanding (MOU) between the NRC and the Electric Power Research Institute (EPRI), PNNL is collaborating with EPRI (who is conducting independent research in this area) to evaluate NDE capabilities for CFRP repairs in Class 2 and 3 safety-related piping.

As part of a project, PNNL is surveying CFRP subject-matter experts to help identify and prioritize the critical flaws and defects found during both the CFRP repair installation process as well as throughout the anticipated lifetime of the repair. In addition, we hope to better understand how the variables associated with CFRP fabrication/application techniques impact the NDE used to ensure the integrity of repairs.

Your answers are very appreciated and will be helpful in guiding the fabrication of mockups for use in NDE research.

During the preliminary review and workshop held at EPRI, PNNL-NRC-EPRI identified a list of conditions (variables related to the design as well as flaws/defects) that are to be simulated in the NDE mockups being fabricated. As it is not feasible to fabricate mockups that include every possible condition, the team would like to identify the most important ones that should be considered in the design and fabrication of our NDE mockups. Below, we are asking you to please provide your thoughts on what design considerations and flaws/defects will impact the structural integrity of the CFRP repair, and thus, are necessary to mockup to assess NDE capabilities.

1. Please select profession/mention level of expertise relative to composite material repairs: Designer / Asset Owner / Fabricator / Installer / NDE Researcher / NDE Level Certified Tech / Other

For an *internal* CFRP repair of a steel piping system operating below 300 PSIG and 200F and between 30 – 48 inches in diameter, please provide details of possible attribute ranges and configurations that may be used for the repair.

2. Typical carbon fiber fabric weight
3. Typical glass fiber fabric weight
4. Carbon fiber fabric orientation (bi-directional or unidirectional)
5. Number of carbon fiber layers (total)
6. Number of carbon fiber layers (unidirectional fabric) in hoop direction
7. Number of carbon fiber layers (unidirectional fabric) in longitudinal direction
8. Number of glass fiber layers (total)
9. Example configurations of fabric installation design (e.g., 1-Glass, 1-Hoop, 1-Longtidunal, 1-Glass, 1-Hoop)
10. Do you use thickened epoxy between layers?
11. Do you use thickened epoxy as a topcoat?
12. Do you use thickened epoxy at interface to substrate?
13. Please describe nature of any thickened epoxy used (e.g., epoxy + fumed silica vs. other)
14. Total range of CFRP repair thickness (inches)

For an external CFRP repair of a steel piping system operating below 300 PSIG and 200F and between 30 – 48 inches in diameter, please provide details of possible attribute ranges and configurations that may be used for the repair.

15. Typical carbon fiber fabric weight
16. Typical glass fiber fabric weight
17. Carbon fiber fabric orientation (bi-directional or unidirectional)
18. Number of carbon fiber layers (total)
19. Number of carbon fiber layers (unidirectional fabric) in hoop direction
20. Number of carbon fiber layers (unidirectional fabric) in longitudinal direction
21. Number of glass fiber layers (total)
22. Example configurations of fabric installation design (e.g., 1-Glass, 1-Hoop, 1-Longtidunal, 1-Glass, 1-Hoop)
23. Do you use thickened epoxy between layers?
24. Do you use thickened epoxy as a topcoat?
25. Do you use thickened epoxy at interface to substrate?
26. Please describe nature of any thickened epoxy used (e.g., epoxy + fumed silica vs. other)
27. Total range of CFRP repair thickness (inches)

Below is a list of postulated design-related flaws that could have an impact on CFRP integrity and/or performance. Please list/describe any that may be missing:

- Loss of adhesion to substrate
- Delamination between layers
- Air voids within epoxy matrix
- Cracking of epoxy matrix
- Under saturation of fabric
- Over saturation of the fabric
- Air bubbles / blisters in final layer or topcoat
- Presence of foreign object debris

28. Comments on any flaw/defects missing
29. Comments on any flaw/defects described above

For each postulated design-related flaw, please indicate your view on the potential degree of criticality this flaw type could have CFRP performance. The range is 1-5, with 1 being very critical, and 5 being relatively inconsequential.

30. Loss of adhesion to substrate (terminal end regions)
    a. Flaw size < 2 in.
    b. Flaw size 2-5 in.
    c. Flaw size > 5 in.
31. Delamination between layers
    a. Flaw size < 2 in.
    b. Flaw size 2-5 in.
    c. Flaw size > 5 in.
32. Air voids (<0.1 in. diameter) throughout epoxy matrix
    a. <2% of area
    b. 2-5% of area
    c. >5% of area
33. Cracking of epoxy matrix
    a. Flaw size > 2 in.
    b. Flaw size > 5 in.
    c. Flaw size > 10 in.
34. Undersaturation of fabric

   a. Flaw size > 2 in.
   b. Flaw size > 5 in.
   c. Flaw size > 10 in.
35. Oversaturation of fabric
   a. Flaw size > 2 in.
   b. Flaw size > 5 in.
   c. Flaw size > 10 in.
36. Air bubbles / blisters in final layer or topcoat
   a. Flaw size > 2 in.
   b. Flaw size > 5 in.
   c. Flaw size > 10 in.
37. Presence of foreign object debris
   a. < 0.25 in.
   b. 0.25-1 in.
   c. > 1 in.
38. Please list / describe any flaw types that would be of concern to detect and size during the lifetime of the composite (e.g., in-service induced flaws). Please include range of sizes of potential interest to detect based on impact to possible CFRP performance, considering both normal operations and during design basis event).

Questions related to NDE

39. If in situ monitoring was readily available, what metrics, flaws or attributes would be most important to monitor (substrate disbonds, interply delamination, strength of bonds, glass transition temperature, etc.)?
40. What fabrication methods do you recommend for creating intentional flaws in the CFRP mockup?
41. What techniques do you use for NDE and what flaws are identifiable with that technique?
42. Does the NDE technique you use, have any limitations on the surface of the CFRP repair? Like surface color, surface preparation requirements?
43. Does the NDE technique have limitations in detecting flaws on the flat plates vs. the piping?
44. How is the curing temperature monitored during the installation?
45. Are there any other comments that you would like to provide?

Appendix D – EPRI Mockup Manual Tap Testing Data

Table D.1. Summary of delamination detection using MTT.

Mockup Set #	Mockup Plate #	Total No. of Layers in Mockup	Defect Placed on Top of Layer#	Delamination Size	MTT in Ambient	MTT with Noise
1	1	2	Base	Small	x	
1	1	2	Base	Medium	x	
1	1	2	Base	Large	x	x
1	1	2	1	Small	x	x
1	1	2	1	Medium	x	x
1	2	3	Base	Small		
1	2	3	Base	Medium		
1	2	3	Base	Large	x	x
1	2	3	2	Small	x	x
1	2	3	2	Medium	x	x
1	2	3	2	Large	x	x
1	3	4	Base	Large	x	x
1	3	4	1	Small	x	x
1	3	4	1	Medium	x	x
1	3	4	2	Small	x	
1	3	4	2	Medium	x	x
1	5	5	Base	Large	x	x
1	5	5	1	Large	x	
1	5	5	2	Large	x	x
1	5	5	4	Small	x	x
1	5	5	4	Medium	x	x
1	7	6	Base	Large	x	x
1	7	6	2	Large	x	x
1	7	6	5	Large	x	x

Table D.2. Summary of air bubbles detection using MTT.

Mockup Set #	Mockup Plate #	Defect Placed on Top of Layer #	Delamination Size	MTT in Ambient	MTT with Noise
2A	1	Base	Unfilled air bubble 4 in.^{2}	x	x
2A	1	Base	Filled air bubble 10 in.^{2}		
2A	3	2	Unfilled air bubble 4 in.^{2}	x	x
2A	3	2	Filled air bubble 10 in.^{2}.		
2A	4	3	Unfilled air bubble 4 in.^{2}	x	x
2A	4	3	Filled air bubble 10 in.^{2}		
2A	5	4	Unfilled air bubble 4 in.^{2}	x	x
2A	5	4	Filled air bubble 10 in.^{2}		
2A	6	5	Unfilled air bubble 4 in.^{2}	x	x
2A	6	5	Filled air bubble 10 in.^{2}		
2A	7	2	Unfilled air bubble 10 in.^{2}	x	x
2A	7	2	Filled air bubble 10 in.^{2}		
2A	8	4	Unfilled air bubble 10 in.^{2}	x	x
2A	8	4	Filled air bubble 10 in.^{2}		
2B	11	2	Unfilled air bubble 4 in.^{2}	x	x
2B	11	2	Filled air bubble 10 in.^{2}		
2B	12	3	Unfilled air bubble 4 in.^{2}	x	x
2B	12	3	Filled air bubble 10 in.^{2}		
2B	13	4	Unfilled air bubble 4 in.^{2}	x	x
2B	13	4	Filled air bubble 10 in.^{2}		
2B	15	3	Unfilled air bubble 10 in.^{2}	x	x
2B	15	3	Filled air bubble 10 in.^{2}		
2B	16	3	Filled air bubble (1/16 in. thick)		
2B	16	3	Filled air bubble (1/8 in. thick)		
2B	16	3	Filled air bubble (3/16 in. thick)	x	x

Table D.3. Summary of dry spot detection using MTT.

Mockup Set #	Mockup Plate #	Defect Placed on Top of Layer#	Delamination Size	MTT in Ambient	MTT with Noise
2A	1	1	Dry spot 1 in.^{2}		
2A	1	1	Dry spot 2 in.^{2}		
2A	1	1	Dry spot 4 in.^{2}	x	
2A	1	1	Dry spot 6 in.^{2}	x	x
2A	3	3	Dry spot 1 in.^{2}	x	
2A	3	3	Dry spot 2 in.^{2}	x	
2A	3	3	Dry spot 4 in.^{2}	x	x
2A	3	3	Dry spot 6 in.^{2}	x	x
2A	4	4	Dry spot 1 in.^{2}	x	x
2A	4	4	Dry spot 2 in.^{2}	x	x
2A	4	4	Dry spot 4 in.^{2}	x	x
2A	4	4	Dry spot 6 in.^{2}	x	x
2A	5	5	Dry spot 1 in.^{2}		
2A	5	5	Dry spot 2 in.^{2}	x	
2A	5	5	Dry spot 4 in.^{2}	x	x
2A	5	5	Dry spot 6 in.^{2}.	x	x
2A	6	6	Dry spot 1 in.^{2}	x	x
2A	6	6	Dry spot 2 in.^{2}		
2A	6	6	Dry spot 4 in.^{2}	x	x
2A	6	6	Dry spot 6 in.^{2}	x	x
2A	7	3	Dry Spot 10 in.^{2}	x	x
2A	8	5	Dry Spot 10 in.^{2}	x	x
2B	11	3	Dry spot 1 in.^{2}		
2B	11	3	Dry spot 2 in.^{2}		
2B	11	3	Dry spot 4 in.^{2}		
2B	11	3	Dry spot 6 in.^{2}	x	x
2B	12	4	Dry spot 1 in.^{2}		
2B	12	4	Dry spot 2 in.^{2}		
2B	12	4	Dry spot 4 in.^{2}		
2B	12	4	Dry spot 6 in.^{2}	x	x
2B	13	5	Dry spot 1 in.^{2}		
2B	13	5	Dry spot 2 in.^{2}		
2B	13	5	Dry spot 4 in.^{2}	x	
2B	13	5	Dry spot 6 in.^{2}	x	
2B	15	4	Dry Spot 10 in.^{2}	x	x

Table D.4. Summary of overlap detection using MTT.

Mockup Set #	Mockup Plate #	Defect Placed on Top of Layer#	Delamination Size	MTT in Ambient	MTT with Noise
2A	8	3	Overlap		

Appendix E – NDE Plots of PNNL Mockups

The NDE results from MTT, ATT, UT, and DRS are compared together in this appendix. The images below are organized as shown in Figure E.1: the top left quadrant is the MTT results, the top right quadrant is the ATT results obtained using EVOTIS, the bottom left quadrant has the 1.0 MHz UT results, and the bottom right quadrant is the DRS results. Plots are overlaid with the true-state maps.

Note that 1.0 MHz UT plots on the bottom left quadrant were obtained by stitching the results collected on each quadrant of the plate, which may have different gain settings. Also, different gate (depth) settings were needed to identify the defects; not all defects may be visible in a single screenshot.

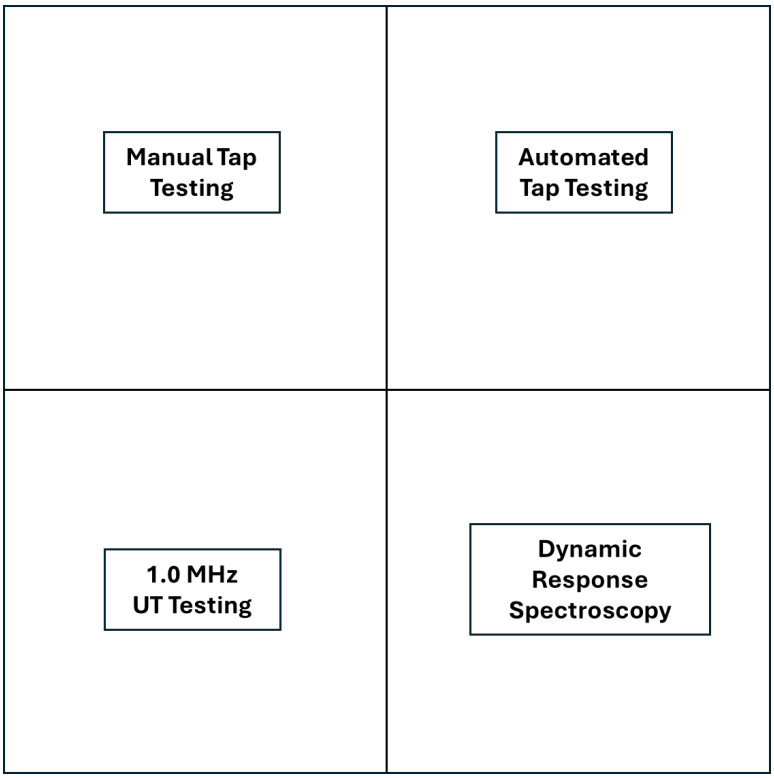

Figure E.1. Figures in this appendix will be organized according to this map.

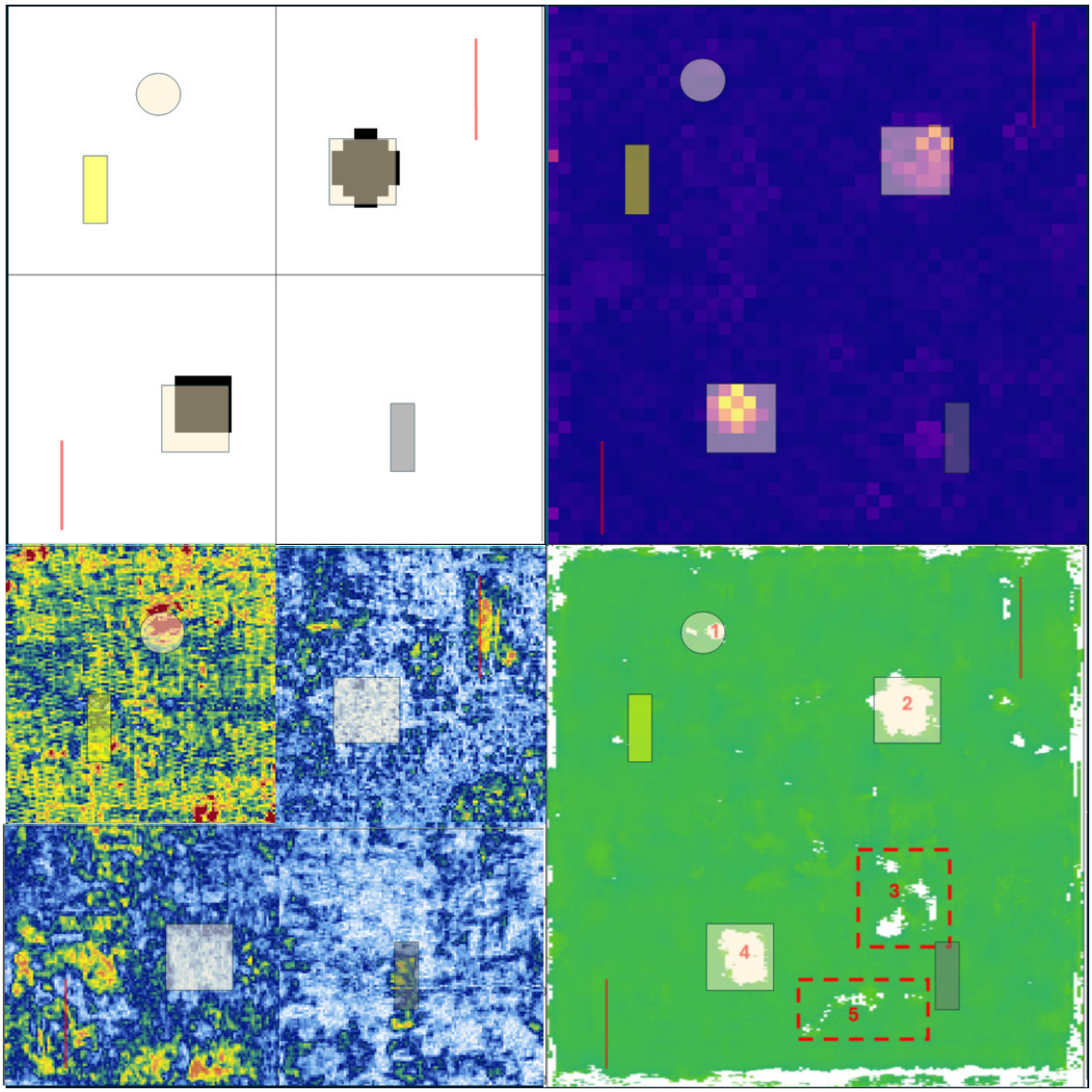

Figure E.2. NDE of CFRP Plate 1.

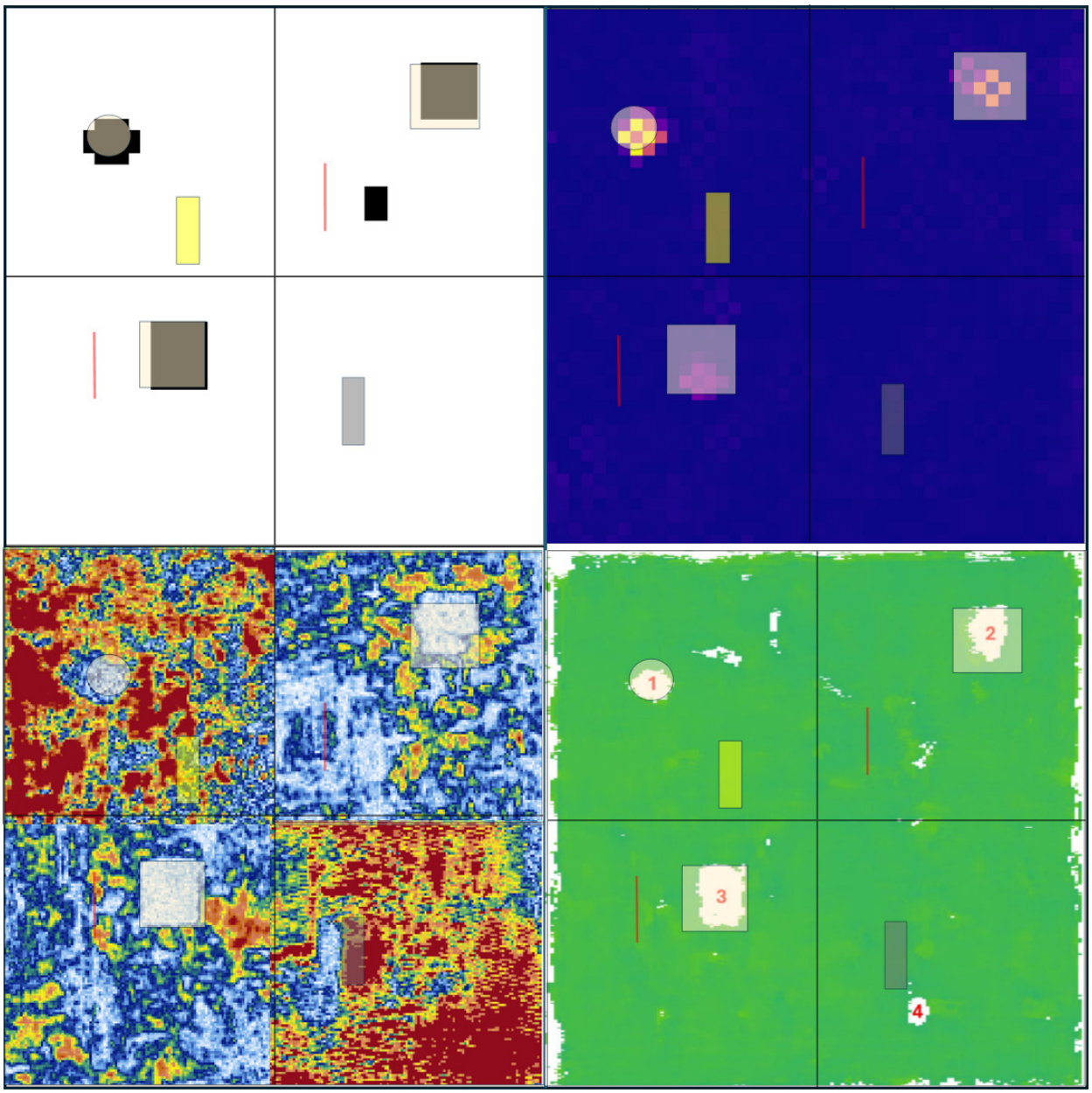

Figure E.3. NDE of CFRP Plate 2.

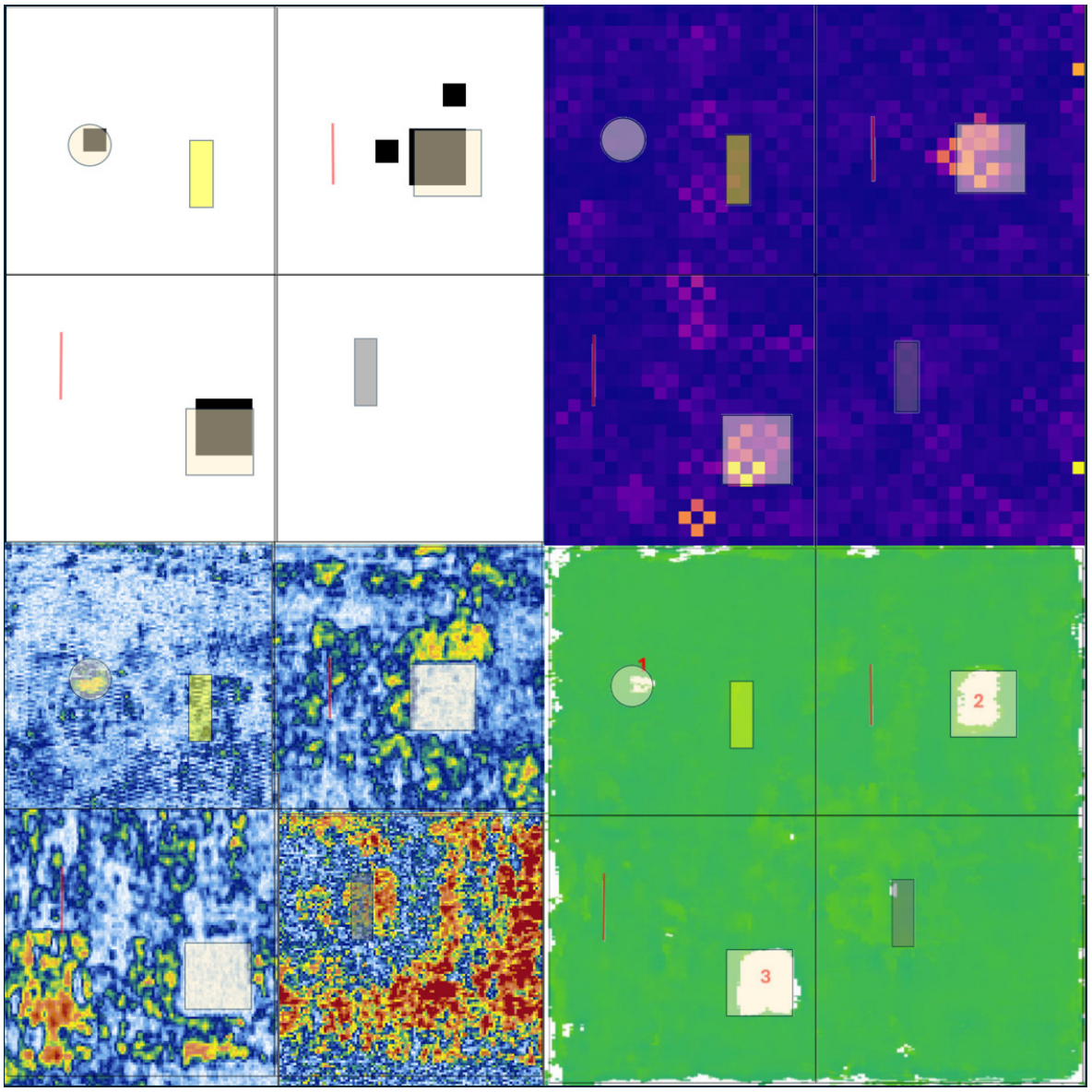

Figure E.4. NDE of CFRP Plate 3.

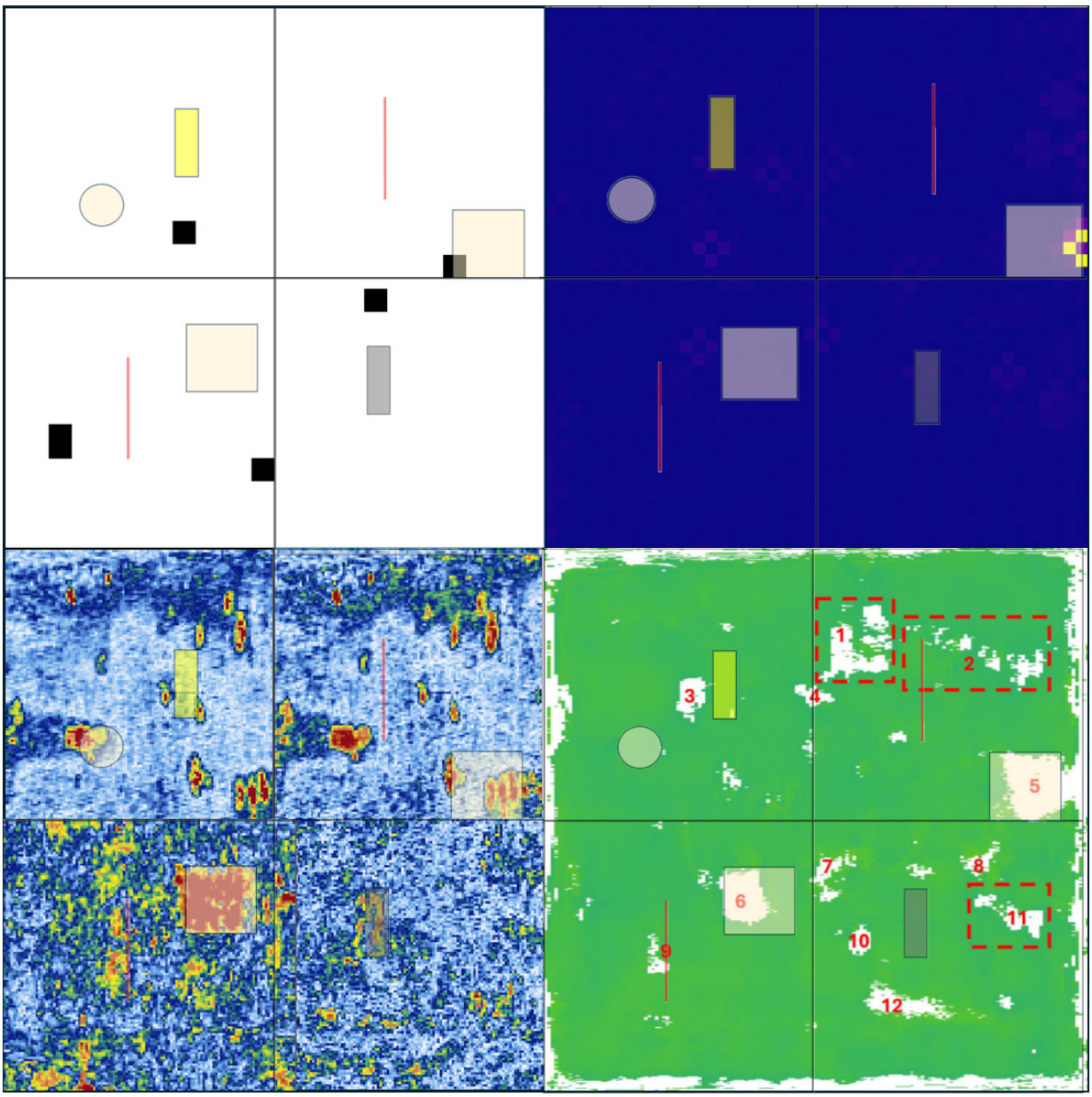

Figure E.5. NDE of CFRP Plate 4.

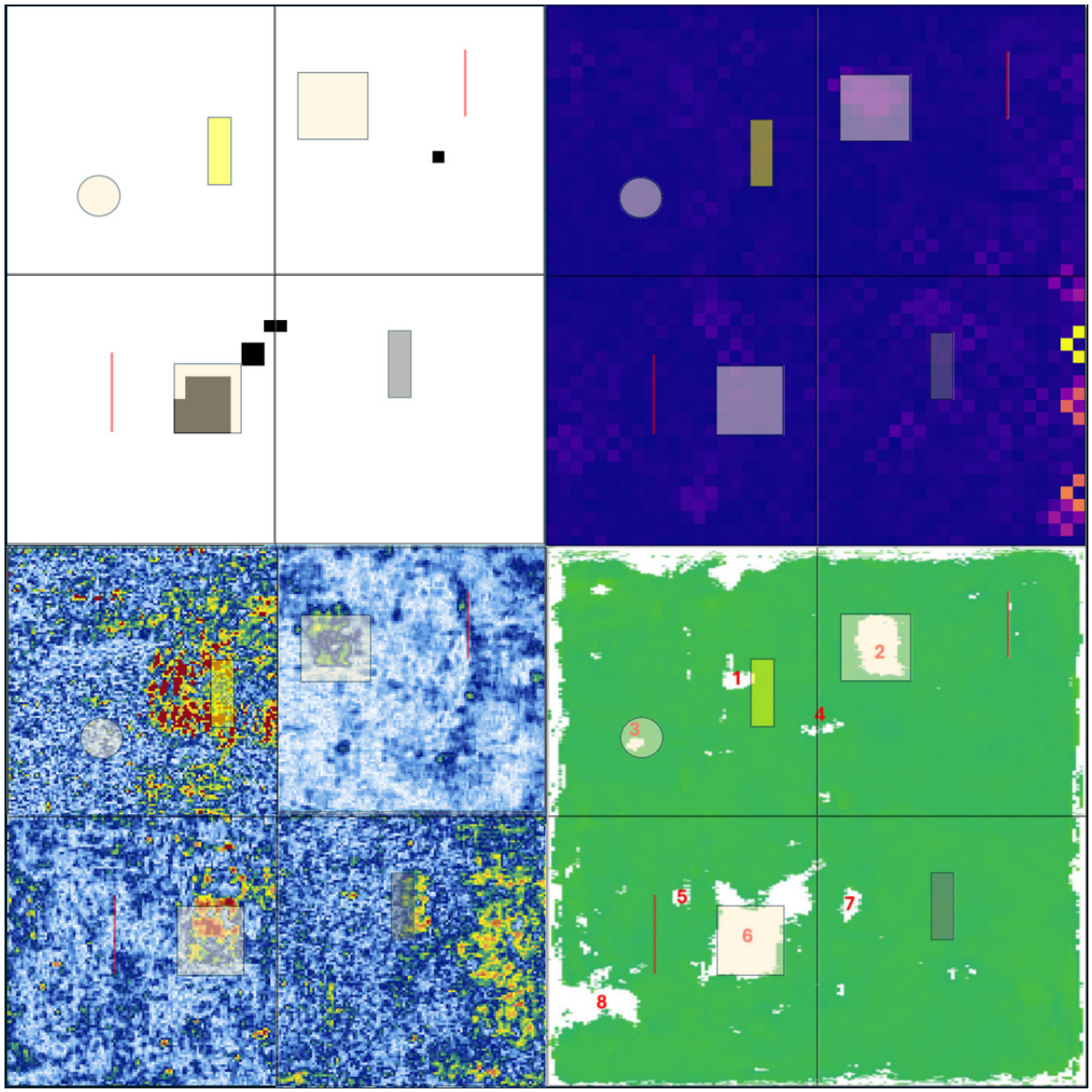

Figure E.6. NDE of CFRP Plate 5.

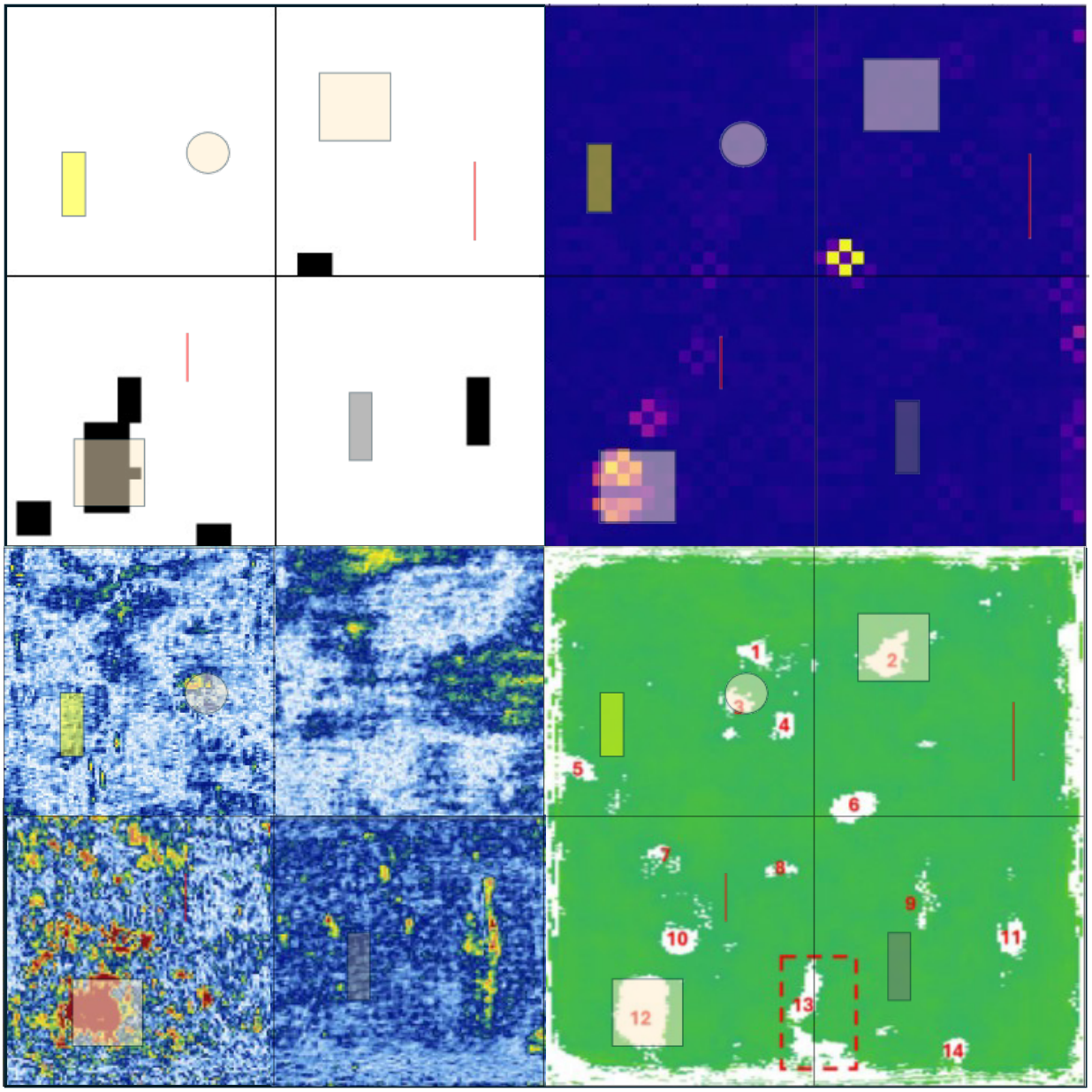

Figure E.7. NDE of CFRP Plate 6.

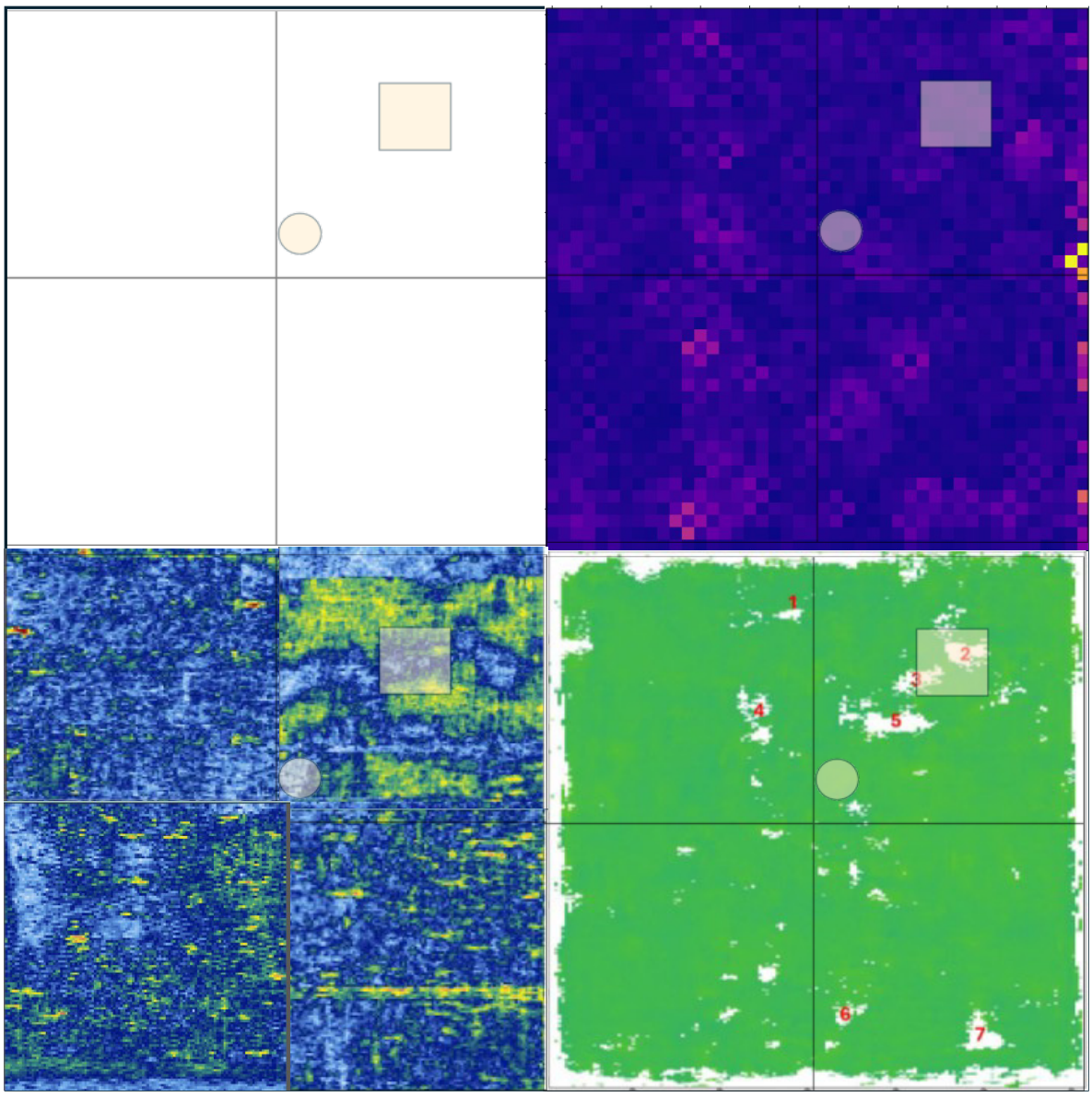

Figure E.8. NDE of CFRP Plate 7.

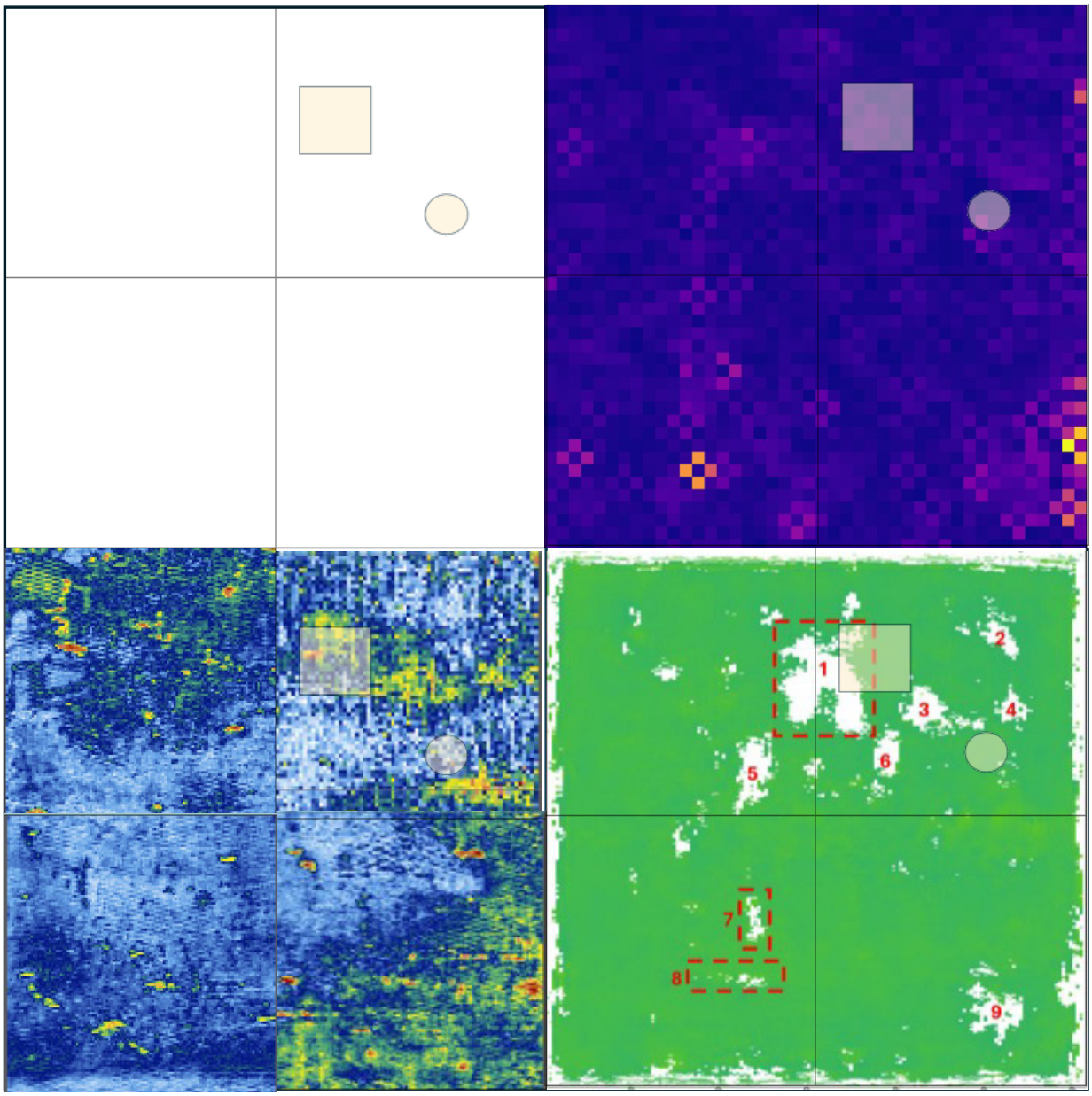

Figure E.9. NDE of CFRP Plate 8.

Pacific Northwest National Laboratory

902 Battelle Boulevard
P.O. Box 999
Richland, WA 99354

1-888-375-PNNL (7665)

www.pnnl.gov